THE SINGULAR FUNCTION BOUNDARY INTEGRAL METHOD FOR LAPLACIAN AND BIHARMONIC PROBLEMS WITH BOUNDARY SINGULARITIES

Miltiades Ch. Elliotis

PhD Dissertation

DEPARTMENT OF MATHEMATICS AND STATISTICS

UNIVERSITY OF CYPRUS

Supervisor: Professor Georgios Georgiou

Co-supervisor: Assistant Professor Christos Xenophontos

Nicosia

May, 2005

To my wife Ioulia

and to the rest of my family.

To the memory of my father Charalambos Elliotis.

To my mother Agathoniki, brother Loizos and sister Eleni.

Περίληψη

Στη διατριβή αυτή αναπτύσσουμε την Μέθοδο Συνοριακού Ολοκληρώματος με Ιδιόμορφες Συναρτήσεις (ΜΣΟΙΣ) σε Λαπλασιανά και διαρμονικά προβλήματα με ιδιόμορφα συνοριακά σημεία. Τέτοια προβλήματα συναντώνται σε αρκετές φυσικές και βιολογικές επιστήμες. Στην προτεινόμενη μέθοδο η λύση στη γειτονιά του ιδιόμορφου σημείου προσεγγίζεται απο τους πρώτους όρους του ασυμπτωτικού αναπτύγματος της τοπικής λύσης των οποίων οι συντελεστές ονομάζονται *ιδιόμορφοι συντελεστές*. Με εφαρμογή της μεθόδου Galerkin διακριτοποιείται η διέπουσα μερική διαφορική εξίσωση και με τη βοήθεια του θεωρήματος Green το χωρικό ολοκλήρωμα ανάγεται σε συνοριακό. Οι συνοριακές συνθήκες Dirichlet εφαρμόζονται ασθενώς με πολλαπλασιαστές Lagrange που προσεγγίζονται τοπικά με δευτεροβάθμιες συναρτήσεις βάσης. Προκύπτει έτσι, ένα γραμμικό σύστημα διακριτοποιημένων εξισώσεων με άγνωστους τους ιδιόμορφους συντελεστές και τους πολλαπλασιαστές Lagrange.

Στο πρώτο μέρος της διατριβής, η ΜΣΟΙΣ εφαρμόζεται σε δυο Λαπλασιανά προβλήματα σε χωρία σχήματος L. Τα αποτελέσματα της μεθόδου συγκρίνονται με αυτά άλλων μεθόδων και της *hp* εκδοχής των πεπερασμένων στοιχείων. Ακολούθως, η ΜΣΟΙΣ επεκτείνεται στην επίλυση διαρμονικών προβλημάτων με ιδιόμορφο συνοριακό σημείο και εφαρμόζεται στο ρευστοδυναμικό πρόβλημα ολίσθησης-μη ολίσθησης (stick-slip problem) και στο θραυστομηχανικό πρόβλημα Schiff. Στα προβλήματα αυτά η μέθοδος οδηγεί σε ταχείς ρυθμούς σύγκλισης και αποτελέσματα μεγάλης ακρίβειας που συγκρίνονται ευμενώς με αυτά άλλων τεχνικών της βιβλιογραφίας και με τις αναλυτικές λύσεις. Στο τελευταίο μέρος της διατριβής ασχολούμαστε με τη θεωρητική ανάλυση της μεθόδου για προβλήματα Laplace και αποδεικνύουμε ότι υπό προϋποθέσεις, η σύγκλισή της είναι εκθετική.

Abstract

In this dissertation we develop the Singular Function Boundary Integral Method (SFBIM) for Laplacian and biharmonic boundary value problems with boundary singularities. Such problems are encountered in many physical and biological applications. In the proposed method the solution in the neighbourhood of the singular point is approximated by the truncated local asymptotic expansion which is expressed as a series of singular functions, the coefficients of which are called *singular coefficients*. The Galerkin method is employed in order to discretize the governing partial differential equation. By means of the divergence theorem, the volume integrals are reduced to boundary integrals, and the Dirichlet boundary conditions are weakly enforced by means of Lagrange multiplier functions, which are expressed in terms of quadratic basis functions. The resulting linearized system of discretized equations, is solved for the unknown singular coefficients and the Lagrange multipliers.

In the first part of the thesis, the SFBIM is applied to two Laplacian Problems over L-shaped domains. The results are compared with those of other methods and the p/hp finite element method. Then, the SFBIM is developed for the solution of two biharmonic problems with a boundary singularity and applied to the Newtonian stick-slip problem of fluid mechanics and the so-called Schiff problem of fracture mechanics. In all the above problems the method exhibits high accuracy and fast rate of convergence. The results compare favorably with the analytical solution and available numerical results in the literature. In the last part of the dissertation, we deal with the theoretical analysis of the method for Laplacian problems and we show that, under certain conditions, the convergence is exponential.

Acknowledgements

Many thanks are due to the academic and administrative staff of the Department of Mathematics and Statistics of the University of Cyprus and in general to everyone who supported me in this effort. Obviously, special thanks are due to my wife Ioulia and to my mother, brother and sister for their encouragement and help. Naturally, I would like to express my gratidute to my supervisor Professor Georgios Georgiou and to my co-supervisor Professor Christos Xenophontos, for their encouragement, guidance and support throughout the whole period of my studies at the Masters and PhD levels, research and preparation of this work.

Miltiades Ch. Elliotis

Department of Mathematics and Statistics

University of Cyprus, May 2005

Contents

List of Figures

List of Tables

Chapter 1

Introduction

In many engineering problems (e.g., in fracture and fluid mechanics), governed by Laplacian or biharmonic partial differential equations, boundary singularities arise when there is a sudden change in the boundary conditions (along a smooth boundary) or in the geometry of the boundary itself [31]. This causes most standard numerical methods, such as finite-element, boundary-element, finite-difference and spectral methods, to perform poorly. Many specialized numerical schemes have been developed during the last three decades in order to alleviate this problem. For example, in the context of the finite element method, this can be achieved by adaptive grid refinement (e.g., [10, 20]), the use of the *hp* version on geometrically graded meshes [6] or the use of the multigrid finite element method [12]. While these methods yield adequate accuracy, and even exponential convergence rates in the case of the *hp* version, the computational cost required is significant.

With this in mind, in this dissertation we are concerned with the development of a special boundary integral method for the solution of Laplacian and biharmonic problems with boundary singularities. This method, called Singular Function Boundary Integral Method (SFBIM), belongs to the family of numerical schemes which incorporate the form of the singularity in the approximation. (cf. [29, 30, 32, 36, 44]). In fact, the SFBIM is based on the approximation of the solution by the leading terms of the local solution expansion near the point of singularity,

which for most problems is known. The main advantage of this method is its exponential convergence rate. Moreover, because the discretized equations are reduced to boundary integrals, by means of the divergence theorem, the computational cost of the method is significantly reduced compared to other methods. In addition, the leading singular coefficients of the local solution expansion, which are desired in most problems, are calculated directly (i.e., no post-processing is required).

Clearly, knowledge of the local solution is a prerequisite in using the SFBIM. Hence, the rest of this chapter is devoted to the description of the local solutions for certain Laplacian and biharmonic problems. In Section 1.1 the concept of a boundary singularity is discussed and the local solutions in 2-D Laplacian problems are presented. In Section 1.2 the local solutions for planar biharmonic problems are discussed. In Section 1.3 the definition of some function spaces and associated norms, used in this thesis are given, and finally in Section 1.4 we elaborate on the format of the structure of the dissertation.

1.1 Local solutions for 2-D Laplacian problems

In many elliptic problems defined on the plane[1] there are boundary singularities which are usually due to sudden geometric changes on the boundary (e.g. existence of a re-entrant corner) or due to an abrupt change in the conditions on a smooth boundary (see Figure 1.1). The local solution in the vicinity of a singular point can be determined by a local analysis, as summarized below.

Let us consider the Laplace equation

$$\nabla^2 u = 0 \quad \text{in} \quad \Omega, \tag{1.1}$$

[1] In this work we deal with 2-D problems only.

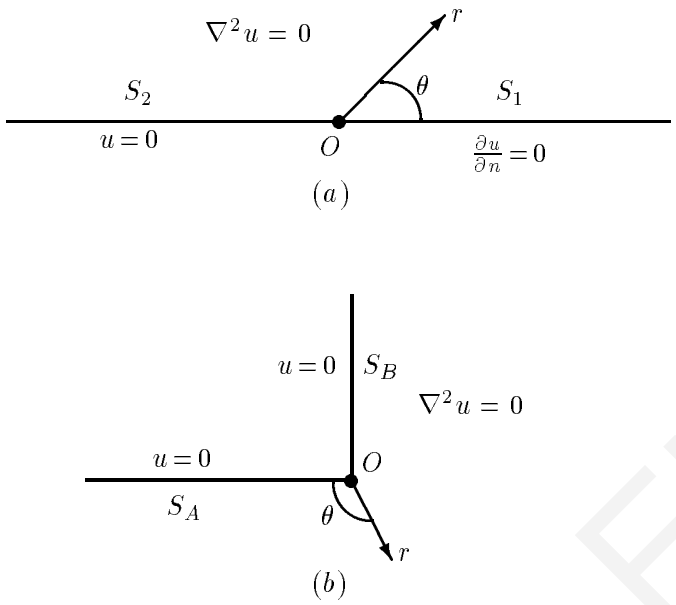

Figure 1.1. *Examples of boundary singularities : (a) Sudden change in boundary conditions on a smooth boundary (b) Sudden geometric change (re-entrant corner). The variables (r, θ) denote polar coordinates centered at the singular point.*

where $\Omega \subset \mathbf{R^2}$ is a bounded domain and let us assume that there is a boundary singularity at O (See Figure 1.1(a) or 1.2). This singular point is shared by the straight boundary parts S_1 and S_2 on which there are different boundary conditions. In order to find the local asymptotic solution we use polar coordinates and we follow the classical technique of separation of variables. Thus, u is expressed as $u(r,\theta) = R_\mu(r)\, f_\mu(\theta)$, where $\mu \in \mathbf{R}$ is the eigenvalue of the operator, and we find that

$$u(r,\theta) = \sum_{i=1}^{\infty} \alpha_i\, r^{\mu_i}\, f_{\mu_i}(\theta)\,, \tag{1.2}$$

where the coefficients $\alpha_i \in \mathbf{R}$ are calculated from the boundary conditions on the rest of the boundary, and f_{μ_i} is a trigonometric function which for the examples in Figures 1.1(a) and 1.2 has the form $f_{\mu_i} = \cos(\mu_i\, \theta)$.

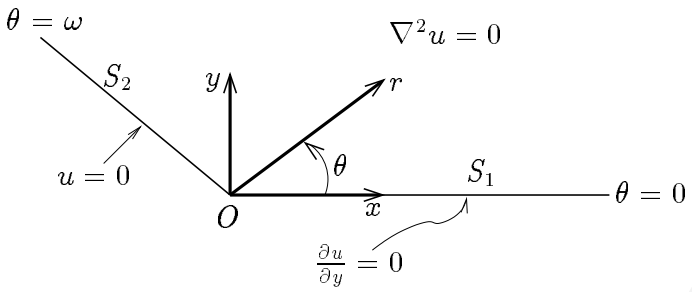

Figure 1.2. *Example of a boundary singularity combining a sudden change both in the geometry of the boundary and the boundary conditions.*

1.2 Local solutions for 2-D biharmonic problems

The biharmonic equation is

$$\nabla^2 (\nabla^2 u) \;=\; \nabla^4 u \;=\; 0 \quad \text{in} \quad \Omega\,, \tag{1.3}$$

where $\Omega \subset \mathbf{R^2}$ is a bounded domain. This 4^{th} order partial differential equation is routinely used to model Stokes flow. An example is the case of a viscous flow between two rigid boundaries fixed at an angle 2α, which has a singularity at the point O of intersection of the two boundaries, as shown in Figure 1.3. In this problem u is called stream-function.

As in the case of the singular Laplacian problems, the solution of a singular biharmonic equation can be expressed in a series of the form

$$u(r,\theta) \;=\; \sum_{j=1}^{\infty} a_j \, r^{\mu_j + 1} \, f_{\mu_j}(\theta)\,, \tag{1.4}$$

where $f_{\mu_j}(\theta)$ has the following general form obtained after employing separation of variables:

$$f_{\mu_j}(\theta) \;=\; A_{\mu_j} \cos(\mu_j + 1)\theta + B_{\mu_j} \sin(\mu_j + 1)\theta + C_{\mu_j} \cos(\mu_j - 1)\theta + D_{\mu_j} \sin(\mu_j - 1)\theta\,, \tag{1.5}$$

where the coefficients A_{μ_j}, B_{μ_j}, C_{μ_j} and D_{μ_j} are real or complex numbers.

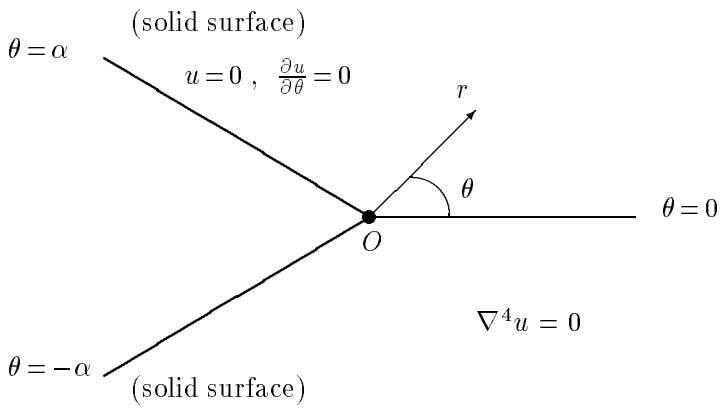

Figure 1.3. *Example of a singular biharmonic problem which corresponds to a viscous flow near a corner.*

Because we are going to concentrate on the viscous flow problem depicted in Figure 1.3, the terminology which will be used in the rest of this section, will pertain to this problem. Hence, as indicated by Dean and Montagnon [19], a disturbance far away from the region of the corner can cause either an axisymmetric or a symmetric flow pattern in the neighbourhood of the corner, and therefore the stream-function u is an even or odd function of θ, respectively. Due to the linearity property of the solutions of the biharmonic equation, we treat the two types of flows separately. Furthermore, we consider the case where $\alpha=\pi$. This is the case of a flow near a wall and a free surface, meeting at an angle π. In the bibliography, this case is also known as the stick-slip problem (Figure 1.4)

Axisymmetric problem (even solutions)

For this type of flow $f_{\mu_j}(\theta)$ is even ($B_{\mu_j}=D_{\mu_j}=0$) and thus we have

$$f_{\mu_j}(\theta) \;=\; A_{\mu_j}\,\cos(\mu_j\,+1)\,\theta\;+C_{\mu_j}\cos(\mu_j\,-1)\,\theta\,. \tag{1.6}$$

The even solutions must satisfy the conditions on the solid and free surfaces, i.e. the boundary conditions to the left and to the right of the singularity as shown in Figure 1.4. Therefore, we

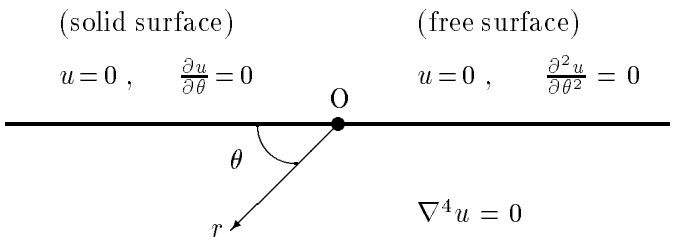

Figure 1.4. *Boundary singularity for the case of the stick-slip biharmonic problem.*

obtain the following expression for the axisymmetric flow:

$$f_1(\theta,\mu_j) \;=\; \alpha_j\;[\cos(\mu_j\;+1)\,\theta\;-\;\cos(\mu_j\;-1)\,\theta]\;,\qquad \mu_j\;=\;j\;-\frac{1}{2}\,,\quad j\;=\;1,2,\cdots\,. \tag{1.7}$$

Symmetric problem (odd solutions)

For this type of flow $f_{\mu_j}(\theta)$ is odd (A_{μ_j}=C_{μ_j}=0) and thus

$$f_{\mu_j}(\theta)\;=\;B_{\mu_j}\;\sin(\mu_j\;+1)\,\theta\;+D_{\mu_j}\;\sin(\mu_j\;-1)\,\theta\,. \tag{1.8}$$

As in the case of the even solutions, the odd solutions must satisfy the conditions on the solid and free surfaces, i.e. the boundary conditions on the boundary parts sharing the singular point. Thus, eventually, we obtain the following expression for the odd solutions:

$$f_2(\theta,\mu_j) = \beta_j\,[(\mu_j\;-1)\;\sin(\mu_j\;+1)\,\theta\;-(\mu_j\;+1)\;\sin(\mu_j\;-1)\,\theta]\,,\quad \mu_j = j{+}1,\quad j\;=\;1,2,\cdots. \tag{1.9}$$

Combining all the above information, the local solution is

$$u\;=\;\sum_{j=1}^{\infty}\;\alpha_j\,W_1^j\;+\;\sum_{j=1}^{\infty}\;\beta_j\,W_2^j\,, \tag{1.10}$$

where

$$W_1^j\;\equiv\;r^{\mu_j+1}\,f_1(\theta,\mu_j)\,,\qquad\qquad W_2^j\;\equiv\;r^{\mu_j+1}\,f_2(\theta,\mu_j)\,. \tag{1.11}$$

The above form of the local solution will be used in Chapter 4 where we discuss the extension of the SFBIM to the planar stick-slip problem. A similar analysis is made in order to determine the local solution for the case of biharmonic problems in fracture mechanics, as will be done in Chapter 5 for the so-called Schiff problem [65].

1.3 Preliminaries

In this work we will be using some standard function spaces and associated norms, the definitions of which are given in this section. First, we define the space $L^2(\Omega)$, of the square integrable functions, as

$$L^2(\Omega) \;=\; \left\{ v \;:\; \Omega \;\rightarrow\; R \;\;\text{measurable}\,, \;\; \int_\Omega \, v^2 \;<\; \infty \right\}\,, \tag{1.12}$$

equipped with the inner product $\langle u,\, v\rangle_\Omega \;=\; \int_\Omega \; u\, v$, and with the (Euclidean) norm

$$||u||_2 \;=\; \langle u,\, u\rangle_\Omega^{\frac{1}{2}}\,. \tag{1.13}$$

We also define the Sobolev space of order q [17]

$$H^q(\Omega) \;=\; \left\{ v \in L^2(\Omega) \,|\, D^\alpha \, v \in L^2(\Omega),\, |\alpha| \leq q \right\}. \tag{1.14}$$

Here, q is the value of the maximum order among the derivatives of the continuous functions in $L^2(\Omega)$, in the sence of distributions (cf. [14]), and the generalized derivative D^α of the function $v(x_1, x_2, \cdots, x_n)$ is defined as

$$D^\alpha v \;=\; \frac{\partial^{|\alpha|} v}{\partial x_1^{\alpha_1}\, \partial x_2^{\alpha_2} \cdots \partial x_n^{\alpha_n}} \qquad \text{where} \qquad |\alpha| \;=\; \sum_{i=1}^{n} \, \alpha_i\,. \tag{1.15}$$

The value of q determines the inner product which, in this case, is defined as

$$\langle u,\, v\rangle_{q,\Omega} \;=\; \sum_{|\alpha|\leq q} \; \int_\Omega \; D^\alpha u \, D^\alpha v\,. \tag{1.16}$$

The norm of $H^q(\Omega)$ is defined as

$$||u||_q \;=\; (\langle u,\, u\rangle_{q,\Omega})^{\frac{1}{2}}\,. \tag{1.17}$$

We will also encounter the space $H_0^1(\Omega)$ defined as

$$H_0^1(\Omega) \;=\; \Big\{u \in H^1(\Omega)\;:u|_{\partial\Omega} \;=\; 0\Big\}\,. \tag{1.18}$$

1.4 Structure of the Dissertation

We emphasize that there is some material overlap between chapters since most of them originally appeared as independent works. This means, of course, that one can follow any chapter without having to refer to the previous one.

Chapter 2 is concerned with the solution of a Laplacian problem on an L-shaped domain with Dirichlet boundary conditions, by the SFBIM. Emphasis is placed on the numerical calculations in order to show the high accuracy and rate of convergence of the method.

In Chapter 3 we compare the SFBIM with the p/hp version of the finite element method for a Laplacian problem on an L-shaped domain, with mixed boundary conditions. Again the high accuracy and rate of convergence of this method is demonstrated and numerical results are compared with those obtained by the p/hp finite element method.

In Chapter 4 we develop the SFBIM for the solution of a biharmonic problem with a boundary singularity, namely the Newtonian stick-slip problem of fluid mechanics. Calculations are presented and compared with those obtained with other methods in the literature and with the analytical solution, in order to demonstrate again the robustness and accuracy of the method.

In Chapter 5 the method is extended for the solution of a planar biharmonic problem in fracture mechanics known as Schiff problem. Emphasis again is placed on the numerical

calculations, and comparisons are made with another method.

Chapter 6 contains the analysis of the SFBIM for the case of Laplacian problems. In this Chapter the convergence rate of the method is established and the numerical results of the previous chapters are justified.

Finally, Chapter 7 summarizes this work and suggests future directions.

All the programs developed were written in FORTRAN 77 and compiled on UNIX system on an IBM RS6000, F80 machine.

Chapter 2

The SFBIM for Laplacian problems

In this chapter[1], the singular function boundary integral method is applied for the solution of a Laplace equation problem over an L-shaped domain. The solution is approximated by the leading terms of the local asymptotic solution expansion while the Dirichlet boundary conditions are weakly enforced by means of Lagrange multipliers. Estimates of great accuracy are obtained for the leading singular coefficients, as well as for the Lagrange multipliers. Comparisons are made with recent numerical results in the literature.

2.1 Introduction

In many engineering problems (e.g., fracture mechanics applications [2]), governed by elliptic partial differential equations, boundary singularities arise when there is a sudden change in the boundary conditions (along a smooth boundary) or on the boundary itself. Singularities are known to affect adversely the accuracy and the convergence of standard numerical methods, such as finite-element, boundary-element, finite difference and spectral methods. Grid refinement is the most usual approach in these methods, aiming to improve the convergence rate and accuracy. However, most adaptive grid refinement schemes cause significant computational cost and their efficiency is not always satisfactory. To take into account the form of

[1] The material of this chapter appears in J. Commun. Numer. Meth. Eng. [22].

the singularity more effectively and achieve better accuracy and faster convergence, special methods are often required which incorporate the form of the singularity in the numerical scheme, which is, in general, more effective than mesh refinement (see [41], [54] and [67] and references therein). We should also add here the early works of Symm [70] Papamichael and Symm [58] and Xanthis et al. [78] who developed singular boundary integral methods. Two notable alternatives to singular methods are the *hp* version of the finite element method with geometrically graded meshes [6, 16], and a recently proposed multigrid finite element method on quasi-uniform meshes [12]. The former method has the potential of approximating singular solutions at an exponential rate of convergence, and the latter method is the only known way, to our knowledge, through which the $O(h^p)$ convergence rate can be retained using quasi-uniform meshes on problems with corner singularities (here h is the meshwidth and p the degree of the approximating polynomial).

For the two-dimensional Laplace equation, the asymptotic solution in polar coordinates (r, θ) centered at the singular point, is given by [31]

$$u(r,\theta) = \sum_{j=1}^{\infty} \alpha_j \, r^{\mu_j} \, f_j(\theta) \,, \qquad r,\theta \in V \,, \tag{2.1}$$

where V is a simply connected domain, u is the dependent variable, α_j are the unknown singular coefficients, μ_j are the singularity powers arranged in ascending order, and the functions $f_j(\theta)$ represent the θ-dependence of the eigensolution. Of particular interest to engineering mechanics, especially in the field of elasticity, are the leading singular coefficients α_j of the asymptotic expansion [71]. In fracture mechanics, the first coefficient α_1 represents the so-called opening mode stress intensity factor [35], a measure of the stress intensity near the fracture tip. In the case of Laplacian problems, the singular coefficients are also called generalized stress intensity factors [71] or flux intensity factors [2].

Of special interest are numerical methods for the solution of problems with singularities in which the singular coefficients are calculated directly (see [54], [60] and [78]). In the work of Babuška and Miller [8, 9], the singular coefficients were calculated by *post-processing* the finite element solution. This was done using both an influence function extraction technique and the well-known energy release principle of fracture mechanics. Szabó and Yosibash [72, 73], also used a finite element post-solution operation method, based on the complementary energy principle, in order to calculate the singular coefficients in heat transfer and elasticity problems involving re-entrant corners and abrupt changes in material properties. Their method is applicable in cases where the singularities are characterized by complex eigenpairs. Brenner [13], used a multigrid finite element method for the computation of singular solutions and stress intensity factors with piecewise linear functions on quasi-uniform meshes. This method was shown to be efficient and convergent at the optimal $O(h)$ rate. A review of singular intensity factor evaluation and modelling of singularities in boundary integral methods is provided by Mukhopadhyay et al. [50].

In Refs. [29] and [30], Georgiou and co-workers developed a singular function boundary integral method for the solution of plane Laplacian problems with boundary singularities. This is based on the approximation of the solution by the leading terms of the local solution expansion:

$$\bar{u} \;=\; \sum_{j=1}^{N_\alpha} \bar{\alpha}_j \, W^j \tag{2.2}$$

where N_α is the number of basis functions, and

$$W^j \;\equiv\; r^{\mu_j} \, f_j(\theta) \tag{2.3}$$

are the singular functions which exactly satisfy the governing equation and the boundary conditions along the boundary causing the singularity. Using Galerkin's principle, the Laplace

equation is weighted by the singular functions. The volume integral is then reduced to a boundary one using Green's second identity. The Dirichlet boundary conditions are weakly enforced by means of Lagrange multipliers. Since the final discretized equations are boundary integrals, the dimension of the problem is reduced by one, and thus the computational cost is significantly reduced. The method has been tested on standard Laplacian problems, such as the so-called Motz problem, yielding extremely accurate estimates of the leading singular coefficients. It also exhibits exponential convergence with respect to the number of singular functions [29, 30]. The method of Georgiou and co-workers [29, 30] is applicable only if the expansion (2.2) is valid over the entire domain of solution.

The objective of this chapter is to calculate the singular coefficients in problems involving re-entrant corners (i.e., with L-shaped domains) and compare the results of the singular function boundary integral method [29, 30] with those of Arad et al. [2], and the multigrid finite element results of Brenner [13]. The method of Arad et al. [2] is similar to ours since it is based on the approximation of the solution by the leading terms of the local expansion. An essential difference is that, instead of using Lagrange multipliers for the enforcement of the boundary conditions away from the boundary causing the singularity, they minimize a discrete functional which sums the squares of the distances between the approximation and the boundary conditions at a given number of boundary points. (Note that the same idea was used earlier by Li et al. [40].) Arad et al. [2] used their method to solve the Motz problem and a Laplacian problem over an L-shaped domain. In the case of the Motz problem, their results for the leading singular coefficients are as accurate as those obtained with the singular boundary integral method. However, the convergence of their method with the number of singular functions appears to be much slower [2, 29]. Moreover, their method is computationally more

costly due to the nonlinearity introduced by the least squares method.

Symm [70] solved two other Laplacian problems over L-shaped domains using a singular boundary integral method. The accuracy of his solution was restricted to four significant digits; he did not provide estimates for the leading singular coefficients. In Symm's method, the approximation of the solution is expanded around the singularity into a series of special solutions to the Laplace equation and is regularized by subtracting the four leading terms of the local expansion. The regularized solution is then calculated by the standard boundary element method, under the assumption that it vanishes together with its normal derivative at nodal points near the singular point. As noted by Igarashi and Honma [33], this assumption is valid only when those nodal points are located sufficiently near the singular points. Igarashi and Honma [33] modified Symm's method by relaxing the above assumption, and showed that, in the case of the Motz problem, their method gives almost the same results as those of the Symm's method, when the boundary is subdivided into sufficiently fine elements. However, their results for the leading singular coefficients converge only up to five significant digits and are not as accurate as those calculated by the methods of Olson et al. [54], Li et al. [40], Georgiou et al. [29] and Arad et al. [2]. Igarashi and Honma [33] also applied their method to a Laplacian problem over an L-shaped domain and showed that with their method the convergence in the computation of the capacitance of the solution is improved compared with the method of Wigley [77] which involves a time-consuming iterative procedure. The accuracy of the calculated singular coefficients is restricted to five significant digits.

The outline of this chapter is as follows: in Section 2.2, we consider the Laplacian problem over an L-shaped domain solved by Arad et al. [2], and present the formulation of the singular function boundary integral method. The numerical results are presented in Section 2.3,

where the fast convergence of the method with respect to the number of singular functions is demonstrated, and comparisons are made with the results provided by Arad et al. [2] and by Brenner [13]. The conclusions are summarized in Section 2.4.

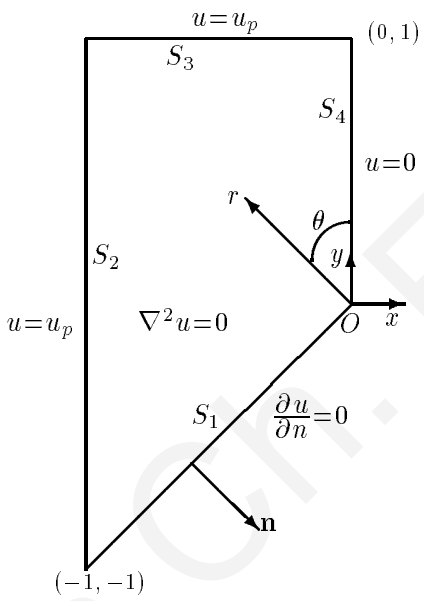

Figure 2.1. *Geometry and boundary conditions of the Laplacian problem.*

2.2 The singular function boundary integral method (SFBIM)

Consider the Laplace equation problem depicted in Figure 2.1. This is equivalent to a Poisson equation problem, $\nabla^2 v=-1$, over an L-shaped domain, with homogeneous Dirichlet boundary conditions along the whole boundary. Note that along boundary parts S_2 and S_3 essential boundary conditions are applied. Due to symmetry about an axis lying along S_1, only half of

the domain is considered. Also, the transformation $v=u+u_p$, where

$$u_p(r,\theta) \;=\; -\frac{r^2}{6\pi}\left[\frac{3\pi}{2} \;+\; 2\ln r\;\sin 2\theta \;+\; \left(2\theta - \frac{3\pi}{2}\right)\cos 2\theta\right] \;, \tag{2.4}$$

leads to the problem shown in Figure 2.1. A singularity arises at $x=y=0$. The local solution is given by

$$u \;=\; \sum_{j=1}^{\infty} \alpha_j \; r^{2(2j-1)/3} \; \sin\left[\frac{2}{3}(2j-1)\theta\right] \;. \tag{2.5}$$

This problem is important in fracture mechanics and the 'stress intensity factor', defined by $2\alpha_1/3$, is of great significance [2].

In the singular function boundary integral method [29], the solution is approximated as a linear combination of the leading singular functions of the local expansion (2.5),

$$\bar{u} \;=\; \sum_{j=1}^{N_a} \bar{\alpha}_j \, W^j \;=\; \sum_{j=1}^{N_a} \bar{\alpha}_j \, r^{2(2j-1)/3} \; \sin\left[\frac{2}{3}(2j-1)\theta\right] \;, \tag{2.6}$$

where N_α is the number of singular functions, and $\bar{\alpha}_j$ are the approximations of the singular coefficients to be calculated. Obviously, the method can be used only if the solution expansion is valid everywhere in the problem domain. Note also that the singular functions W^j satisfy the governing equation over the domain, and the boundary conditions along the parts of the boundary that cause the singularity.

Applying Galerkin's principle, the governing equation is weighted by the singular functions,

$$\int_\Omega \nabla^2 u \, W^i \, dV \;=\; 0 \;, \qquad\qquad i = 1, 2, \ldots, N_\alpha \;. \tag{2.7}$$

Given that the singular functions W^j satisfy the Laplace equation, application of Green's second identity reduces the volume integral into a boundary one:

$$\int_{\partial\Omega} \left(\frac{\partial \bar{u}}{\partial n} \, W^i \;-\; \bar{u} \, \frac{\partial W^i}{\partial n}\right) \, dS \;=\; 0 \;, \qquad\qquad i = 1, 2, \ldots, N_a \;, \tag{2.8}$$

where n denotes the direction normal to the boundary. The above integral is identically zero along boundary parts S_1 and S_4 since the boundary conditions are identically satisfied there (see Figure 2.1). This is an important feature of the singular function boundary integral method since integration over the boundary parts causing the singularity is avoided.

To impose the Dirichlet conditions along the remaining parts, S_2 and S_3, we employ Lagrange multipliers which replace the corresponding normal derivatives. The boundary is then partitioned into three-node elements, i.e., the Lagrange multipliers are expanded in terms of quadratic basis functions, M^j:

$$\lambda_A \;=\; \frac{\partial \bar{u}}{\partial x} \;=\; \sum_{j=1}^{N_{\lambda_A}} \lambda_A^j \, M^j \quad \text{and} \quad \lambda_B \;=\; \frac{\partial \bar{u}}{\partial y} \;=\; \sum_{j=1}^{N_{\lambda_B}} \lambda_B^j \, M^j \,, \tag{2.9}$$

where N_{λ_A} and N_{λ_B} are the numbers of quadratic nodes along boundaries S_2 and S_3, respectively. The nodal values of λ_A and λ_B are additional unknowns of the problem. Finally, the Dirichlet boundary conditions are weighted by the quadratic basis functions. The following system of $N_\alpha + N_{\lambda_A} + N_{\lambda_B}$ equations is thus obtained:

$$-\int_{S_2} \left(\lambda_A W^i - \bar{u} \frac{\partial W^i}{\partial x} \right) dy + \int_{S_3} \left(\lambda_B W^i - \bar{u} \frac{\partial W^i}{\partial y} \right) dx \;=\; 0 \,, \qquad i = 1, 2, \ldots, N_\alpha \,, \tag{2.10}$$

$$-\int_{S_2} \bar{u} \, M^i \, dy \;=\; \int_{S_2} u_p \, M^i \, dy \,, \qquad i = 1, 2, \ldots, N_{\lambda_A} \,, \tag{2.11}$$

$$\int_{S_3} \bar{u} \, M^i \, dx \;=\; -\int_{S_3} u_p \, M^i \, dx \,, \qquad i = 1, 2, \ldots, N_{\lambda_B} \,. \tag{2.12}$$

The above system of equations can be written in the following block form :

$$\begin{bmatrix} K_1 & K_2 & K_3 \\ {K_2}^T & 0 & 0 \\ {K_3}^T & 0 & 0 \end{bmatrix} \begin{bmatrix} A \\ \Lambda_A \\ \Lambda_B \end{bmatrix} = \begin{bmatrix} 0 \\ \Gamma_2 \\ \Gamma_3 \end{bmatrix} \,, \tag{2.13}$$

where sub-matrices K_1, K_2 and K_3 contain the coefficients of the unknowns $\bar{\alpha}_j$, λ_A^j and λ_B^j, respectively, as they are found after expanding Eqs. (2.10) – (2.12) and expressing them in

linear algebraic form. Also, A is the vector of the singular coefficients and Λ_A and Λ_B are the vectors of the Lagrange multipliers. Vectors Γ_2 and Γ_3 contain the values of the RHS of integrals (2.11) and (2.12), respectively. Note that the integrands in Eq. (2.10) are nonsingular and that all integrals are calculated far from the boundaries causing the singularity. It is easily shown that the coefficient matrix is symmetric. Moreover, it is singular if $N_a < N_\lambda$, where $N_\lambda = N_{\lambda_A} + N_{\lambda_B}$.

2.3 Numerical results

In all results presented in this section, boundaries S_2 and S_3 are subdivided uniformly into $2N$ and N elements, respectively. Therefore, the number of Lagrange multipliers is

$$N_\lambda = N_{\lambda_A} + N_{\lambda_B} = 6N + 2 .$$

As in Refs. [29, 30], the integrals in Eqs. (2.10) – (2.12) are calculated numerically by subdividing each quadratic element into 10 subintervals and using a 15-point Gauss-Legendre quadrature for the numerical integration over each subinterval. The symmetry of the coefficient matrix is taken into account during the calculation of its elements, which means that only the elements on and above the main diagonal are calculated.

As pointed out above, the number of the singular functions, N_α, should be much greater than the number of the Lagrange multipliers, N_λ, because otherwise the stiffness matrix is ill-conditioned or singular. On the other hand, large values of N_α should be avoided because the contributions of the high-order singular functions become either negligible (for $r < 1$) or very large (if $r > 1$) beyond the limits double precision can handle.

We performed several series of runs to find the "optimal" values of N_α and N_λ. We varied N_λ from 8 up to 68, and N_α from a value slightly above N_λ up to $3N_\lambda$. For every run plots

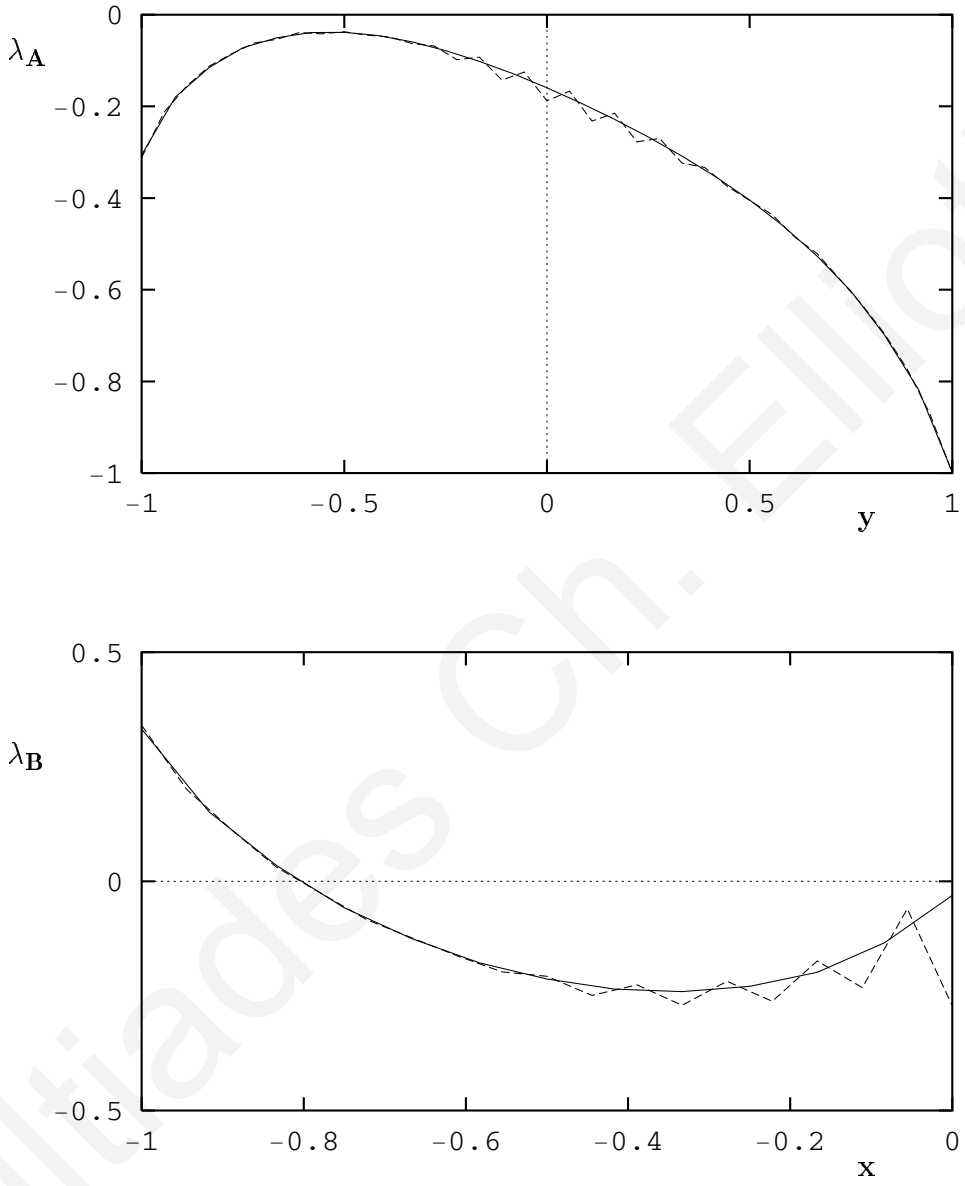

Figure 2.2. *Calculated Lagrange multipliers with N_α=80 and N_λ=38 (solid line) and 56 (dashed line).*

Table 2.1. *Convergence of the solution with N_λ when N_α=80.*

N_λ	α_1	α_2	α_3	α_5	α_{10}	α_{15}
8	0.40187481	0.09363398	-0.0094030	-0.0083099	-0.0002086	-0.0002264
14	0.40192971	0.09364730	-0.0093818	-0.0083517	-0.0005154	-0.0001607
26	0.40193100	0.09364829	-0.0093831	-0.0083588	-0.0005649	-0.0001351
38	0.40193103	0.09364829	-0.0093830	-0.0083588	-0.0005653	-0.0001378
50	0.40193103	0.09364828	-0.0093830	-0.0083589	-0.0005652	-0.0001376
56	0.40193103	0.09364827	-0.0093831	-0.0083588	-0.0005653	-0.0001376
62	0.40193104	0.09364828	-0.0093830	-0.0083589	-0.0005653	-0.0001375

of λ_A vs. y and λ_B vs. x were obtained. In using the singular function boundary integral method, we observed that λ_A and λ_B were characterized by oscillations at all values of N_α when $N_\lambda \geq 44$. This is illustrated in Figure 2.2, where the graphs of λ_A and λ_B are presented for both N_λ=38 and N_λ=56 while keeping the number of singular functions equal to 80. These plots indicate that, indeed, as N_λ approaches the value of N_α, the coefficient matrix becomes ill-conditioned and oscillations appear.

The smoothness of the calculated Lagrange multipliers (checked by plotting λ_A vs. y and λ_B vs. x) provides a good measure of the quality of the solution. Our calculations with different values of N_α and N_λ show that the "optimal" value for N_λ is 38 (see Figure 2.2). For smaller values of N_λ, λ_A and λ_B are still smooth but their approximations are, of course, less satisfactory because the boundary is less refined. In all runs, we observed that for $N_\lambda \leq$ 38 the approximation of the solution was the best possible when the value of N_α was about

Table 2.2. *Convergence of the solution with N_α when N_λ=38.*

N_α	α_1	α_2	α_5	α_{10}	α_{15}
50	0.401931033	0.093648287	-0.00835895	-0.00056546	-0.0001374
60	0.401931032	0.093648288	-0.00835882	-0.00056548	-0.0001377
70	0.401931032	0.093648287	-0.00835882	-0.00056532	-0.0001379
80	0.401931032	0.093648286	-0.00835881	-0.00056534	-0.0001378
90	0.401931033	0.093648287	-0.00835882	-0.00056536	-0.0001378
100	0.401931033	0.093648288	-0.00835882	-0.00056561	-0.0001375
110	0.401931033	0.093648289	-0.00835880	-0.00056535	-0.0001380
120	0.401931033	0.093648285	-0.00835883	-0.00056522	-0.0001381
130	0.401931032	0.093648283	-0.00835885	-0.00056513	-0.0001382

$2N_\lambda$. For $N_\alpha > 2N_\lambda$ the solution deteriorated. This means that there is an upper bound on the number of singular coefficients one should use. In Table 2.1, we show the effect of N_λ on the calculated values of α_1, α_2, α_3, α_5, α_{10} and α_{15}, obtained with N_α=80. The results indicate that the values of singular coefficients converge rapidly with N_λ and that very accurate estimates are obtained, at least for the 15 leading coefficients. Also, one notices that when the difference between N_λ and N_α is large then the solution is not accurate, as emphasized above. In Table 2.2, we show the effect of N_α on the values of some singular coefficients calculated with N_λ=38. The method exhibits exponential convergence with respect to N_α. However, for values of N_α greater than 90, the accuracy of the solution appears to start deteriorating due to the fact that the system becomes ill-contioned.

Table 2.3. *Converged values of the leading singular coefficients with N_λ=38 and N_α=80.*

i	α_i
1	0.40193103
2	0.09364829
3	-0.0093830
4	-0.0298851
5	-0.0083588
6	-0.0047302
7	-0.0015451
8	-0.001098
9	-0.000719
10	-0.000565
11	-0.000395
12	-0.000296
13	-0.000219
14	-0.000173
15	-0.000138

In Table 2.3, we tabulate the converged values of the singular coefficients calculated with "optimal" choices of N_α=80 and N_λ=38. Evidently, the contributions of the higher order terms are progressively vanishing. The CPU time required for the above run is 2.14 s on an IBM RS6000 (Processor type: Power PC 604e/375 MHz).

Note that the value 0.40193103 of the leading singular coefficient is accurate to the eighth significant digit (this accuracy is obtained even for N_α=50 and N_λ=38), while Arad et al. [2] provide the value 0.401920085 which is accurate only to the fourth significant digit. (Arad et al. [2] have not studied the convergence of their method in the case of the present problem.) Brenner [13] reported for the first singular coefficient the values 0.40193219, 0.40193032 and 0.40193057, which are accurate to the fifth decimal digit. These values have been obtained by the standard full multigrid algorithm and two modified full multigrid algorithms, respectively (see [13] for more details). Neither Arad et al. [2] nor Brenner [13] provide numerical estimates for the higher-order singular coefficients.

As a conclusion, using Lagrange multipliers for the enforcement of the essential boundary conditions is more effective than the minimization of a least-squares functional suggested by Arad et al. [2]. It is also computationally less costly, since it preserves the linearity of the problem. Finally, when compared to the multigrid methods from Ref. [13], the singular function boundary integral method yields more accurate estimates not only for the first but also for the other leading singular coefficients.

2.4 Conclusions

A Laplace equation problem over an L-shaped domain has been solved using the singular function boundary integral method. The calculated values of the singular coefficients are of great accuracy. Comparisons between the results of the present method and those of the method of Arad et al. [2] indicate that the singular boundary integral method converges faster with respect to the number of singular functions and yields more accurate estimates for the leading singular coefficients.

In the following chapters we will see that the method can be applied to other singular problems with a different shape of the domain and with different singularities, provided that the local solution expansion is known and holds over the entire domain.

Chapter 3

Comparisons with the p/hp FEM

In this chapter[1] we solve a Laplacian problem over an L-shaped domain using the singular function boundary integral method and the p/hp finite element method. In the former method, the solution is approximated by the leading terms of the local asymptotic solution expansion, and the unknown singular coefficients are calculated directly. In the latter method, these coefficients are computed by post-processing the finite element solution. The predictions of the two methods are discussed and compared with recent numerical results in the literature.

3.1 Introduction

In the past few decades, many different methods have been proposed for the numerical solution of plane elliptic boundary value problems with boundary singularities, aiming at improving the accuracy and resolving the convergence difficulties that are known to appear in the neighborhood of such singular points. These methods range from special mesh-refinement schemes to sophisticated techniques that incorporate, directly or indirectly, the form of the local asymptotic expansion, which is known in many occasions. In polar coordinates (r, θ) centered at the

[1] The material in this chapter is in press in J. Appl. Math. Comput. [23].

singular point, the local solution is of the general form

$$u(r,\theta) \;=\; \sum_{j=1}^{\infty} a_j \, r^{\mu_j} \;\; f_j(\theta)\,, \tag{3.1}$$

where μ_j are the eigenvalues and f_j are the eigenfunctions of the problem, which are uniquely determined by the geometry and the boundary conditions along the boundaries sharing the singular point. The singular coefficients α_j, also known as generalized stress intensity factors [71] or flux intensity factors [2], are determined by the boundary conditions in the remaining part of the boundary. Knowledge of the singular coefficients is of importance in many engineering applications.

An exhaustive survey of treatment of singularities in elliptic boundary value problems is provided in the recent article by Li and Lu [43], who classify the proposed methods into three categories: methods involving local refinement, methods involving singular functions supplementing the approximation spaces of standard numerical methods, and combined methods which incorporate local singular and analytical solutions. A review of singular intensity factor evaluation and modelling of singularities in boundary integral methods is provided by Mukhopadhyay et al. [50].

In the Finite Element Method (FEM), which is the most commonly used method for solving structural mechanics problems, the singular coefficients are calculated by post-processing the numerical solution. Generally speaking, the most effective versions of the FEM are the high-order p and hp versions, in which instead of simply refining the mesh, convergence is achieved by: (i) increasing the degree of the piecewise polynomials in the case of the p version, and (ii) by increasing p **and** decreasing h in the case of the hp version. The reason for the success of these methods is that they are able to approximate singular components of the solution to elliptic boundary value problems (that arise, for example, at corners of the domain) very efficiently. For

instance, the *hp* version, over appropriately designed meshes, approximates these singularities at an *exponential* rate of convergence ([6]). Different solution post-processing methods for the calculation of the singular coefficients from the finite element solution have been proposed by Babuška and Miller [8, 9], Szabó and Yosibash [72, 73], and Brenner [13].

In the past few years, Georgiou and co-workers [29, 30, 22] developed the Singular Function Boundary Integral Method (SFBIM), in which the unknown singular coefficients are calculated directly. The solution is approximated by the leading terms of the local asymptotic solution expansion and the Dirichlet boundary conditions are weakly enforced by means of Lagrange multipliers. The method has been tested on standard Laplacian problems, yielding extremely accurate estimates of the leading singular coefficients, and exhibiting exponential convergence with respect to the number of singular functions.

The objective of the present chapter is to compare the predictions of the SFBIM against those of the *p*/*hp* version of the FEM. We consider as a test problem the Laplacian problem over an L-shaped domain solved by Igarashi and Honma [33]. They used a modified version of the singular boundary integral method proposed by Symm [70]. The approximation of the solution around the singularity is expanded into a series of special harmonic functions and is regularized by subtracting the four leading terms of the local expansion. It is then calculated by the standard boundary element method. The accuracy of the calculated singular coefficients is restricted to five significant digits. As shown below, the predictions of both the SFBIM and the *p*/*hp*-FEM are of much higher accuracy.

The outline of this chapter is as follows: in Section 2, we present the SFBIM in the case of a general Laplacian problem over an arbitrary domain with a boundary singularity. In Section 3, the SFBIM is applied to the test problem. In Sections 4 and 5, the results of the SFBIM and

the p/hp-FEM, respectively, are presented and discussed. Comparisons are also made with the results provided by Igarashi and Honma [33]. The conclusions are summarized in Section 6.

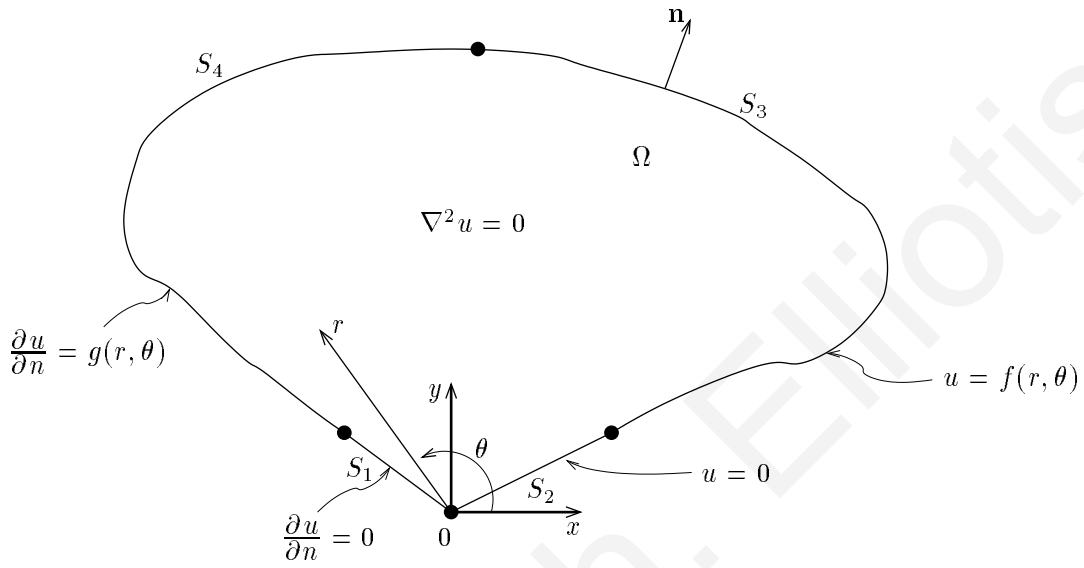

Figure 3.1. *A Laplacian problem with one singular point.*

3.2 The singular function boundary integral method (SFBIM)

In order to present and formulate the singular function boundary integral method, we consider the rather general Laplace equation problem over a two-dimensional domain Ω, shown in Figure 3.1. This is characterized by the presence of a boundary singularity at the corner O, formed by the straight boundary segments S_1 and S_2. With the exception of O, the boundary of Ω is everywhere smooth. In the remaining parts of the boundary, either Dirichlet or Neumann boundary conditions apply. Without loss of generality, the following problem is considered:

$$\nabla^2 u = 0 \qquad \text{in } \Omega\,, \tag{3.2}$$

with

$$\left.\begin{array}{lll} \dfrac{\partial u}{\partial n} = 0 & \text{on} & S_1 \\ u = 0 & \text{on} & S_2 \\ u = f(r,\theta) & \text{on} & S_3 \\ \dfrac{\partial u}{\partial n} = g(r,\theta) & \text{on} & S_4 \end{array}\right\}, \tag{3.3}$$

where $\partial\Omega = S_1 \cup S_2 \cup S_3 \cup S_4$, and f and g are given functions such that no other boundary singularity is present.

The asymptotic solution in polar coordinates (r, θ) centered at the singular point, is given by [31]

$$u(r,\theta) = \sum_{j=1}^{\infty} \alpha_j \, r^{\mu_j} \, f_j(\theta) \,, \qquad (r,\theta) \in \Omega \,, \tag{3.4}$$

where α_j are the unknown singular coefficients, μ_j are the singularity powers arranged in ascending order, and the functions $f_j(\theta)$ represent the θ-dependence of the eigensolution.

The SFBIM [29, 30, 22] is based on the approximation of the solution by the leading terms of the local solution expansion:

$$\bar{u} = \sum_{j=1}^{N_\alpha} \bar{\alpha}_j \, W^j \tag{3.5}$$

where N_α is the number of basis functions, and

$$W^j \equiv r^{\mu_j} \, f_j(\theta) \tag{3.6}$$

are the singular functions. It should be noted that this approximation is valid only if Ω is a subset of the convergence domain of the expansion (3.4). If not, it may still be possible to use this approach provided there exist (possibly different) expansions similar to (3.4) in different sectors of the domain Ω (see e.g. [40]).

Application of Galerkin's principle gives the following set of discretized equations:

$$\int_\Omega \nabla^2 u \, W^i \, dV = 0 \,, \qquad i = 1, 2, \ldots, N_\alpha \,. \tag{3.7}$$

By using Green's second identity and taking into account that the singular functions, W^i, are harmonic, the above volume integral is reduced to a boundary one:

$$\int_{\partial\Omega} \left(\frac{\partial \bar{u}}{\partial n} W^i \; - \; \bar{u} \, \frac{\partial W^i}{\partial n} \right) dS \; = \; 0 \, , \qquad\qquad i = 1, 2, \ldots, N_a \, . \tag{3.8}$$

The dimension of the problem is, thus, reduced by one, which leads to a considerable reduction of the computational cost. Since, now, W^i exactly satisfy the boundary conditions along S_1 and S_2, the above integral along these boundary segments is identically zero. Therefore, we have:

$$\int_{S_3} \left(\frac{\partial \bar{u}}{\partial n} W^i \; - \; \bar{u} \, \frac{\partial W^i}{\partial n} \right) dS + \int_{S_4} \left(W^i \, \frac{\partial \bar{u}}{\partial n} \; - \; \bar{u} \, \frac{\partial W^i}{\partial n} \right) dS \; = \; 0 \, , \quad i = 1, 2, \ldots, N_a \, . \tag{3.9}$$

To impose the Neumann condition along S_4, we simply substitute the normal derivative by the known function g [Eq. (3.3)]. The Dirichlet condition along S_3 is imposed by means of a Lagrange multiplier function, λ, replacing the normal derivative. The function λ is expanded in terms of standard, polynomial basis functions M^j,

$$\lambda \; = \; \frac{\partial \bar{u}}{\partial n} \; = \; \sum_{j=1}^{N_\lambda} \lambda_j \, M^j , \tag{3.10}$$

where N_λ represents the total number of the unknown discrete Lagrange multipliers (or, equivalently, the total number of Lagrange-multiplier nodes) along S_3. The basis functions M^j are used to weight the Dirichlet condition along the corresponding boundary segment S_3. We thus obtain the following system of $N_\alpha + N_\lambda$ discretized equations:

$$\int_{S_3} \left(\lambda \, W^i \; - \; \bar{u} \, \frac{\partial W^i}{\partial n} \right) dS - \int_{S_4} \bar{u} \, \frac{\partial W^i}{\partial n} \, dS \; = \; - \int_{S_4} W^i \, g(r, \theta) \, dS \, , \quad i = 1, 2, \ldots, N_a \, , \tag{3.11}$$

$$\int_{S_3} \bar{u} \, M^i \, dS \; = \; \int_{S_3} f(r, \theta) \, M^i \, dS , \qquad\qquad i = 1, 2, \ldots, N_\lambda \, . \tag{3.12}$$

It is easily shown that the linear system of Eqs. (3.11) and (3.12) is symmetric. This can be

written in the following block form:

$$\begin{bmatrix} K_1 & K_2 \\ K_2^T & O \end{bmatrix} \begin{bmatrix} A \\ \Lambda \end{bmatrix} = \begin{bmatrix} F_1 \\ F_2 \end{bmatrix} \tag{3.13}$$

where A is the vector of the unknown singular coefficients, $\bar{\alpha}_i$, Λ is the vector of the unknown Lagrange multipliers λ_i, submatrices K_1 and K_2 contain the coefficients of the unknowns. Obviously, K_1 is symmetric. Vectors F_1 and F_2 contain the RHS contributions of Eqs. (3.11) and (3.12), respectively. It should be noted that the integrands in Eq. (3.11) are non-singular and all integrations are carried out far from the boundaries causing the singularity.

3.3 Application of the SFBIM to a test problem

We consider the same Laplacian problem over an L-shaped domain as in [33]; this is shown in Figure 3.2. The local solution around the singularity at $x=y=0$ is given by

$$u \;=\; \sum_{j=1}^{\infty} \alpha_j \, r^{2(2j-1)/3} \, \sin\left[\frac{2}{3}(2j-1)\,\theta\right] \;. \tag{3.14}$$

Taking into account the symmetry of the problem, we consider only half of the domain and note that even-numbered coefficients are zero. Therefor, u may be written as follows:

$$u \;=\; \sum_{j=1}^{\infty} \alpha_j \, W^j \;, \tag{3.15}$$

where

$$W^j \;=\; r^{2(4j-3)/3} \, \sin\left[\frac{2}{3}(4j-3)\,\theta\right] \tag{3.16}$$

are the singular functions.

Setting $f=1$ and $g=0$, Eqs. (3.11) and (3.12) are simplified as follows:

$$-\int_{S_3} (\lambda \, W^i \;-\; \bar{u} \, \frac{\partial W^i}{\partial x}) \, dy - \int_{S_4} \bar{u} \, \frac{\partial W^i}{\partial y} \, dx \;=\; 0 \;, \qquad i = 1, 2, \cdots, N_\alpha \;, \tag{3.17}$$

$$\int_{S_3} \bar{u}\, M^i\, dy \;=\; \int_{S_3} M^i\, dy\,, \qquad\qquad i = 1, 2, \cdots, N_\lambda\,. \tag{3.18}$$

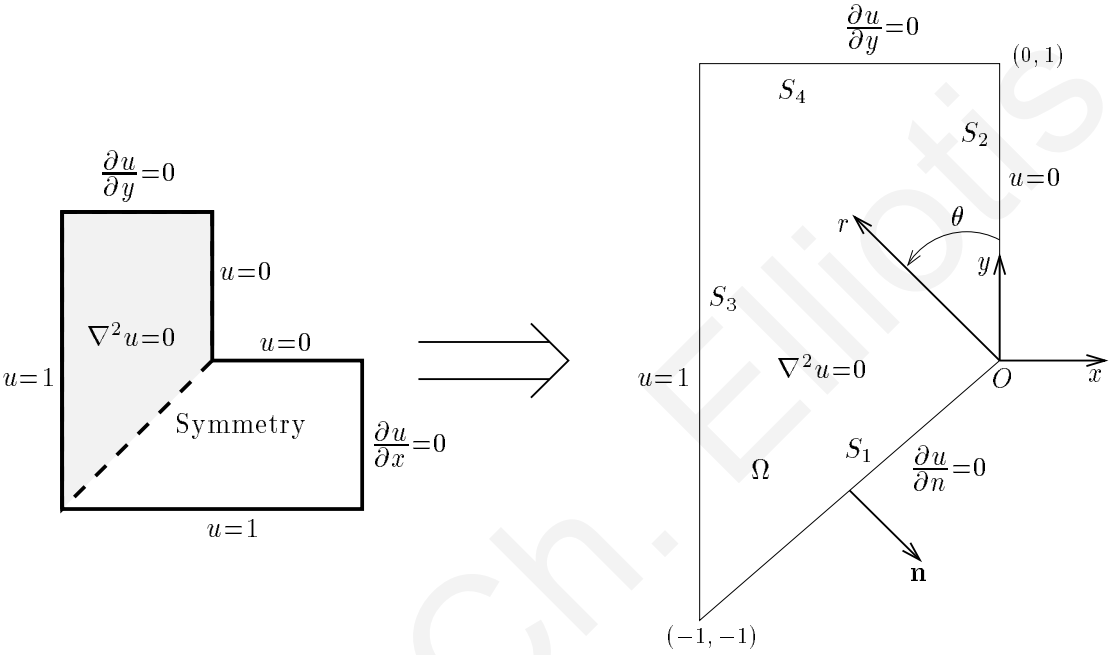

Figure 3.2. *Geometry and boundary conditions of the test problem.*

In [33], the quantity

$$C := 2 \int_{S_3 \cup S_4} \frac{\partial u}{\partial n}\, dS \tag{3.19}$$

referred to as the capacitance, was of interest. Note that due to the geometry and boundary conditions, (3.19) reduces to

$$C \;=\; -2 \int_{-1}^{1} \left.\frac{\partial u}{\partial x}\right|_{x=-1} dy\,. \tag{3.20}$$

3.4 Numerical results with the SFBIM

The Lagrange multiplier function λ used to impose the Dirichlet condition along S_3 is expanded in terms of quadratic basis functions. Boundaries S_3 and S_4 are subdivided, respectively, into

$2N$ and N quadratic elements of equal size. Thus, the number of Lagrange multipliers is N_λ=$4N$+1. The integrals in Eqs. (3.17) and (3.18) involve the singular functions that are not polynomial and become highly oscillatory as N_α increases. These are calculated numerically by subdividing each quadratic element into 10 subintervals and using a 15-point Gauss-Legendre quadrature over each subinterval. In computing the coefficient matrix, its symmetry is taken into account.

Several series of runs were performed in order to obtain the "optimal" values of N_α and N_λ. Our search was guided by the fact that N_λ should be large enough in order to assure accurate integrations along the boundary (which is divided into smaller elements) but much smaller than N_α in order to avoid ill-conditioning of the stiffness matrix. On the other hand, N_α cannot be very high, given that the computer accuracy cannot handle the contributions of the higher-order singular functions which become very small for $r < 1$ or very large for $r > 1$. Hence, N_λ was varied from 5 up to 65 and N_α from a value slightly above N_λ up to 100.

The convergence of the solution with the number of Lagrange multipliers is shown in Table 3.1, where we tabulate the values of the five leading singular coefficients and the capacitance C calculated with N_α=60. We observe that the values of the singular coefficients converge rapidly with N_λ, up to N_λ=41, and that very accurate estimates are obtained. For higher values of N_λ, however, signs of divergence are observed, due to the ill-conditioning of the stiffness matrix. In addition to the divergence of the singular coefficients, another manifestation of ill-conditioning is the appearance of wiggles on the calculated Lagrange multiplier function [22]. The quality of the solution for N_α=60 and N_λ=41 was checked by plotting λ as a function of y (Figure 3.3) and verifying that λ is smooth and free of oscillations.

The values of the leading singular coefficients and the capacitance C calculated for N_λ=41

Table 3.1. *Convergence of the solution with N_λ; SFBIM with N_α=60.*

N_λ	α_1	α_2	α_3	α_5	C
5	1.12797118414119	0.16993982990692	-0.02304003771255	0.00096430271538	2.5585187
9	1.12798030920688	0.16993376833638	-0.02304036610151	0.00091656933158	2.5585226
17	1.12798039995306	0.16993386409437	-0.02304096729203	0.00091515473431	2.5585229
25	1.12798040098244	0.16993386632558	-0.02304097349784	0.00091515689483	2.5585231
33	1.12798040105726	0.16993386650219	-0.02304097400496	0.00091515710753	2.5585226
41	1.12798040105939	0.16993386650225	-0.02304097399348	0.00091515709910	2.5585231
49	1.12798038900362	0.16993384321933	-0.02304098436389	0.00091522372105	2.5556215

Table 3.2. *Convergence of the solution with N_α; SFBIM with N_λ=41.*

N_α	α_1	α_2	α_3	α_5	C
45	1.12798046929652	0.16993391450191	-0.02304128110013	0.00091337482002	2.5467734
50	1.12798040111620	0.16993386693468	-0.02304097583682	0.00091509465304	2.5585230
55	1.12798040105939	0.16993386650225	-0.02304097399348	0.00091515709909	2.5585231
60	1.12798040105939	0.16993386650225	-0.02304097399348	0.00091515709910	2.5585231
65	1.12798040105939	0.16993386650223	-0.02304097399351	0.00091515709917	2.5585231
70	1.12798040105938	0.16993386650176	-0.02304097399413	0.00091515710049	2.5585230
75	1.12798040105929	0.16993386650304	-0.02304097399577	0.00091515709264	2.5585230
80	1.12798040105953	0.16993386650246	-0.02304097399337	0.00091515710302	2.5585232

Table 3.3. *Converged values of the singular coefficients; SFBIM with N_λ=41 and N_α=60.*

i	α_i	Ref. [33]
1	1.12798040105939	1.1280
2	0.16993386650225	0.1699
3	-0.02304097399348	-0.0230
4	0.0034711966582	0.0035
5	0.0009151570991	0.0009
6	-0.0001128038345	
7	0.0000877165245	
8	0.0000277603137	
9	-0.0000044161578	
10	0.0000027539457	
11	0.0000009219619	
12	-0.0000001554459	
13	0.0000001088408	
14	0.0000000379699	
15	-0.0000000066619	
16	0.000000004711	
17	0.00000000168	
18	-0.00000000030	
19	0.00000000022	
20	0.00000000008	
C	2.5585231	2.5585

and various values of N_α are shown in Table 3.2. Exponential convergence with respect to N_α is observed(see Figure 3.4 ahead) and extremely accurate estimates of the singular coefficients are obtained. Our calculations with different values of N_α and N_λ show that the "optimal" values are N_α=60 and N_λ=41. In Table 3.3, the converged values of the singular coefficients calculated with these "optimal" choices of N_α and N_λ are presented. The CPU time required for the above run is 1.6 s on an IBM RS6000 (Processor type: Power PC 604e/375 MHz).

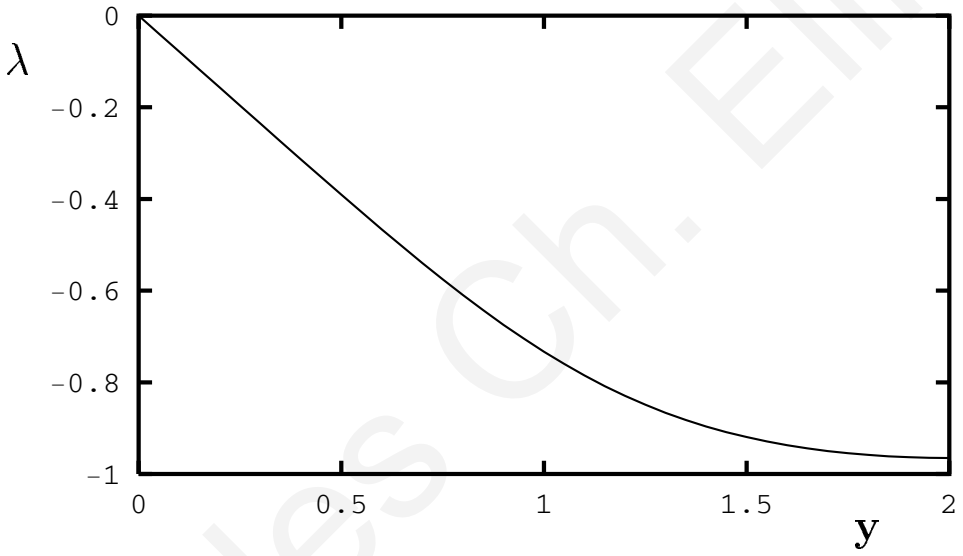

Figure 3.3. *Calculated Lagrange multipliers with* N_α=60 *and* N_λ=41.

In Table 3.3, we see that the contributions of the higher-order terms are progressively vanishing. Note that the converged value of α_1 (1.12798040105939) is accurate to fifteen significant digits, while the value provided by Igarashi and Honma [33] (1.1280) is accurate only to five significant digits. The improved accuracy is also reflected on the calculated value of the capacitance, which is converged to eight significant digits, C=2.5585231.

Finally, in Figure 3.4, we plot the errors in the calculated values of the leading singular

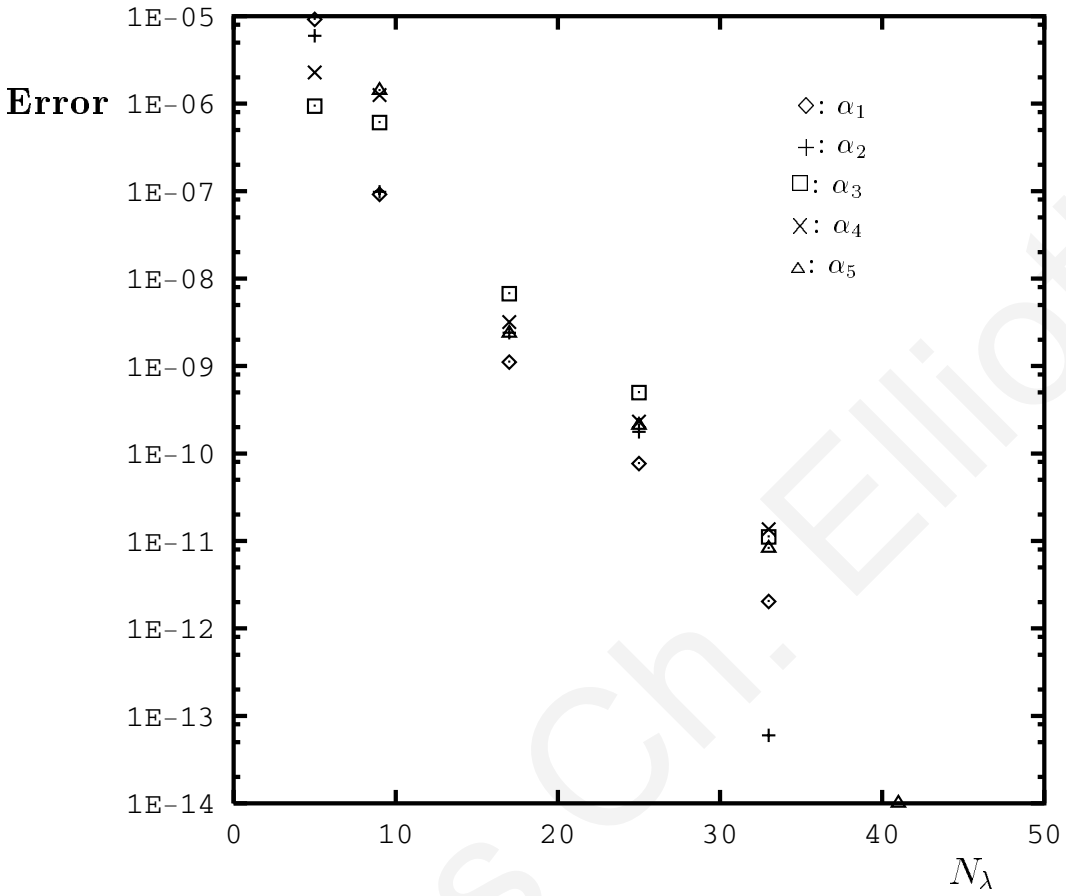

Figure 3.4. *Convergence of the SFBIM with N_λ; N_α=60.*

coefficients for N_α=60 versus the number of Lagrange multipliers. The errors are based on the converged values tabulated in Table 3.3. It is clear that the SFBIM converges exponentially with N_λ, and the error is reduced rapidly down to machine accuracy.

3.5 Numerical results with the p/hp FEM

In this section we present the results of solving the same test problem, using the p/hp version of the FEM over a geometrically graded mesh seen in Figure 3.5. This is, to our knowledge, the most effective technique for approximating the solution to elliptic boundary value problems

with corner singularities in the context of the FEM. We refer to [71] for more details on corner singularities and geometrically graded meshes in conjunction with the p and hp versions of the FEM. Once the solution u_{FEM} is obtained, the singular coefficients α_j, are computed as a post-solution operation. In particular, the algorithm for computing the α_j's is based on an L^2 projection of u_{FEM} into the space of functions characterized by the asymptotic expansion in terms of the eigenpairs (which are computed using a modified Steklov method). See [72, 73] for details.

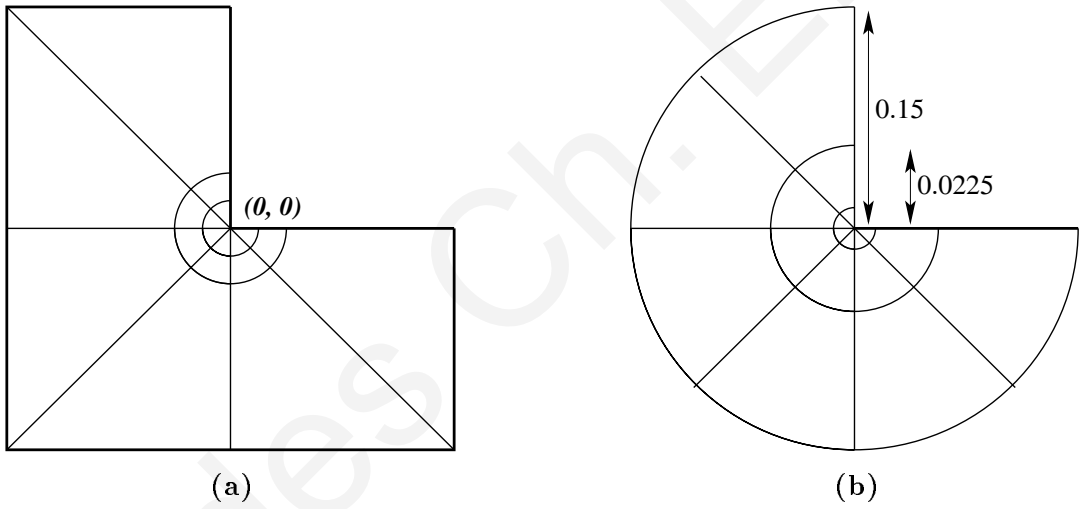

Figure 3.5. *(a) Geometrically graded mesh over the domain Ω; (b) Mesh detail near the re-entrant corner.*

The computations were performed using the commercial FEM package STRESSCHECK (E.S.R.D. St. Louis, MO) on an IBM Pentium III machine. Since this is a p version package, the geometrically graded mesh was constructed a priori and the polynomial shape functions were taken to have degree $p = 1, ..., 8$, uniformly over all elements in the (fixed) mesh. The CPU time was approximately 9 seconds for the calculation of u_{FEM} and about 2 seconds for

Table 3.4. *Values of the potential energy and the percentage relative error in the p/hp FEM.*

p	DOF	Energy	Error (%)
1	10	1.3385078	21.52
2	39	1.2819648	4.60
3	74	1.2806200	3.26
4	127	1.2793571	0.85
5	198	1.2792877	0.43
6	287	1.2792738	0.28
7	394	1.2792690	0.20
8	519	1.2792667	0.15

the calculation of the α_j's. Table 3.4 shows the potential energy as well as the (estimated) percentage relative error in the energy norm,

$$Error = 100 \times \frac{||u_{EX} - u_{FEM}||_{E(\Omega)}}{||u_{EX}||_{E(\Omega)}},$$

indicating that u_{FEM} is computed accurately. Table 3.5 shows the computed singular coefficients, which were obtained using u_{FEM} corresponding to $p = 8$. These results show that the p version of the FEM (on geometrically graded meshes) seems to perform quite well when compared with the results obtained using other methods found in the literature.

The capacitance, C, was calculated from the solution corresponding to $p = 8$. Since u_{FEM} is a polynomial of degree 8 in x and y, we see from (3.20) that a 5-point Gaussian quadrature formula is sufficient to exactly evaluate the integral involved. We obtained $C_{FEM} = 2.557256$, an approximation which is not as good as that obtained using the SFBIM. We believe this is

Table 3.5. *Values of the leading singular coefficients obtained with the p/hp FEM.*

i	α_i, DOF=519	α_i, DOF=691
1	1.12797960	1.12798010
2	0.16993396	0.16993387
3	-0.0230434	-0.0230419
4	-0.0034780	-0.0034755
5	0.0009115	0.0009126
C	2.557256	2.558588

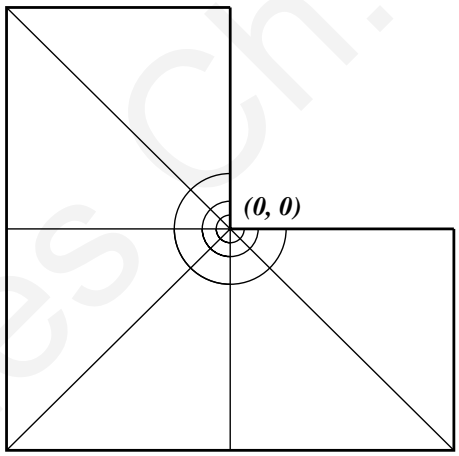

Figure 3.6. *Refined mesh.*

due to the *pollution* effects that are influencing the extraction of the data of interest (see e.g. [71]). Pollution is a phenomenon that occurs when singularities are present in the solution of an elliptic boundary value problem. These singularities cause the numerical method to yield inaccurate results *away* from the point of singularity (as is the case here), when certain

quantities of engineering interest are computed. The p version of the FEM is much more susceptible to pollution effects than the h and hp versions. We repeated the calculation using a more refined mesh near the re-entrant corner, as seen in Figure 3.6. The newly computed singular coefficients are shown in Table 3.5 and the capacitance is recomputed as $C_{FEM} = 2.558588$, which is a much better approximation. The refined mesh required 691 degrees of freedom (for $p = 8$), as opposed to 519 used before, and the CPU time increased by 1 second.

3.6 Conclusions

We have solved a Laplacian problem over an L-shaped domain using both the SFBIM and the p/hp finite element method, and studied the convergence of the solution with the numbers of singular functions and of Lagrange multipliers, and the number of degrees of freedom, respectively. With the SFBIM the leading singular coefficients of (3.5) are calculated explicitly, whereas with the p/hp-FEM they are calculated by postprocessing the numerical solution.

Fast convergence is achieved and highly accurate results are obtained with both methods, which perform considerably better than other techniques found in the literature (e.g. that of Igarashi and Honma [33]). Given that there are no known exact values for the singular coefficients, the very good agreement between the SFBIM and the p/hp FEM serves as *validation* for the computational results presented here. We should point out that, in terms of efficiency, the SFBIM is a better choice, since the singular coefficients are computed directly and no post-processing is necessary. On the other hand, the FEM can be applied to a much wider class of problems than those that can efficiently and effectively be handled by the SFBIM. Finally, we should mention that in Chapter 6 we present the mathematical theory that establishes the observed exponential convergence rate of the SFBIM.

Chapter 4

Solution of the stick-slip problem

In this chapter, the singular function boundary integral method (SFBIM) is developed for solving biharmonic problems with boundary singularities[1]. The method is applied to the Newtonian stick-slip flow problem. The streamfunction is approximated by the leading terms of the local asymptotic solution expansion which are also used to weight the governing biharmonic equation in the Galerkin sense. By means of the divergence theorem the discretized equations are reduced to boundary integrals. The Dirichlet boundary conditions are weakly enforced by means of Lagrange multipliers, the values of which are calculated together with the singular coefficients. The method converges very fast with the number of singular functions and the number of Lagrange multipliers, and accurate estimates of the leading singular coefficients are obtained. Comparisons with the analytical solution and results obtained with other numerical methods are also made.

4.1 Introduction

In the past few decades, many different numerical methods have been proposed for the treatment of boundary singularities in plane elliptic boundary value problems, in order to improve the solution accuracy and resolve the convergence difficulties occurring in the neighborhood

[1] The material of this chapter appears in [24].

of such singular points. These methods range from special mesh-refinement schemes to sophisticated techniques that incorporate, directly or indirectly, the form of the local asymptotic expansion, which is known in many occasions. An exhaustive survey of treatment of singularities in elliptic boundary value problems is provided in the recent articles by Li and Lu [43], by Dosiyev [21] and by Shi et al. [68]. Knowledge of the coefficients appearing in the local solution expansion is often desired in many engineering applications. These coefficients, referred to as *singular coefficients* or *generalized stress intensity factors* [71], are calculated either directly (see [22] and references therein) or by post-processing the numerical solution [9, 73].

In the past few years, we have developed the Singular Function Boundary Integral Method (SFBIM) for Laplacian problems with boundary singularities [22, 29, 30], in which the unknown singular coefficients are calculated directly. The solution is approximated by the leading terms of the local asymptotic solution expansion which are also used to weight the governing equation in the Galerkin sense. With a double application of Green's theorem, the discretized equations are reduced to boundary integrals over those parts of the boundary that do not involve the singular point. The Dirichlet boundary conditions are weakly enforced by means of Lagrange multipliers, which are calculated simultaneously with the singular coefficients. The method has been tested on standard Laplacian problems, yielding extremely accurate estimates of the leading singular coefficients, and exhibiting exponential convergence with respect to the number of singular functions [22, 29, 30].

The objective of the present chapter is to extend the SFBIM to biharmonic problems with boundary singularities. For that purpose we have chosen to solve the Newtonian planar stick-slip problem, which is a benchmark Stokes flow problem used to test various numerical methods proposed in the literature for the solution of viscous and non-Newtonian flows, such as

the extrudate-swell flow. This concerns the extrusion of a fluid from a slit or an axisymmetric die into the atmosphere. Due to the relaxation of stresses, the fluid swells as it exits the die. Swelling is particularly pronounced in the case of elastic fluids, but it is also observed in the Newtonian case, provided that the Reynolds number is sufficiently low. The stick-slip problem is a special case of the extrudate-swell problem: in the limit of infinite surface tension, no swelling occurs, and the free surface becomes flat (in the case of slit die). A boundary inverse-square-root stress singularity appears at the exit of the die due to the sudden change of the boundary conditions from the wall to the flat free surface, which is the cause of numerical difficulties that become more severe in the case of non-Newtonian or viscoelastic flows [74, 4].

The creeping planar stick-slip problem was solved analytically by Richardson who used a Wiener-Hopf technique [62] and by Sturges who used the method of matched eigenfunction expansions [69]. Both methods have been used by Trogdon and Joseph [76] to obtain analytical solutions for the round stick-slip problem.

Direct estimates of the leading singular coefficients in the case of the planar stick-slip problem have been reported by various researchers who employed a variety of numerical methods and techniques to incorporate the leading terms of the local asymptotic solution (which is equivalent to subtracting the leading terms of the singularity). Kelmanson employed a direct modified boundary integral equation method (BIEM) incorporating a subtraction of the singular terms technique that accelerated the rate of convergence, and reported estimates for the leading four coefficients [38]. Estimates for these coefficients have also been reported by Georgiou et al. [28] who solved the problem using the integrated singular basis function method (ISBFM). In this method, the singular functions are directly subtracted from the original problem formulation which leads to a modified problem with the regular part of the solution and

the singular coefficients as unknowns. The smooth problem is then solved using finite elements. The integrals involving singular contributions are reduced to boundary ones by means of a double integration by parts and the original essential boundary conditions are enforced by means of Lagrange multipliers. These two features are encountered also with the SFBIM that we propose in the present work. However, the two methods are quite different for the following reasons:

(a) With the ISBFM the problem is formulated in terms of the two velocity components and the pressure, while with the SFBIM it is formulated in terms of the streamfunction.

(b) In the ISBFM the unknown fields are the smooth parts of the primary variables which are approximated by means of standard polynomial basis functions. In the SFBIM, however, there is no subtraction of the singularity and the unknown field, i.e. the streamfunction, is approximated as a linear combination of the leading terms of the local asymptotic expansion. It is clear that such an approximation is valid only if the domain of the problem falls within the domain of convergence of the local solution.

(c) In the ISBFM, the discretized equations are double integrals, whereas in the SFBIM, these are boundary ones. Hence, the dimension of the problem is reduced by one, and the computational cost of the SFBIM is considerably lower than that of the ISBFM.

Karageorghis [37] obtained direct estimates of the first four singular coefficients using a modified method of fundamental solutions (MFS) that was based on the direct subtraction of the leading terms of the singular local solution. A similar method was also used by Poullikas et al. [61] who subtracted only the leading term of the singular local solution, assuming that its form is unknown and part of the problem.

Georgiou et al. [27] developed a singular finite element method (SFEM), in which special

elements incorporating the radial form of the local singularity expansion are employed in a small region around the singular point, in order to resolve the convergence difficulties and improve the accuracy of the global solution. They obtained more accurate results than those achieved with ordinary elements and calculated the leading singular coefficients by post-processing the finite element solution. A similar post-processing technique has been employed by Salamon et al. [64] who obtained accurate results near the singularity using high resolution finite elements with quasi-orthogonal mesh generation and local, adaptive mesh refinement with irregular imbedded elements. Ngamaramvaranggul and Webster [51] developed a semi-implicit Taylor-Galerkin/pressure-correction finite element method (STGFEM) for free surface flows and applied it to various Newtonian flows including the plane and axisymmetric stick-slip and extrudate-swell problems. More recently, Normandin et al. [53] solved the Newtonian stick-slip problem using a finite element Galerkin technique associated with stream-tube analysis and presented comparisons of the computed streamlines with previous results.

The stick-slip flow of non-Newtonian and viscoelastic fluids has also received considerable attention due to the convergence difficulties associated with the presence of the singularity and the relevance to the extrudate-swell problem. We discuss briefly the literature with emphasis on works reporting results for the Newtonian case. Tanner and Huang [74] applied the J-integral method for solving the planar stick-slip flow of power-law fluids, corrected the numerical estimate of singularity strength in Richardson's Newtonian analysis [62], and calculated the first singular coefficient for various power-law exponents. Owens and Phillips [55] presented solutions of the planar stick-slip problem obtained with a spectral domain decomposition method (DDM) for an Oldroyd-B fluid. In a subsequent article, they applied an algebraic mapping to treat the flow domain without truncation and computed the singular co-

efficients using a post-processing technique [56]. Baaijens investigated the numerical stability of a discontinuous Galerkin method using a Phan-Thien-Tanner model incorporating monotonicity enforcement [3] and applied low-order discontinuous Galerkin methods to solve the planar stick-slip problem using the Phan-Thien-Tanner and the Maxwell model [4]. More recently, Ngamaramvaranggul and Webster used a Taylor-Galerkin/pressure-correction method with consistent streamline upwinding and velocity gradient recovery to solve the axisymmetric stick-slip flow for an Oldroyd-B flow [52].

The rest of this chapter is organized as follows: in Section 4.2, the Newtonian planar stick-slip problem is introduced and the governing equations and the local asymptotic solution expansion are presented. The SFBIM is developed in Section 4.3, where four different formulations of the method corresponding to different techniques of imposing the Dirichlet boundary conditions are presented. The numerical results are given in Section 4.4, where the fast convergence of the method with respect to the number of singular functions is demonstrated and comparisons are made with the analytical solution [62] and the results obtained with the boundary integral equation method of Ingham and Kelmanson [38], the spectral domain decomposition method of Owens and Phillips [56], the high-resolution finite element method of Salamon et al. [64], the STGFEM of Ngamaramvaranggul and Webster [51], and other methods. The conclusions are summarized in Section 4.5.

4.2 Governing equations and asymptotic solution

The planar stick-slip problem is the idealization of the extrusion of a Newtonian fluid between parallel plates at infinite surface tension. The geometry of the flow is depicted in Figure 4.1. Due to symmetry, only the upper half of the flow domain is considered, i.e. boundary part S_D

denotes the plane of symmetry. Boundary parts S_A and S_B represent the wall and the flat free surface, respectively. The latter is flat in the limit of infinite surface tension. Finally, S_C and S_E are, respectively, the artificial inlet and outlet boundaries.

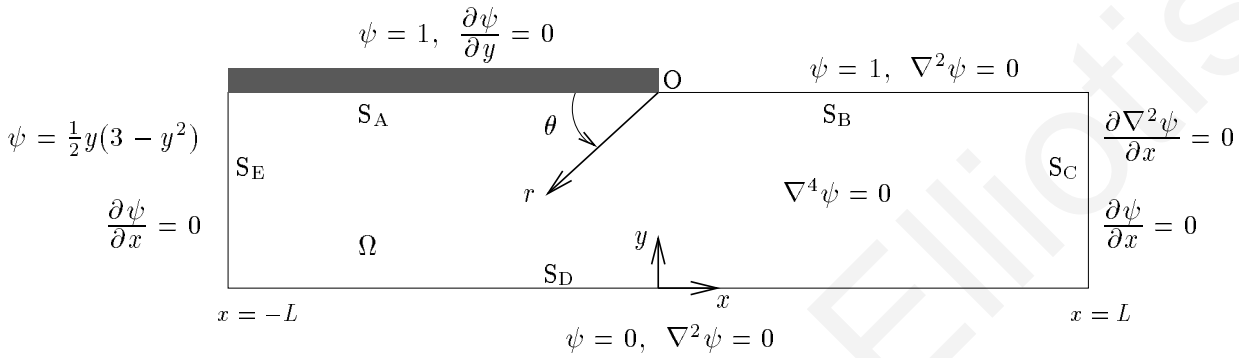

Figure 4.1. *The planar stick-slip problem in terms of the stream-function ψ.*

In the creeping case, the flow is governed by the biharmonic equation:

$$\nabla^4 \psi \ = \ 0 \qquad \text{in} \ \ \Omega \, , \tag{4.1}$$

where ψ is the stream-function defined by

$$u_x \equiv \frac{\partial \psi}{\partial y} \qquad \text{and} \qquad u_y \equiv -\frac{\partial \psi}{\partial x} \, , \tag{4.2}$$

u_x and u_y being the velocity components in the $x-$ and $y-$ directions, respectively.

The boundary conditions of the flow are also depicted in Figure 4.1. Along the wall S_A there is no slip and no penetration (i.e. the two velocity components are zero). Along the free surface, both u_y and the xy-stress component are zero which leads to $\nabla^2 \psi$=0. The inflow and outflow planes are taken at a distance L before and after the die exit. This distance is assumed to be sufficiently large so that the flow corresponds to the fully developed Poiseuille flow at the inflow plane and to a plug (i.e. uniform) flow at the outflow plane. Finally, along the symmetry

plane, the vertical velocity component and the shear stress are zero, i.e. the centerline is a slip surface. The stick-slip flow is characterized by the presence of a stress singularity at the exit O caused by the sudden change in the boundary conditions, from no slip (stick) along the wall S_A to full slip along the flat free surface S_B.

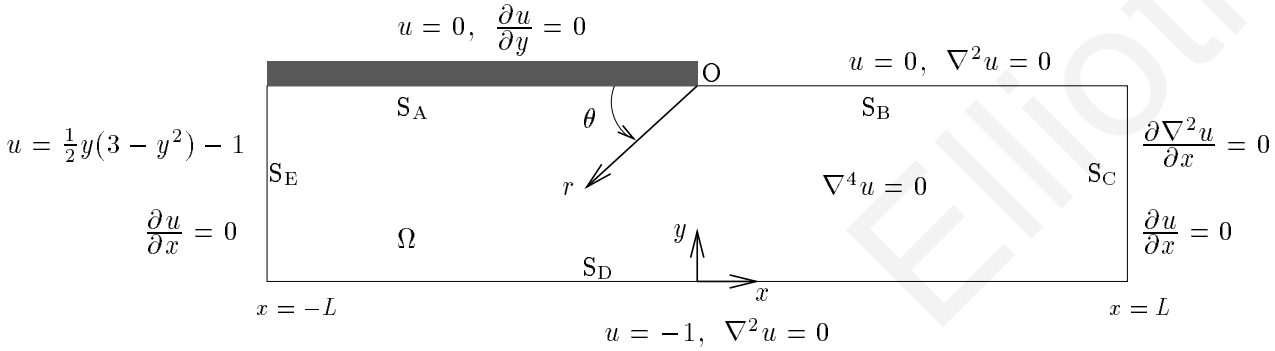

Figure 4.2. *The modified planar stick-slip problem in terms of $u=\psi-1$.*

After using the transformation $\psi=u+1$, the problem of Figure 4.1 is transformed as follows:

$$\nabla^4 u \;=\; 0 \qquad \text{in } \Omega\,, \tag{4.3}$$

with

$$\left.\begin{array}{ll} u \;=\; 0, & \dfrac{\partial u}{\partial y} \;=\; 0 \quad \text{on } S_A \\ u \;=\; 0, & \nabla^2 u \;=\; 0 \quad \text{on } S_B \\ \dfrac{\partial \nabla^2 u}{\partial x} \;=\; 0, & \dfrac{\partial u}{\partial x} \;=\; 0 \quad \text{on } S_C \\ u \;=\; -1, & \nabla^2 u \;=\; 0 \quad \text{on } S_D \\ u \;=\; \frac{1}{2}\, y\,(3 \,-\, y^2) \,-\, 1, & \dfrac{\partial u}{\partial x} \;=\; 0 \quad \text{on } S_E \end{array}\right\}. \tag{4.4}$$

The transformed problem is also shown in Figure 4.2. Note that the weak condition

$$\frac{\partial\,(\nabla^2 u)}{\partial x} \;=\; 0 \tag{4.5}$$

along S_C can be replaced by the stronger Dirichlet condition

$$u \;=\; y \;-\; 1\,, \tag{4.6}$$

which leads to a different formulation, since with the SFBIM, imposing Dirichlet conditions requires the introduction of (unknown) Lagrange multipliers.

The asymptotic solution in the neighbourhood of the singularity can be expressed in terms of an eigenfunction expansion of the form [62, 38, 28]:

$$u(r,\theta) \;=\; \sum_{j=1}^{\infty} a_j\, r^{\mu_j + 1}\;\; f(\theta,\mu_j)\,, \qquad (r,\theta) \in \Omega\,, \tag{4.7}$$

where $(r,\ \theta)$ are the polar coordinates centered at the singular point, μ_j, with j=1, 2, $\cdots$, are the singularity powers arranged in ascending order, the functions $f(\theta,\mu_j)$ represent the θ-dependence of the eigensolution, and α_j are the unknown singular coefficients determined by the global flow.

The functions $W^j \equiv r^{\mu_j+1} f(\theta,\mu_j)$ are referred to as singular functions. The local solution (4.7) consists of even and odd solutions, the corresponding singular functions of which will be denoted by W_1^j and W_2^j, respectively. In the case of even solutions [62],

$$W_1^j \;\equiv\; r^{\mu_j+1}\, f_1(\theta,\mu_j)\,, \tag{4.8}$$

with

$$f_1(\theta,\mu_j) \;=\; \cos(\mu_j \;+\; 1)\;\theta \;-\; \cos(\mu_j \;-\; 1)\;\theta\,,\;\; \mu_j \;=\; j \;-\; \frac{1}{2}\,,\quad j = 1,2,\cdots\,, \tag{4.9}$$

whereas in the case of odd solutions,

$$W_2^j \;\equiv\; r^{\mu_j+1}\, f_2(\theta,\mu_j)\,, \tag{4.10}$$

with

$$f_2(\theta,\mu_j) \;=\; (\mu_j \;-\; 1)\,\sin\,(\mu_j \;+\; 1)\,\theta \;-\; (\mu_j \;+\; 1)\,\sin\,(\mu_j \;-\; 1)\,\theta\,,\;\; \mu_j \;=\; j \;+\; 1\,,\quad j = 1,2,\cdots. \tag{4.11}$$

Thus the first singular function is

$$W_1^1 \;=\; r^{3/2}\,\left(\cos\frac{3\theta}{2} \;-\; \cos\frac{\theta}{2}\right)\,,$$

which indicates that the velocity gradients and the stresses vary as the inverse square root of the radial distance from the singular point.

In what follows we will be using the symbols α_j and β_j for the singular coefficients corresponding to the even and odd singular functions, respectively. Thus, the local solution is written as follows:

$$u \;=\; \sum_{j=1}^{\infty}\,\alpha_j\,W_1^j \;+\; \sum_{j=1}^{\infty}\,\beta_j\,W_2^j\,. \tag{4.12}$$

4.3 The singular function boundary integral method (SFBIM)

In the SFBIM [22] the solution of the problem (4.3)–(4.4) is approximated by the leading terms of the local solution expansion (4.12). By employing the first N_α terms in both sums of (4.12) the approximate solution $\bar{u}$ is

$$\bar{u} \;=\; \sum_{j=1}^{N_\alpha}\,\bar{\alpha}_j\,W_1^j \;+\; \sum_{j=1}^{N_\alpha}\,\bar{\beta}_j\,W_2^j \tag{4.13}$$

where $\bar{\alpha}_j$ and $\bar{\beta}_j$ are the approximations of the singular coefficients. Obviously, the total number of singular functions involved in the approximation (4.13) is $2N_\alpha$.

By applying Galerkin's principle, the governing equation is weighted by the singular functions used in the approximation of the solution. Hence, the following set of discretized equations is obtained:

$$\int_{\Omega} \nabla^4 \bar{u}\, W_k^i \, dV \;=\; 0\,, \qquad\qquad i = 1, 2, \cdots, N_\alpha\,, \quad k = 1, 2\,. \tag{4.14}$$

By applying Green's theorem twice and taking into account that the singular functions W_k^i, are biharmonic, the above volume integrals are reduced to boundary ones:

$$\int_{\partial\Omega} \left(\frac{\partial \bar{u}}{\partial n}\, \nabla^2 W_k^i \;-\; \bar{u}\, \frac{\partial\, (\nabla^2 W_k^i)}{\partial n} \right) dS \;+ \int_{\partial\Omega} \left(\frac{\partial\, (\nabla^2 \bar{u})}{\partial n}\, W_k^i \;-\; \nabla^2 \bar{u}\, \frac{\partial W_k^i}{\partial n} \right) dS \;=\; 0\,,$$

$$i = 1, 2, \ldots, N_a\,, \qquad k = 1, 2\,. \tag{4.15}$$

where $\partial\Omega = S_A \cup S_B \cup S_C \cup S_D \cup S_E$. The dimension of the problem is, thus, reduced by one, which leads to a considerable reduction of the computational cost. Since W_k^i satisfy exactly the boundary conditions along S_A and S_B, the above integral along these boundary segments, is identically zero. Therefore,

$$\int_{S_C \cup S_D \cup S_E} \left(\frac{\partial \bar{u}}{\partial n}\, \nabla^2 W_k^i \;-\; \bar{u}\, \frac{\partial\, (\nabla^2 W_k^i)}{\partial n} \right) dS + \int_{S_C \cup S_D \cup S_E} \left(\frac{\partial\, (\nabla^2 \bar{u})}{\partial n}\, W_k^i \;-\; \nabla^2 \bar{u}\, \frac{\partial W_k^i}{\partial n} \right) dS = 0,$$

$$i = 1, 2, \ldots, N_a\,, \qquad k = 1, 2\,. \tag{4.16}$$

In the SFBIM the Dirichlet boundary conditions are imposed by means of Lagrange multipliers which replace the normal derivative of the solution u. In the problem under study Dirichlet boundary conditions appear only along boundary parts S_D and S_E. Since along S_E the normal derivative $\partial u/\partial x$ vanishes, Lagrange multipliers are chosen to replace $\partial(\nabla^2 u)/\partial x$ in the boundary integrals of Eq. (4.16). Boundary parts S_D and S_E are partitioned into three-node elements and the corresponding Lagrange multipliers, denoted respectively by λ_D

and λ_E, are expanded in terms of quadratic basis functions M^j:

$$\lambda_D \;=\; \frac{\partial \bar{u}}{\partial y} \;=\; \sum_{j=1}^{N_{\lambda_D}} \lambda_D^j \, M^j \qquad \text{on} \quad S_D \,, \tag{4.17}$$

and

$$\lambda_E \;=\; \frac{\partial \left(\nabla^2 \bar{u}\right)}{\partial x} \;=\; \sum_{j=1}^{N_{\lambda_E}} \lambda_E^j \, M^j \qquad \text{on} \quad S_E \,, \tag{4.18}$$

where N_{λ_D} and N_{λ_E} are the numbers of the discrete Lagrange multipliers λ_D^j and λ_E^j along the corresponding boundaries. The nodal values of λ_D and λ_E are additional unknowns of the problem. The required $N_{\lambda_D}+N_{\lambda_E}$ additional equations are obtained by weighting the Dirichlet boundary conditions along S_D and S_E by the quadratic basis functions M^j in the Galerkin sense. The following linear system of $2N_\alpha+N_{\lambda_D}+N_{\lambda_E}$ discretized equations is thus obtained:

$$\begin{aligned}
&\int_{S_C} \left(-\,\bar{u}\,\frac{\partial \left(\nabla^2 W_k^i\right)}{\partial x} \;-\; \nabla^2 \bar{u}\,\frac{\partial W_k^i}{\partial x} \right) dy \;+ \\
&\int_{S_D} \left(-\lambda_D\,\nabla^2 W_k^i \;+\; \bar{u}\,\frac{\partial \left(\nabla^2 W_k^i\right)}{\partial y} \;-\; \frac{\partial \left(\nabla^2 \bar{u}\right)}{\partial y}\, W_k^i \right) dx \;+ \\
&\int_{S_E} \left(-\lambda_E\, W_k^i \;+\; \bar{u}\,\frac{\partial \left(\nabla^2 W_k^i\right)}{\partial x} \;+\; \nabla^2 \bar{u}\,\frac{\partial W_k^i}{\partial x} \right) dy \;=\; 0 \,, \; i = 1, \ldots, N_a \,, \; k = 1, 2 \,,
\end{aligned} \tag{4.19}$$

$$\int_{S_D} \bar{u}\, M^i \, dx \;=\; -\int_{S_D} M^i \, dx, \qquad\qquad i = 1, 2, \ldots, N_{\lambda_D} \,, \tag{4.20}$$

$$\int_{S_E} \bar{u}\, M^i \, dy \;=\; \int_{S_E} \left[\frac{1}{2}\, y\,(3 \;-\; y^2) \;-\; 1 \right] M^i \, dy, \qquad\qquad i = 1, 2, \ldots, N_{\lambda_E} \,. \tag{4.21}$$

The above linear system is not symmetric. This can be written in block form as follows:

$$\begin{bmatrix} K & K_D' & K_E \\ K_D'' & O & O \\ {K_E}^T & O & O \end{bmatrix} \begin{bmatrix} X_{\bar{\alpha},\bar{\beta}} \\ \Lambda_D \\ \Lambda_E \end{bmatrix} \;=\; \begin{bmatrix} O \\ B \\ C \end{bmatrix} \,, \tag{4.22}$$

where $X_{\bar{\alpha},\bar{\beta}}$, Λ_D and Λ_E are the vectors of the unknowns:

$$X_{\bar{\alpha},\bar{\beta}} \;=\; \left[\bar{\alpha}_1, \cdots, \bar{\alpha}_{N_\alpha}, \bar{\beta}_1, \cdots, \bar{\beta}_{N_\alpha}\right]^T$$

$$\Lambda_D \;=\; \left[\lambda_D^1, \lambda_D^2, \cdots, \lambda_D^{N_{\lambda_D}}\right]^T$$

$$\Lambda_E \;=\; \left[\lambda_E^1, \lambda_E^2, \cdots, \lambda_E^{N_{\lambda_E}}\right]^T \;.$$

It should be noted that the integrands in the above equations are non-singular and all integrations are carried out far from the boundaries causing the singularity. Note that the stiffness matrix is not symmetric and that it becomes singular if $N_\lambda > 2\,N_\alpha$ where N_λ=N_{λ_D}+N_{λ_E}. The above formulation will be referred to as Formulation A. We have also considered three alternative formulations which are briefly discussed below.

Formulation B

The only difference between this formulation and Formulation A is that function λ_D along boundary part S_D replaces the normal derivative of the Laplacian of u:

$$\lambda_D \;=\; \frac{\partial\left(\nabla^2 \bar{u}\right)}{\partial y} \;=\; \sum_{j=1}^{N_{\lambda_D}} \lambda_D^j\, M^j \qquad \text{on} \quad S_D \;, \tag{4.23}$$

instead of the normal derivative of u. Therefore, the only change in the formulation is in the boundary integral along the centerline plane, S_D, which becomes:

$$\int_{S_D} \left(-\lambda_D\, W_k^i \;+\; \bar{u}\,\frac{\partial\left(\nabla^2 W_k^i\right)}{\partial y} \;-\; \frac{\partial \bar{u}}{\partial y}\,\nabla^2 W_k^i \right) dx \;.$$

In contrast to formulation A, the resulting linear system of equations is symmetric. As before the stiffness matrix is singular if $N_\lambda > 2\,N_\alpha$.

Formulation C

In this formulation, the weak boundary condition $\partial\nabla^2 u/\partial x$=0 along S_C is replaced by

$$u \;=\; y \;-\; 1 \qquad \text{on} \qquad S_C \;. \tag{4.24}$$

The use of this essential boundary condition requires the introduction of an additional Lagrange multiplier function, λ_C, which replaces the normal derivative of the Laplacian of u and is

expressed in terms of quadratic basis functions M^j:

$$\lambda_C \;=\; \frac{\partial\,(\nabla^2 \bar{u})}{\partial x} \;=\; \sum_{j=1}^{N_{\lambda_C}} \lambda_C^j\, M^j, \qquad \text{on} \quad S_C\,. \tag{4.25}$$

As is the case with the other essential boundary conditions, the condition (4.24) is weighted by means of the basis functions M^j. A linear system of $2N_\alpha+N_{\lambda_C}+N_{\lambda_D}+N_{\lambda_E}$ equations is thus obtained:

$$\int_{S_C} \left(\lambda_C\, W_k^i \;-\; \bar{u}\,\frac{\partial\,(\nabla^2 W_k^i)}{\partial x} \;-\; \nabla^2\bar{u}\,\frac{\partial W_k^i}{\partial x}\right) dy \;+$$

$$\int_{S_D} \left(-\lambda_D\,\nabla^2 W_k^i \;+\; \bar{u}\,\frac{\partial\,(\nabla^2 W_k^i)}{\partial y} \;-\; \frac{\partial\,(\nabla^2\bar{u})}{\partial y}\,W_k^i\right) dx \;+$$

$$\int_{S_E} \left(-\lambda_E\, W_k^i \;+\; \bar{u}\,\frac{\partial\,(\nabla^2 W_k^i)}{\partial x} \;+\; \nabla^2\bar{u}\,\frac{\partial W_k^i}{\partial x}\right) dy \;=\; 0\,,\; i=1,\ldots,N_a\,,\; k=1,2\,, \tag{4.26}$$

$$\int_{S_C} \bar{u}\, M^i\, dy \;=\; \int_{S_C} (y \;-\; 1)\, M^i\, dy, \qquad i=1,2,\ldots,N_{\lambda_C}\,, \tag{4.27}$$

$$\int_{S_D} \bar{u}\, M^i\, dx \;=\; -\int_{S_D} M^i\, dx, \qquad i=1,2,\ldots,N_{\lambda_D}\,, \tag{4.28}$$

$$\int_{S_E} \bar{u}\, M^i\, dy \;=\; \int_{S_E} \left[\frac{1}{2}\, y\,(3 \;-\; y^2) \;-\; 1\right] M^i\, dy, \qquad i=1,2,\ldots,N_{\lambda_E}\,. \tag{4.29}$$

The above linear system is not symmetric. The stiffness matrix is singular if $N_\lambda > 2\,N_\alpha$ where here N_λ=N_{λ_C}+N_{λ_D}+N_{λ_E}.

Formulation D

As in Formulation B, the Lagrange multiplier function λ_D, used to impose the Dirichlet boundary conditions along S_D, replaces the normal derivative of the Laplacian of u (Eq. (4.23)). The resulting linear system of discretized equations is the same as that of Formulation C except from the integral along S_D in Eq. (4.26), which becomes:

$$\int_{S_D} \left(-\lambda_D\, W_k^i \;+\; \bar{u}\,\frac{\partial\,(\nabla^2 W_k^i)}{\partial y} \;-\; \frac{\partial\bar{u}}{\partial y}\,\nabla^2 W_k^i\right) dx\,.$$

As in formulation B, the system of the discretized equations is symmetric.

4.4 Numerical results

Calculations have been carried out with all four formulations presented in Section 3. In order to implement the SFBIM, the boundary parts S_C, S_D and S_E (i.e. the boundary parts away from the singularity) are subdivided into quadratic elements. Specifically, we employ N_E elements over each one of boundaries S_E and S_C and N_D elements over boundary S_D. Thus, the total number of Lagrange multipliers in formulations A and B is $N_\lambda=N_{\lambda_E}+N_{\lambda_D}$ and in formulations C and D is $N_\lambda=N_{\lambda_C}+N_{\lambda_D}+N_{\lambda_E}=2N_{\lambda_E}+N_{\lambda_D}$ (where $N_{\lambda_E}=2N_E+1$ and $N_{\lambda_D}=2N_D+1$). As in [22] and [23], the integrals in all formulations are calculated numerically by subdividing each quadratic element into 10 subintervals and using a 15-point Gauss-Legendre quadrature over each subinterval. Unless otherwise indicated, the semi-length L of the domain has been taken equal to 3.

As already mentioned, the number of the singular functions $2N_\alpha$ should be much greater than the number of Lagrange multipliers N_λ, since otherwise the stiffness matrix is ill-conditioned or singular. On the other hand, large values of $2N_\alpha$ should be avoided because the contributions of the high-order singular functions become either negligible (for $r < 1$) or very large (for $r > 1$) beyond the limits double precision can handle.

Systematic runs have been carried out in order to study the effects of both N_α and N_λ on the numerical results. The effect of $2N_\alpha$ on the leading singular coefficients can be observed in Tables 4.1 and 4.2, which show results obtained using formulation A with N_λ=32. Fast convergence is observed as $2N_\alpha$ is increased and accurate estimates of the leading singular coefficients are obtained. However, at very high values of $2N_\alpha$ (i.e. above $2N_\alpha$=88) slow divergence is observed due to the inaccuracies introduced by the high-order singular functions.

The convergence of the method with the number of Lagrange multipliers is shown in Ta-

Table 4.1. *Convergence of the singular coefficients α_i with $2N_\alpha$; N_λ=32, formulation A.*

$2N_\alpha$	α_1	α_2	α_3	α_4	α_5	α_{10}
70	0.6909892	0.2645003	0.030364	-0.021405	-0.002845	0.00024
80	0.6909881	0.2645007	0.030376	-0.021407	-0.002900	0.00022
86	0.6909882	0.2645004	0.030374	-0.021405	-0.002892	0.00021
88	0.6909882	0.2645004	0.030374	-0.021404	-0.002891	0.00021
90	0.6909882	0.2645002	0.030375	-0.021403	-0.002895	0.00021
92	0.6909885	0.2645045	0.030371	-0.021436	-0.002875	0.00034
100	0.6909884	0.2644998	0.030371	-0.021401	-0.002878	0.00020
110	0.6909883	0.2645004	0.030374	-0.021405	-0.002891	0.00021
120	0.6909883	0.2645003	0.030374	-0.021404	-0.002890	0.00021
130	0.6909882	0.2645003	0.030375	-0.021404	-0.002897	0.00020
140	0.6909873	0.2644989	0.030387	-0.021393	-0.002943	0.00019
150	0.6909883	0.2645008	0.030373	-0.021407	-0.002886	0.00021

Table 4.2. *Convergence of the singular coefficients β_i, with $2N_\alpha$; N_λ=32, formulation A.*

$2N_\alpha$	β_1	β_2	β_3	β_4	β_5	β_{10}
70	-0.0808635	-0.017115	0.001726	0.001231	-0.000282	-0.000001
80	-0.0808617	-0.017119	0.001720	0.001240	-0.000270	-0.000006
86	-0.0808619	-0.017119	0.001720	0.001238	-0.000271	-0.000005
88	-0.0808619	-0.017119	0.001720	0.001238	-0.000271	-0.000005
90	-0.0808617	-0.017119	0.001720	0.001238	-0.000270	-0.000005
92	-0.0808645	-0.017122	0.001729	0.001245	-0.000287	-0.000009
100	-0.0808621	-0.017117	0.001721	0.001234	-0.000273	-0.000003
110	-0.0808619	-0.017119	0.001720	0.001238	-0.000272	-0.000005
120	-0.0808619	-0.017118	0.001720	0.001237	-0.000271	-0.000005
130	-0.0808617	-0.017119	0.001720	0.001239	-0.000270	-0.000006
140	-0.0808590	-0.017121	0.001711	0.001231	-0.000258	-0.000008
150	-0.0808623	-0.017119	0.001721	0.001237	-0.000273	-0.000005

Table 4.3. *Convergence of the singular coefficients α_i with N_λ; $2N_\alpha$=88, formulation A.*

N_λ=N_{λ_D}+N_{λ_E}	α_1	α_2	α_3	α_4	α_5	α_{10}
13 + 5	0.6909940	0.2645260	0.030339	-0.021474	-0.002801	0.00041
17 + 7	0.6909864	0.2644962	0.030396	-0.021382	-0.002969	0.00019
21 + 5	0.6909883	0.2645002	0.030374	-0.021403	-0.002890	0.00021
21 + 7	0.6909882	0.2645007	0.030375	-0.021407	-0.002893	0.00022
25 + 5	0.6909883	0.2645002	0.030373	-0.021403	-0.002888	0.00021
25 + 7	0.6909882	0.2645004	0.030374	-0.021404	-0.002891	0.00021
25 + 9	0.6909882	0.2645005	0.030375	-0.021405	-0.002895	0.00021
29 + 7	0.6909883	0.2645002	0.030374	-0.021403	-0.002892	0.00021
29 + 9	0.6909882	0.2645005	0.030374	-0.021405	-0.002892	0.00021
33 + 7	0.6909883	0.2645004	0.030338	-0.021427	-0.002707	0.00039
33 + 9	0.6909876	0.2645077	0.030435	-0.021461	-0.003168	0.00048

Table 4.4. *Convergence of the singular coefficients β_i with N_λ; $2N_\alpha$=88, formulation A.*

N_λ=N_{λ_D}+N_{λ_E}	β_1	β_2	β_3	β_4	β_5	β_{10}
13 + 5	-0.0808768	-0.017123	0.001747	0.001248	-0.000307	-0.000018
17 + 7	-0.0808566	-0.017121	0.001706	0.001243	-0.000251	-0.000008
21 + 5	-0.0808618	-0.017118	0.001720	0.001237	-0.000271	-0.000005
21 + 7	-0.0808620	-0.017119	0.001721	0.001239	-0.000272	-0.000006
25 + 5	-0.0808619	-0.017118	0.001720	0.001237	-0.000271	-0.000005
25 + 7	-0.0808619	-0.017119	0.001720	0.001238	-0.000271	-0.000005
25 + 9	-0.0808618	-0.017119	0.001720	0.001239	-0.000271	-0.000006
29 + 7	-0.0808618	-0.017118	0.001720	0.001237	-0.000271	-0.000005
29 + 9	-0.0808619	-0.017119	0.001720	0.001238	-0.000271	-0.000005
33 + 7	-0.0808654	-0.017109	0.001747	0.001215	-0.000324	-0.000009
33 + 9	-0.0808571	-0.017146	0.001700	0.001303	-0.000237	-0.000049

bles 4.3 and 4.4 which show the values of the leading singular coefficients calculated with $2N_\alpha$=88 and various values of N_λ=N_{λ_D}+N_{λ_E}. Again, fast convergence is observed initially but as N_λ approaches the value of $2N_\alpha$, the results start diverging slowly, which is attributed to the fact that the stiffness matrix becomes ill-conditioned. Our computations showed that the "optimal" values of N_λ and $2N_\alpha$ are N_λ=32 and $2N_\alpha$=88. For higher values of $2N_\alpha$ (e.g. $2N_\alpha$=120) satisfactory values of the singular coefficients are still obtained, but the quality of the global solution is not very good.

An indication of the quality of the solution is given by the smoothness of the calculated Lagrange multipliers. Thus, for the "optimal" combination N_λ=32 and $2N_\alpha$=88 with formulation A, the calculated Lagrange multiplier function along boundary S_D is smooth. As shown in Figure 4.3a, for a slightly different value of N_λ (i.e. N_λ=36), the calculated Lagrange multiplier function exhibits oscillations, while the values of the singular coefficients are essentially the same. Similar observations are made in Figures 4.3b-d with the results of formulations B-D. Recall here that in formulations A and C, λ_D replaces $\partial u/\partial y$ while in formulations B and D it replaces $\partial\left(\nabla^2 u\right)/\partial y$.

From the results of Figure 4.3, it is clear that formulations A and C are more stable. Since it does not require additional Lagrange multipliers along boundary S_C, formulation A is to be preferred. The converged values of the leading singular coefficients with all formulations are depicted in Table 4.5. Note the slight differences in the values of $2N_\alpha$ and N_λ required for convergence. In Table 4.6, the values of α_1, α_2, α_3 and β_1, calculated using formulation A, are compared with values reported in the literature. To our knowledge, there are no reports in the literature for the values of the higher-order coefficients. The value 0.690988 for α_1 agrees with the analytical solution up to the sixth significant digit and is much more accurate

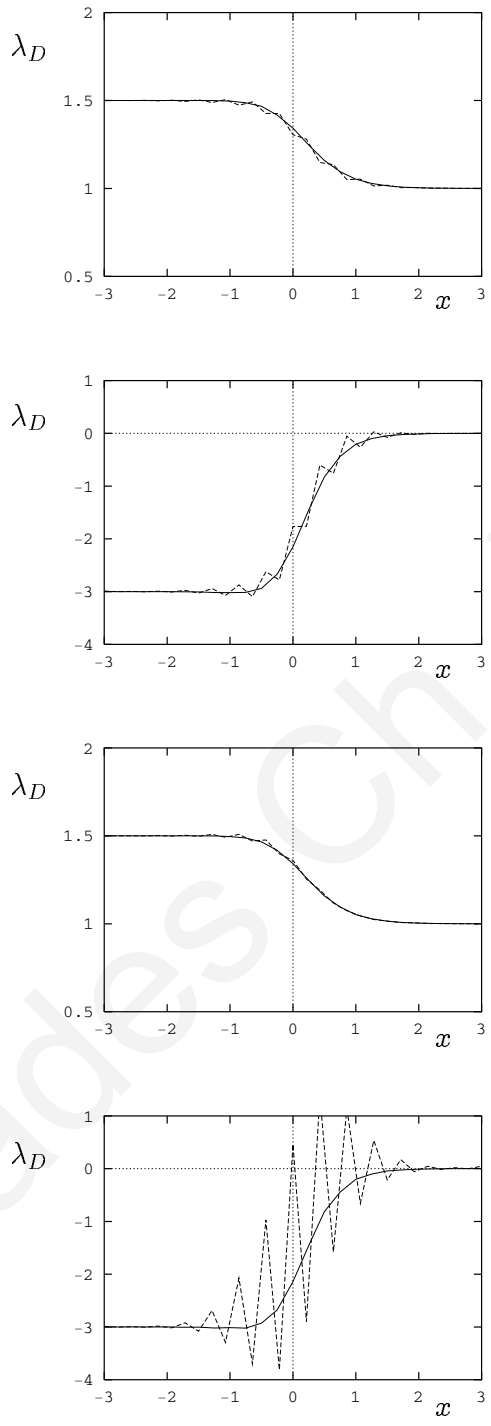

Formulation A
N_λ=32 (solid) and 36 (dashed)
$2N_\alpha$=88

Formulation B
N_λ=32 (solid) and 36 (dashed)
$2N_\alpha$=90

Formulation C
N_λ=39 (solid) and 43 (dashed)
$2N_\alpha$=90

Formulation D
N_λ=39 (solid) and 43 (dashed)
$2N_\alpha$=90

Figure 4.3. *Converged (solid) and oscillatory (dashed) Lagrange multiplier functions along boundary S_D calculated with formulations A-D.*

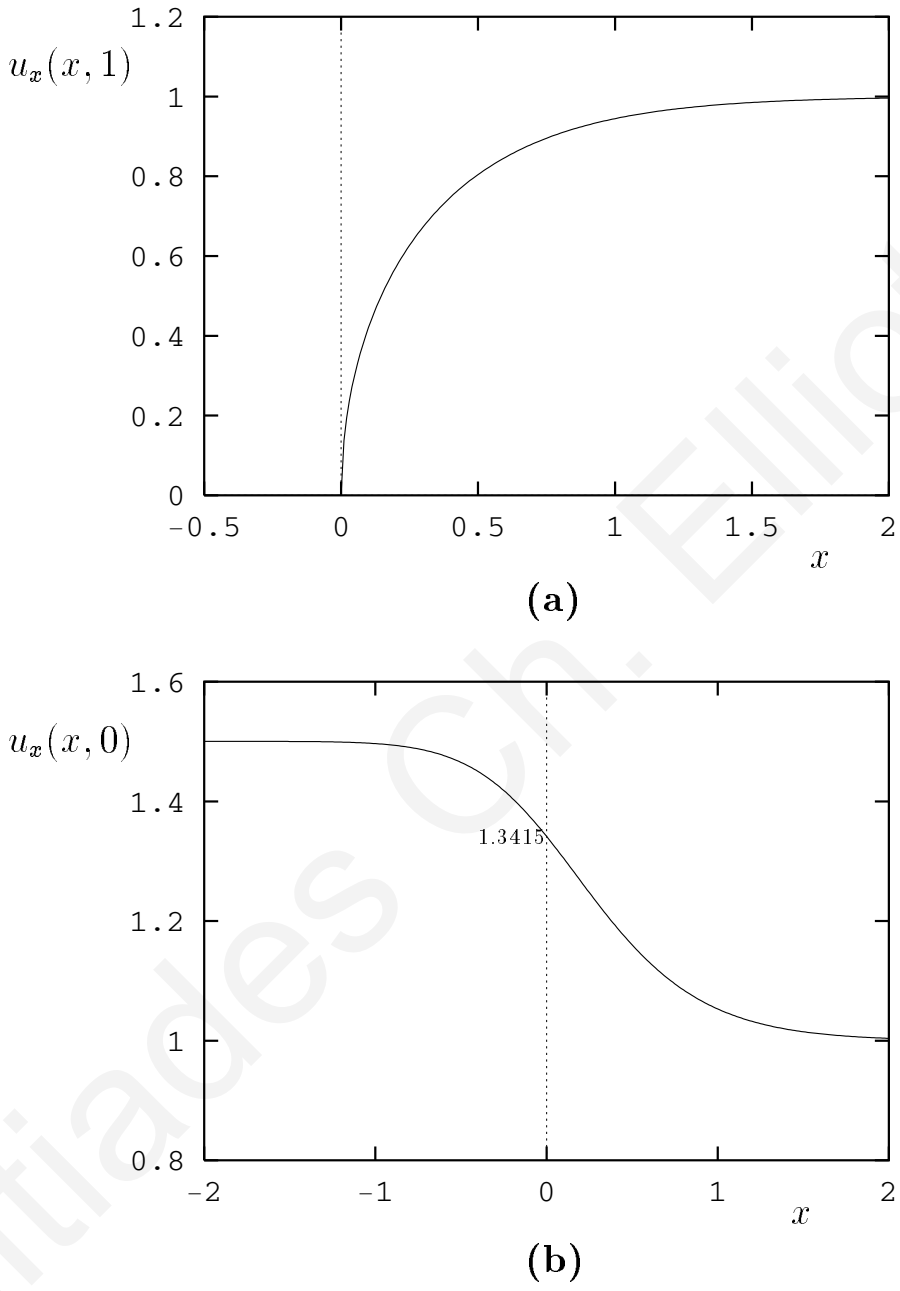

Figure 4.4. *Calculated axial velocity (a) along the slip surface (y=1) and (b) along the centerline (y=0); formulation A with* $2N_\alpha$=88 *and* N_λ=32.

Table 4.5. *Converged values of singular coefficients with formulations A-D.*

Singular coefficient	Formulation A $2N_\alpha$=88, N_λ=32	Formulation B $2N_\alpha$=90, N_λ=32	Formulation C $2N_\alpha$=90, N_λ=39	Formulation D $2N_\alpha$=90, N_λ=39
α_1	0.690988	0.690988	0.690989	0.690989
α_2	0.264500	0.264500	0.264500	0.264500
α_3	0.03037	0.03037	0.03037	0.03037
α_4	-0.02140	-0.02140	-0.02140	-0.02140
α_5	-0.00289	-0.00289	-0.00289	-0.00289
α_6	0.00423	0.00423	0.00423	0.00423
α_7	0.00042	0.00041	0.00041	0.00041
α_8	-0.00093	-0.00093	-0.00093	-0.00093
α_9	-0.00007	-0.00007	-0.00007	-0.00007
α_{10}	0.0002	0.0002	0.0002	0.0002
β_1	-0.080862	-0.080862	-0.080862	-0.080862
β_2	-0.017119	-0.017118	-0.017119	-0.017118
β_3	0.00172	0.00172	0.00172	0.00172
β_4	0.00124	0.00124	0.00124	0.00124
β_5	-0.00027	-0.00027	-0.00027	-0.00027
β_6	-0.00017	-0.00017	-0.00017	-0.00017
β_7	0.00005	0.00005	0.00005	0.00005
β_8	0.00003	0.00003	0.00003	0.00003
β_9	-0.00001	-0.00001	-0.00001	-0.00001
β_{10}	0.00000	0.00000	0.00000	0.00000

Table 4.6. *Comparison of computed singular coefficients (formulation A with $2N_\alpha$=88 and N_λ=32) with the results of other numerical methods.*

Method	α_1	α_2	α_3	β_1
Modified BIEM[1] [38]	0.69108	0.26435	0.04962	-0.07990
Singular FEM[2] [27]	0.69173	0.27168	0.05013	
ISBFM [28]	0.69104	0.26140	-0.01263	
Modified MFS [37]	0.690984	0.274807	-0.022104	-0.043983
J-integral method [74]	0.6910			
Spectral DDM[2] [56]	0.69035	0.26404	0.03069	-0.08051
High-resolution FEM[2] [64]	0.69160	0.27183	0.05232	
Modified MFS[3] [61]	0.69019			
SFBIM (present work)	0.690988	0.264500	0.03037	-0.080862
Analytical solution [62]	0.6909883			

1: extrapolated values.

2: singular coefficients obtained by post-processing the numerical solution.

3: the best reported estimate is listed.

Table 4.7. *Comparison of computed axial velocities (formulation A with $2N_\alpha$=88 and N_λ=32) with the high-resolution finite element predictions of Salamon et al. [64].*

	$u_x(0, 0.975)$	$u_x(0, 0)$	$u_x(1, 1)$
Salamon et al. [64]	0.234855	1.34150	0.944542
Present work	0.234840	1.34151	0.944528

Table 4.8. *Computed velocities along the symmetry plane (formulation A, $2N_\alpha$=88, N_λ=32) compared with other results in the literature.*

x	*Analytical* [62]	*STGFEM* [51]	*SFBIM*
-1.0	1.4964	1.4959	1.4965
-0.8	1.4899	1.4892	1.4903
-0.6	1.4758	1.4749	1.4766
-0.4	1.4484	1.4479	1.4499
-0.2	1.4027	1.4035	1.4051
0.2	1.2798	1.2701	1.2665
0.4	1.1967	1.2006	1.1929
0.6	1.1308	1.1403	1.1310
0.8	1.0834	1.0996	1.0848
1.0	1.0516	1.0702	1.0530

than previously reported values. The values of the other three coefficients compare well with numerical results reported in the literature, especially with those calculated by the spectral domain decomposition method of Owens and Phillips [56].

Once the streamfunction is known, the two velocity components are directly calculated by means of Eq. (4.2). Plots of the axial velocity, u_x, along the slip surface (y=1) and the centerline (y=0), computed using formulation A with $2N_\alpha$=88 and N_λ=32, are shown in Figure 4.4. The calculated slip surface velocity is in good agreement with the predictions of Kelmanson [38] and Owens and Phillips [56], while the centerline velocity agrees very well with the high-resolution finite element predictions of Salamon et al. [64], which is also indicated in Table 4.7, where the values of u_x at three points of the domain are compared. A comparison against the analytical solution along the symmetry plane (as calculated by Ngamaramvaranggul and Webster [51]) is provided in Table 4.8. The small differences observed are due to the fact that the domain used by Richardson [62] was shorter (L=2). However, the predictions of the present method are still much closer to the analytical solution than those of the STGFEM of Ngamaramvaranggul and Webster [51].

Finally, as illustrated in Table 4.9, the calculated value of u_x at (0.2,1) compares well with the analytical solution (based on the graphical information recorded in Reference [62]), and is better than the singular boundary element (SBEM) solution of Ingham and Kelmanson [34], the SFEM and ISBFM results of Georgiou et al. [27, 28] and the STGFEM result as calculated by Ngamaramvaranggul and Webster [51]. It should be noted that Ngamaramvaranggul and Webster [51] used an incorrect value for the analytical solution (0.618040 instead of 0.572).

The pressure corresponding to the local solution (4.12) is given by

$$p(x,y) \;=\; p_1(x,y) \;-\; p_0\,, \tag{4.30}$$

Table 4.9. *Velocity results at x=0.2 on the slip surface.*

Method	*Velocity*
Analytical [62]	0.572
SBEM [34]	0.572608
SFEM [27]	0.571896
ISBFM [28]	0.571259
STGFEM [51]	0.619786
SFBIM	0.571958

where

$$p_1 \;=\; -4\left[\sum_{j=1}^{\infty}\left(j-\frac{1}{2}\right)\alpha_j\, r^{j-\frac{3}{2}}\,\sin\left(j-\frac{3}{2}\right)\theta \;-\; \sum_{j=1}^{\infty}(j+1)(j+2)\,\beta_j\, r^j\,\cos(j\theta)\right]\,,$$

and $p_0{=}p_1(L,1)$ so that the pressure at $(L,1)$ is zero. It is clear that the pressure p is at most as accurate as p_0, the accuracy of which deteriorates as the semi-length L of the domain increases, given that the contributions of the singular functions become larger. This effect is illustrated in Table 4.10, where we show the variation of $p(0^-,1)$ with L. Note that $p_1(0^-,1){=}0$ and thus

$$p(0^-,1) \;=\; -p_0 \;=\; -p_1(L,1)\,.$$

In Figure 4.5a, the pressure along the wall and the slip surface ($y{=}1$) is plotted. This is in good agreement with the results of Salamon et al [64]. The pressure goes to infinity as the singularity is approached from the right, while it remains finite for negative x. This discontinuity cannot be captured by standard numerical methods in which a continuous approximation is used for the pressure. In Figure 4.5b, the computed centerline pressure is compared with the

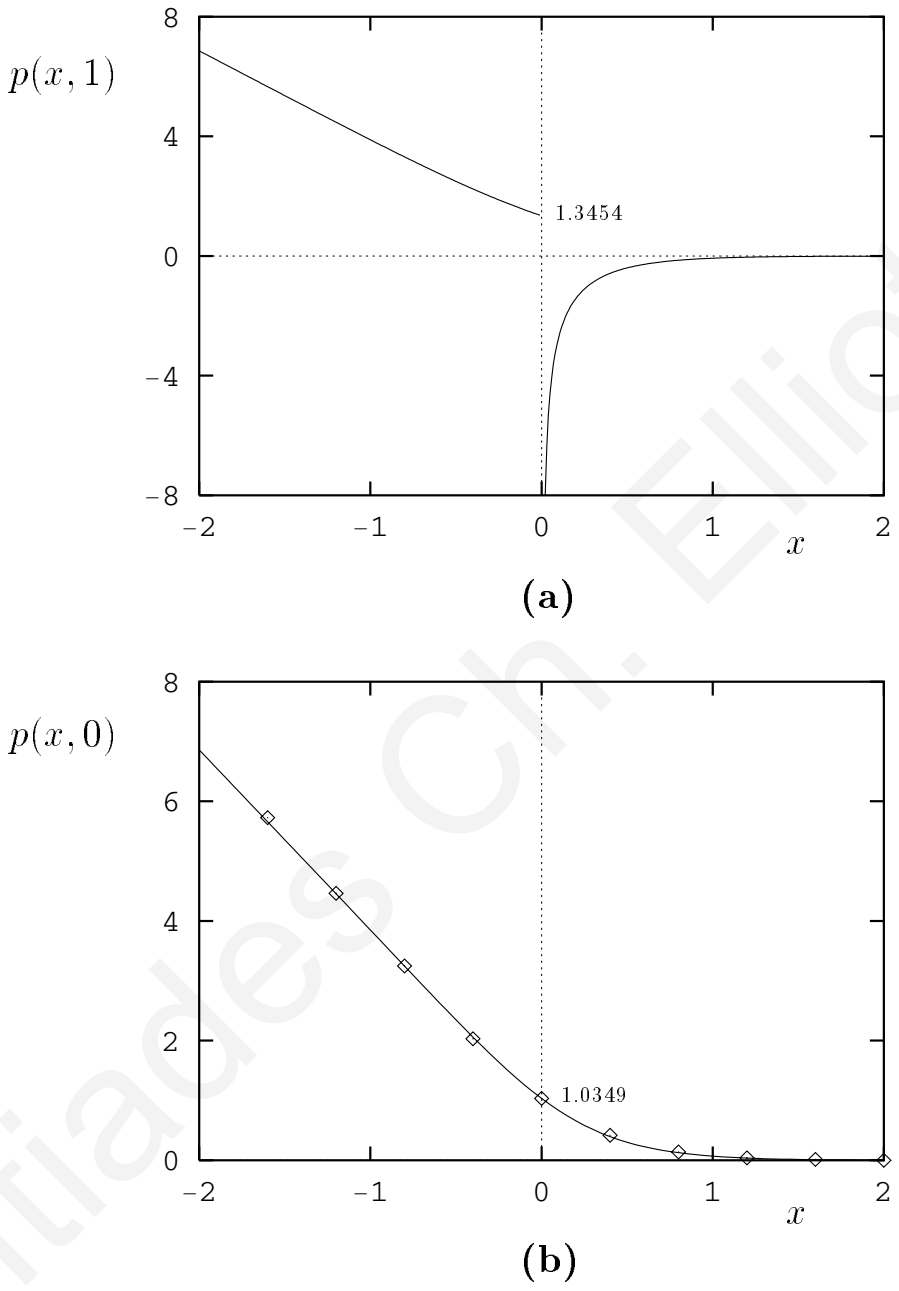

Figure 4.5. *(a) Calculated pressure along y=1; (b) Calculated centerline pressure (continuous curve) compared with the analytical results by Richardson (points) [62]; formulation A with* $2N_\alpha$=88 *and* N_λ=32.

Table 4.10. *Variation of the value of* $p(0^-,1)$ *with the semi-length* L *of the domain; formulation A with* $2N_\alpha$*=88 and* N_λ*=32.*

L	$p(0^-,1)$
2.0	1.3452
2.2	1.3454
2.4	1.3454
2.6	1.3468
2.8	1.3451
3.0	1.3454
3.2	1.3444
3.4	1.3454

Table 4.11. *Comparison of the computed centerline pressure at* x*=0 (formulation A with* $2N_\alpha$*=88 and* N_λ*=32) with the results of other numerical methods.*

Method	$p(0,0)$
Finite differences [1]	1.100
STGFEM [51]	0.9980
SFBIM (present work)	1.0349
Analytical Solution [62]	1.0348

analytical results of Richardson [62] (as given by Ngamaramvaranggul and Webster [51]). The agreement is excellent, which is also seen in Table 4.11, where the computed value of $p(0,0)$ is compared with the analytical value and those of other numerical methods.

The streamlines as well as the contours of the two velocity components (u_x and u_y) and the pressure, computed using formulation A with $2N_\alpha$=88 and N_λ=32, are shown in Figure 4.6. These show the re-adjustment of the flow from a parabolic to a uniform velocity profile and agree well with previous results in the literature [28, 64, 53]. The maximum value of u_y is 0.19364 which compares well with the value of 0.1936 provided by Salamon et al. [64]. (Ngamaramvaranggul and Webster [51] computed the peak value to be 0.17.) According to our calculations, the maximum occurs approximately at the point (0.109,0.712).

The effect of the length of the domain on the computations has also been studied. Table 4.12 depicts the converged values of the first four singular coefficients for N_λ=32 and different values of the semi-length, L, of the domain. As expected, the values of the singular coefficients change dramatically with L for small values of the latter, since the assumptions for fully-developed and uniform flow along the inlet and outlet planes, respectively, are not valid when the two planes are taken close to the die exit. This effect is illustrated in Figure 4.7, where the calculated values of α_1 and β_1 are plotted versus L. We observe that the value L=3 is sufficiently high to assure the validity of the imposed inlet and outlet boundary conditions. At higher values of L, the accuracy of the computed solutions starts deteriorating, due to the fact that the number N_{λ_D} of the corresponding Lagrange multipliers is kept fixed while the length of the boundary S_D increases. As already noted, increasing N_{λ_D} will not improve the accuracy, since it leads to ill-conditioning of the stiffness matrix.

Stream-function, ψ

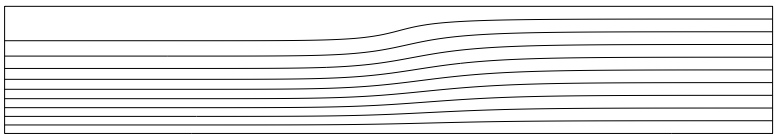

Horizontal velocity component, $u_x = \partial\psi/\partial y$

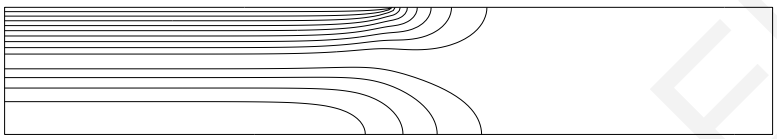

Vertical velocity component, $u_y = -\partial\psi/\partial x$

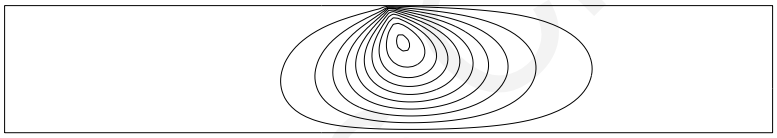

Pressure, p

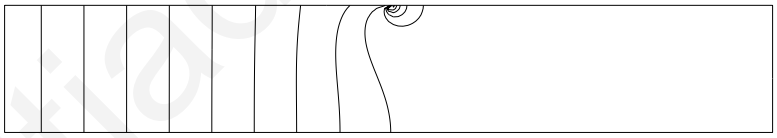

Figure 4.6. *Computed streamlines and contours of the two velocity components and the pressure; formulation A with* $2N_\alpha = 88$ *and* $N_\lambda = 32$.

Table 4.12. *Converged values of the leading singular coefficients with formulation A, N_λ=32 and different values of the semi-length L of the domain S_D; the value of $2N_\alpha$ ranges from 78 to 88, depending on the value of L.*

L	α_1	α_2	β_1	β_2
2.0	0.690973	0.264524	-0.080870	-0.017112
2.1	0.690980	0.264514	-0.080866	-0.017115
2.2	0.690984	0.264508	-0.080864	-0.017117
2.3	0.690986	0.264504	-0.080863	-0.017117
2.4	0.690987	0.264503	-0.080862	-0.017118
2.5	0.690988	0.264502	-0.080862	-0.017118
2.6	0.690988	0.264501	-0.080862	-0.017118
2.7	0.690988	0.264501	-0.080862	-0.017118
2.8	0.690988	0.264501	-0.080862	-0.017118
2.9	0.690988	0.264500	-0.080862	-0.017118
3.0	0.690988	0.264500	-0.080862	-0.017118
3.1	0.690988	0.264500	-0.080862	-0.017118
3.2	0.690988	0.264500	-0.080862	-0.017118
3.3	0.690988	0.264500	-0.080862	-0.017117
3.4	0.690988	0.264500	-0.080862	-0.017118
3.5	0.690988	0.264498	-0.080862	-0.017117
3.6	0.690988	0.264498	-0.080862	-0.017117
3.8	0.690988	0.264498	-0.080862	-0.017118
4.0	0.690988	0.264490	-0.080862	-0.017113

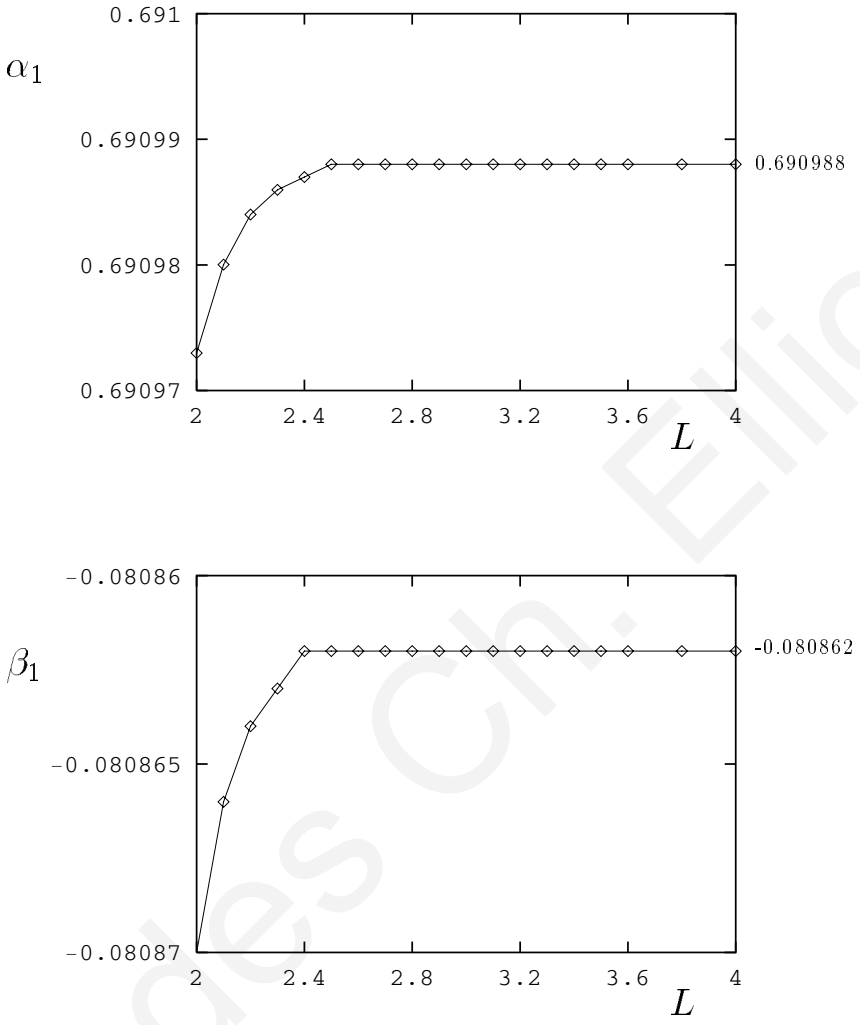

Figure 4.7. *Convergence of α_1 and β_1 with the semi-length L of the domain; formulation A, N_λ=32.*

4.5 Conclusions

The singular function boundary integral method (SFBIM) has been developed for solving a biharmonic problem with a boundary singularity, i.e. the Newtonian planar stick-slip problem in terms of the streamfunction. The solution is approximated by means of the leading singular functions defined by the local asymptotic solution expansion around the singularity. Hence, the method is restricted to Stokes problems with a boundary singularity for which the local solution is available. The proposed approximation is valid only if the domain of the problem is a subset of the domain of convergence of the local solution. If this is not the case, the domain can be partitioned into subdomains over which separate approximations, that obey appropriate compatibility conditions along the interfaces, may be used.

The main features of the SFBIM are as follows:

(a) The singular coefficients are calculated directly.

(b) The governing biharmonic equation is weighted by the singular functions in the Galerkin sense.

(c) The discretized equations are reduced to boundary integrals by means of a double application of the divergence theorem, which leads to a considerable reduction of the computational cost.

(d) The Dirichlet boundary conditions are weakly enforced by means of Lagrange multipliers which may replace either $\partial u/\partial n$ or $\partial\left(\nabla^2 u\right)/\partial n$ in the integrands of the discretized equations. The Lagrange multipliers are calculated together with the singular coefficients.

Four different formulations of the SFBIM, corresponding to different techniques of imposing the Dirichlet boundary conditions, have been investigated. Even though all formulations give about the same results, using a weaker instead of a Dirichlet condition along the outflow plane

is a much better choice, since the number of Lagrange multipliers, N_λ must be much lower than the number of singular functions, $2N_\alpha$ in order to avoid ill-conditioning of the stiffness matrix. Moreover, the best choice for the Lagrange multipliers along the symmetry plane is to replace the normal derivative of the solution and not the normal derivative of its Laplacian.

The SFBIM converges very fast with the number of singular functions and the number of Lagrange multipliers, and accurate estimates of the leading singular coefficients are obtained. In particular, the value 0.690988 for the leading singular coefficient agrees well with the analytical solution up to the sixth significant digit. The effect of the length of the domain on the values of the leading singular coefficients has also been investigated. Finally, the numerical results for the velocity components and the pressure compare very well with the analytical solution of Richardson [62] and the high-resolution finite element results of Salamon et al. [64].

Chapter 5

Solution of a 2-D fracture problem

In this chapter the singular function boundary integral method (SFBIM) is extended for solving two-dimensional fracture problems formulated in terms of the Airy stress function[1]. Our goal is the accurate, direct computation of the associated stress intensity factors, which appear as coefficients in the asymptotic expansion of the solution near the crack tip. As mentioned in previous chapters, in the SFBIM the leading terms of the asymptotic solution are used to approximate the solution and to weight the governing biharmonic equation in the Galerkin sense. The discretized equations are reduced to boundary integrals by means of Green's theorem and the Dirichlet boundary conditions are weakly enforced by means of Lagrange multipliers. The numerical results on a model problem show that the method converges extremely fast and yields accurate estimates of the leading stress intensity factors.

5.1 Introduction

The elastic field near the tip of a fracture in an elastic body is characterized by the *stress intensity factors* (SIFs). These are the coefficients, α_j, that appear in the asymptotic expansion

[1] The material of this chapter appears in [25].

of the Airy stress function u near the crack tip, which is of the general form

$$u = \sum_{i=1}^{\infty} \alpha_j r^{\mu_j} f_j(\theta), \tag{5.1}$$

where (r, θ) denote polar coordinates centered at the crack tip. The eigenvalues μ_j and the corresponding eigenfunctions $f_j(\theta)$ are known, whereas the SIFs are unknown, with their values depending on the global problem. The first SIF, a_1, plays a crucial role in the mathematical description of the propagation of fracture, since

$$K = \sqrt{2\pi} a_1 \tag{5.2}$$

is the *opening mode SIF* [35].

In the last few decades there has been a plethora of work aimed at reliably computing the SIFs. The methods used include the finite element method (FEM) with post-processing [8, 9, 72, 73, 75], the FEM with local mesh refinement [65], enriched and generalized finite elements [63, 66], the method of fundamental solutions [37], as well as certain versions of the Trefftz method [32, 36, 39, 44].

It should be noted that in most of the methods mentioned above, the SIFs are calculated as a *post-solution* operation, i.e. the solution u is approximated first and the SIFs are then calculated using the approximation to u. If the calculation of the SIFs is the main goal of the computation, then it may be beneficial to use a method in which the SIFs are calculated *directly*. Examples of such methods include the Trefftz method [36, 44] and the method of fundamental solutions [37].

The objective of this chapter is to extend the singular function boundary integral method (SFBIM) to two-dimensional fracture problems. The SFBIM was originally developed in Ref. [29] to solve Laplacian problems with boundary singularities aiming at resolving the conver-

gence difficulties encountered with standard numerical methods in the vicinity of singular points. In this method the solution is approximated by the leading terms of the local asymptotic solution expansion, which are also employed to weight the governing equation in the Galerkin sense. Furthermore, the discretized equations are reduced to boundary integrals by means of the divergence theorem, and the Dirichlet boundary conditions are weakly enforced by means of Lagrange multipliers. In addition to reducing the dimension of the problem by one, another important feature of the method is that the singular coefficients α_j are calculated directly (i.e. no postprocessing is required), together with the discrete Lagrange multipliers. In chapters 2 and 3, the SFBIM has been applied to various problems with singularities, such as the Motz problem [29], the cracked-beam problem [30], and to Laplacian problems over L-shaped domains [22, 23], exhibiting fast convergence and yielding very accurate results, especially for the leading singular coefficients.

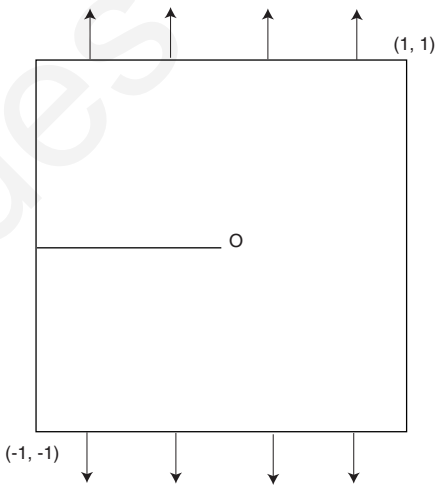

Figure 5.1. *A thin elastic plate with a symmetric crack.*

Since it yields direct estimates of the SIFs, the SFBIM appears to be an excellent candidate for solving fracture problems, which can be expressed as a biharmonic equation in terms of

the Airy stress function. To illustrate the extension of the method to such problems, we have chosen a two-dimensional fracture problem, originally studied by Schiff et al. [65].

The outline of the rest of this chapter is as follows: the model fracture problem and the asymptotic expansion of the solution near the crack tip are presented in Section 5.2, the SFBIM for this particular problem is developed in Section 5.3, while the numerical computations are presented in Section 5.4, in which comparisons are also made with the results obtained by Li et al. [44] using the collocation Trefftz method. Finally, our conclusions are summarized in Section 5.5.

5.2 The model problem and the asymptotic solution

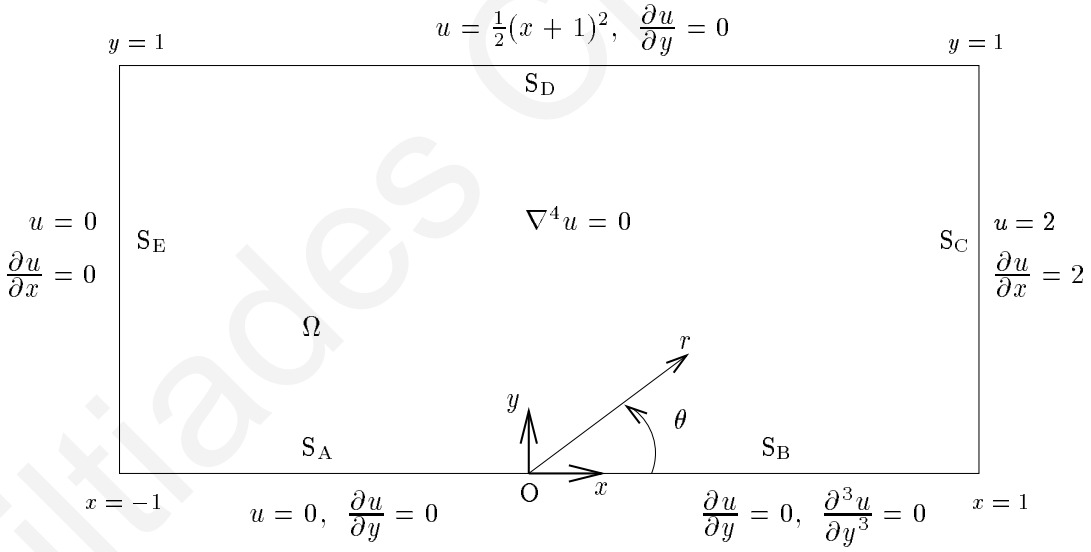

Figure 5.2. *The model fracture problem.*

We consider the model problem studied by Schiff et al. [65]. It deals with a two-dimensional solid elastic plate containing a single edge crack, subjected to a uniform outplane load normal to two of the edges and to the crack. The remaining edges are stress free (see Figure 5.1).

Using symmetry, the problem is formulated on $\Omega = (-1,1)\times(0,1)$, as a biharmonic equation for of the Airy stress function $u(x,y)$, and is depicted graphically in Figure 5.2. For simplicity the load in the original problem from [65] has been taken to be 1.

The resulting boundary value problem is as follows: find u such that

$$\nabla^4 u \;=\; 0 \qquad \text{in } \; \Omega = (-1,1)\times(0,1)\,, \tag{5.3}$$

with

$$\left.\begin{array}{llll} u \;=\; 0, & \dfrac{\partial u}{\partial y} \;=\; 0 & \text{on} & S_A \\ \dfrac{\partial u}{\partial y} \;=\; 0 & \dfrac{\partial^3 u}{\partial y^3} \;=\; 0 & \text{on} & S_B \\ u \;=2, & \dfrac{\partial u}{\partial x} \;=\; 2 & \text{on} & S_C \\ u \;=\tfrac{1}{2}\,(\,x\;+\;1)^2\,, & \dfrac{\partial u}{\partial y} \;=\; 0 & \text{on} & S_D \\ u \;=0, & \dfrac{\partial u}{\partial x} \;=\; 0 & \text{on} & S_E \end{array}\right\}\,. \tag{5.4}$$

where $\partial\Omega = S_A \cup S_B \cup S_C \cup S_D \cup S_E$. The asymptotic expansion for u in the neigbourhood of the singular point O can be expressed in terms of an eigenfunction expansion of the form:

$$u(r,\theta) \;=\; \sum_{j=1}^{\infty} \Big[c_j\, W_1^j(r,\theta) + d_j\, W_2^j(r,\theta)\Big]\,, \tag{5.5}$$

where (r,θ) are the polar coordinates centered at O, and c_j, d_j correspond to the even and odd SIFs, respectively (see also eq. (1.1) in [65]). (Using this notation, we have $a_1 = d_1$ in (5.2).) In expansion (5.5), the two sets of the so-called singular functions $W_k^j, k = 1,2$, are given by

$$W_k^j \;\equiv\; r^{\mu_j\,+\,1}\, f_k(\theta,\mu_j)\,, \qquad k \;=\; 1,2 \tag{5.6}$$

where

$$f_1(\theta,\mu_j) \;=\; \cos(\mu_j \;-\; 1)\;\theta \;-\; \cos(\mu_j \;+\; 1)\;\theta\,,\;\; \mu_j \;=\; j\,,\;\; j = 1,2,\cdots, \tag{5.7}$$

and

$$f_2(\theta,\mu_j) \;=\; \cos(\mu_j \;-\; 1)\;\theta \;-\; \frac{\mu_j \;-\; 1}{\mu_j \;+\; 1}\cos(\mu_j \;+\; 1)\;\theta\,,\;\; \mu_j \;=\; j \;-\; \frac{1}{2}\,,\;\; j = 1,2,\cdots. \tag{5.8}$$

We note that the singular functions W_k^j satisfy the PDE (5.3), as well as the boundary conditions on S_A and S_B.

5.3 The singular function boundary integral method (SFBIM)

In the SFBIM the solution u is approximated by the leading terms of the asymptotic expansion. By employing the first N_α terms in (5.5), the approximate solution $\bar{u}$ is given by

$$\bar{u} \;=\; \sum_{i=1}^{N_\alpha} \bar{c}_i \, W_1^i \;+\; \sum_{i=1}^{N_\alpha} \bar{d}_i \, W_2^i, \tag{5.9}$$

where $\bar{c}_i$ and $\bar{d}_i$ are the approximations to the SIFs. Obviously, the total number of singular functions involved in the approximation is $2N_\alpha$. It should be pointed out that the method is restricted to fracture problems with only one crack for which the asymptotic solution is available. Moreover, the proposed approximation (5.9) is valid only if the domain of the problem is a subset of the domain of convergence of the asymptotic solution. Otherwise, the domain may be partitioned into subdomains over which separate approximations obeying appropriate compatibility conditions along the interfaces should be used.

By applying Galerkin's principle, the governing equation is weighted by the singular functions, which yields to the following set of discretized equations:

$$\int_\Omega \nabla^4 \bar{u} \, W_k^i \, dV \;=\; 0 \,, \quad i = 1, 2, \cdots, N_\alpha \,, \quad k = 1, 2 \,.$$

Next, applying Green's theorem twice and taking into account that the singular functions satisfy the governing biharmonic equation (5.3), the above integrals are reduced to boundary ones:

$$\int_{\partial\Omega} \left(\frac{\partial \bar{u}}{\partial n} \nabla^2 W_k^i - \bar{u} \frac{\partial \left(\nabla^2 W_k^i \right)}{\partial n} \right) dS + \int_{\partial\Omega} \left(\frac{\partial \left(\nabla^2 \bar{u} \right)}{\partial n} W_k^i - \nabla^2 \bar{u} \frac{\partial W_k^i}{\partial n} \right) dS = 0,$$

for $i = 1, 2, \ldots, N_a$, k=1,2. Now, since W_k^i satisfy exactly the boundary conditions along S_A and S_B, the above integral along these boundary segments is identically zero. Therefore,

$$\int_{S_C \cup S_D \cup S_E} \left(\frac{\partial \bar{u}}{\partial n} \nabla^2 W_k^i - \bar{u} \frac{\partial \left(\nabla^2 W_k^i \right)}{\partial n} \right) dS + \int_{S_C \cup S_D \cup S_E} \left(\frac{\partial \left(\nabla^2 \bar{u} \right)}{\partial n} W_k^i - \nabla^2 \bar{u} \frac{\partial W_k^i}{\partial n} \right) dS = 0,$$

for $i = 1, 2, \ldots, N_a$, k=1,2.

In the SFBIM the Dirichlet boundary conditions are imposed by means of Lagrange multipliers. In the case of Laplacian problems, the Lagrange multipliers replace the normal derivative $\partial \bar{u}/\partial n$. In the case of biharmonic problems, another option for the Lagrange multipliers is to replace $\partial \nabla^2 \bar{u}/\partial n$. In the current problem, Dirichlet boundary conditions appear along the three boundary parts of interest, i.e. S_C, S_D and S_E, where the normal derivative of the solution is also specified. Therefore, Lagrange multipliers have been chosen to replace $\partial \nabla^2 \bar{u}/\partial n$ at boundary parts S_C, S_D and S_E. These are partitioned into three-node elements and the corresponding Lagrange multipliers, denoted respectively by λ_C, λ_D and λ_E, are expanded in terms of quadratic basis functions M^j:

$$\lambda_C = \frac{\partial \left(\nabla^2 \bar{u} \right)}{\partial x} = \sum_{j=1}^{N_{\lambda_C}} \lambda_C^j M^j , \quad \text{on } S_C , \tag{5.10}$$

$$\lambda_D = \frac{\partial \left(\nabla^2 \bar{u} \right)}{\partial y} = \sum_{j=1}^{N_{\lambda_D}} \lambda_D^j M^j , \quad \text{at } S_D , \tag{5.11}$$

and

$$\lambda_E = \frac{\partial \left(\nabla^2 \bar{u} \right)}{\partial x} = \sum_{j=1}^{N_{\lambda_E}} \lambda_E^j M^j , \quad \text{at } S_E , \tag{5.12}$$

where N_{λ_C}, N_{λ_D} and N_{λ_E} are the numbers of the discrete Lagrange multipliers λ_C^j, λ_D^j and λ_E^j along the corresponding boundaries. The discrete Lagrange multipliers appear as additional unknowns in the problem. The required $N_{\lambda_C}+N_{\lambda_D}+N_{\lambda_E}$ additional equations are obtained by weighting the Dirichlet boundary conditions along S_C, S_D and S_E by the quadratic basis

functions M^i in the Galerkin sense. The following linear system of $2N_\alpha+N_{\lambda_C}+N_{\lambda_D}+N_{\lambda_E}$ discretized equations is thus obtained:

$$\int_{S_C}\left(\lambda_C\, W_k^i \;-\; \bar{u}\,\frac{\partial\,(\nabla^2 W_k^i)}{\partial x} \;-\; \nabla^2\bar{u}\,\frac{\partial W_k^i}{\partial x}\right)\,dy +$$

$$+\int_{S_D}\left(\lambda_D\, W_k^i \;-\; \bar{u}\,\frac{\partial\,(\nabla^2 W_k^i)}{\partial y} \;-\; \nabla^2\bar{u}\,\frac{\partial W_k^i}{\partial y}\right)\,dx +$$

$$+\int_{S_E}\left(-\lambda_E\, W_k^i \;+\; \bar{u}\,\frac{\partial\,(\nabla^2 W_k^i)}{\partial x} \;+\; \nabla^2\bar{u}\,\frac{\partial W_k^i}{\partial x}\right)\,dy \;=\; -\int_{S_C} 2\,\nabla^2 W_k^i\,dy,$$

$$i=1,\ldots,N_a\;,\;k=1,2\,, \tag{5.13}$$

$$\int_{S_C}\bar{u}M^i dy \;=\; \int_{S_C} 2M^i dy,\;\; i=1,2,\ldots,N_{\lambda_C}, \tag{5.14}$$

$$\int_{S_D}\bar{u}M^i dx \;=\; \int_{S_D}\left[\frac{1}{2}(x+1)^2\right]M^i dx,\;\; i=1,2,\ldots,N_{\lambda_D}, \tag{5.15}$$

$$-\int_{S_E}\bar{u}M^i dy \;=\; 0,\;\; i=1,2,\ldots,N_{\lambda_E}. \tag{5.16}$$

The above linear system can be written in block form as follows:

$$\begin{bmatrix} K & K_C & K_D & K_E \\ {K_C}^T & O & O & O \\ {K_D}^T & O & O & O \\ {K_E}^T & O & O & O \end{bmatrix}\begin{bmatrix} X_{\bar{c},\bar{d}} \\ \Lambda_C \\ \Lambda_D \\ \Lambda_E \end{bmatrix} = \begin{bmatrix} A \\ C \\ D \\ O \end{bmatrix}, \tag{5.17}$$

where $X_{\bar{c},\bar{d}}$, Λ_C, Λ_D and Λ_E are the vectors of unknowns,

$$X_{\bar{c},\bar{d}} \;=\; [\bar{c}_1,\cdots,\bar{c}_{N_\alpha},\bar{d}_1,\cdots,\bar{d}_{N_\alpha}]^T,$$

$$\Lambda_C \;=\; \left[\lambda_C^1,\lambda_C^2,\cdots,\lambda_C^{N_{\lambda_C}}\right]^T,\quad \Lambda_D \;=\; \left[\lambda_D^1,\lambda_D^2,\cdots,\lambda_D^{N_{\lambda_D}}\right]^T,\quad \Lambda_E \;=\; \left[\lambda_E^1,\lambda_E^2,\cdots,\lambda_E^{N_{\lambda_E}}\right]^T.$$

It should be noted that the integrands in equations (5.13)–(5.16) are non-singular and all integrations are carried out far from the boundaries causing the singularity. Also, the stiffness

matrix in (5.17) is symmetric and becomes singular if $N_\lambda > 2\,N_\alpha$ where $N_\lambda = N_{\lambda_C} + N_{\lambda_D} + N_{\lambda_E}$. This last fact will be taken into consideration when choosing specific values for these parameters.

5.4 Numerical results

In order to implement the SFBIM, the boundary parts S_C, S_D and S_E (i.e. the boundary parts away from the singularity) are subdivided into quadratic elements. In particular, we use N_C elements for each of the boundaries S_C and S_E and N_D elements for boundary S_D, which makes the the total number of Lagrange multipliers $N_\lambda = N_{\lambda_C} + N_{\lambda_D} + N_{\lambda_E} = 2N_{\lambda_C} + N_{\lambda_D}$ (where $N_{\lambda_C} = 2N_C + 1$ and $N_{\lambda_D} = 2N_D + 1$). All integrals are calculated numerically by subdividing each quadratic element into 10 subintervals and using a 15-point Gauss-Legendre quadrature over each subinterval [22, 23].

As mentioned above, the number of the singular functions $2N_C$ should be greater than the number of Lagrange multipliers N_λ, because otherwise the stiffness matrix becomes ill-conditioned or singular. On the other hand, large values of $2N_C$ should be avoided because the contributions of the high-order singular functions become either negligible (for $r < 1$) or very large (for $r > 1$) beyond the limits double precision can handle. Since, at the moment, no a-priori way of choosing the "optimal" values for N_λ and N_C exists, we have carried out systematic runs in order to study the effects the variation of these parameters would have on the numerical results.

The effect of $2N_\alpha$ on the leading SIFs can be observed in Tables 5.1 and 5.2, which show results obtained with $N_\lambda = 39$. Initially, we observe fast convergence as $2N_\alpha$ is increased, but at very high values of the latter (i.e. above $2N_\alpha = 94$) slow divergence is observed due to the

Table 5.1. *Convergence of the leading odd SIFs d_i with $2N_\alpha$; N_λ=39.*

$2N_\alpha$	d_1	d_2	d_3	d_4	d_5	d_{10}
70	2.12751291	-1.03669169	0.0371710	0.1177493	-0.1227288	-0.01108
80	2.12751343	-1.03669221	0.0371701	0.1177510	-0.1227319	-0.01103
88	2.12751347	-1.03669218	0.0371701	0.1177511	-0.1227313	-0.01103
90	2.12751342	-1.03669217	0.0371701	0.1177510	-0.1227316	-0.01103
92	2.12751342	-1.03669217	0.0371701	0.1177509	-0.1227316	-0.01103
94	2.12751343	-1.03669217	0.0371702	0.1177509	-0.1227315	-0.01103
96	2.12751343	-1.03669217	0.0371702	0.1177509	-0.1227314	-0.01103
100	2.12751343	-1.03669219	0.0371702	0.1177509	-0.1227315	-0.01103
110	2.12751347	-1.03669237	0.0371705	0.1177508	-0.1227315	-0.01102
120	2.12751343	-1.03669229	0.0371705	0.1177508	-0.1227314	-0.01103

Table 5.2. *Convergence of the leading even SIFs c_i, with $2N_\alpha$; N_λ=39.*

$2N_\alpha$	c_1	c_2	c_3	c_4	c_5	c_{10}
70	0.16676222	0.0624426	-0.1324729	-0.0102230	0.1058502	0.004334
80	0.16676181	0.0624440	-0.1324747	-0.0102203	0.1058466	0.004262
88	0.16676182	0.0624439	-0.1324746	-0.0102211	0.1058471	0.004263
90	0.16676184	0.0624439	-0.1324745	-0.0102208	0.1058474	0.004264
92	0.16676184	0.0624439	-0.1324745	-0.0102208	0.1058474	0.004264
94	0.16676184	0.0624439	-0.1324745	-0.0102209	0.1058472	0.004264
96	0.16676184	0.0624439	-0.1324745	-0.0102208	0.1058471	0.004264
100	0.16676184	0.0624439	-0.1324745	-0.0102207	0.1058470	0.004264
110	0.16676179	0.0624441	-0.1324753	-0.0102196	0.1058450	0.004262
120	0.16676181	0.0624440	-0.1324751	-0.0102200	0.1058457	0.004265

Table 5.3. *Convergence of the leading odd SIFs d_i with N_λ; $2N_\alpha$=94.*

N_λ	d_1	d_2	d_3	d_4	d_5	d_{10}
7+13+7	2.12751309	-1.03669185	0.0371707	0.1177516	-0.1227324	-0.01103
7+17+7	2.12751334	-1.03669214	0.0371702	0.1177509	-0.1227318	-0.01103
7+21+7	2.12751338	-1.03669217	0.0371702	0.1177507	-0.1227319	-0.01103
7+23+7	2.12751343	-1.03669217	0.0371702	0.1177510	-0.1227314	-0.01103
7+25+7	2.12751343	-1.03669217	0.0371702	0.1177509	-0.1227315	-0.01103
7+27+7	2.12751342	-1.03669217	0.0371702	0.1177509	-0.1227315	-0.01103
7+29+7	2.12751347	-1.03669213	0.0371703	0.1177513	-0.1227309	-0.01103
7+31+7	2.12751346	-1.03669213	0.0371703	0.1177513	-0.1227310	-0.01103
7+33+7	2.12751335	-1.03669221	0.0371701	0.1177506	-0.1227324	-0.01103

Table 5.4. *Convergence of the leading even SIFs c_i with N_λ; $2N_\alpha$=94.*

N_λ	c_1	c_2	c_3	c_4	c_5	c_{10}
7+13+7	0.16676176	0.0624436	-0.1324753	-0.0102209	0.1058486	0.004267
7+17+7	0.16676184	0.0624439	-0.1324745	-0.0102207	0.1058479	0.004264
7+21+7	0.16676185	0.0624439	-0.1324744	-0.0102204	0.1058480	0.004266
7+23+7	0.16676185	0.0624439	-0.1324745	-0.0102209	0.1058471	0.004264
7+25+7	0.16676184	0.0624439	-0.1324745	-0.0102209	0.1058472	0.004264
7+27+7	0.16676184	0.0624439	-0.1324745	-0.0102208	0.1058470	0.004263
7+29+7	0.16676180	0.0624438	-0.1324748	-0.0102213	0.1058461	0.004263
7+31+7	0.16676181	0.0624438	-0.1324748	-0.0102212	0.1058462	0.004262
7+33+7	0.16676187	0.0624440	-0.1324743	-0.0102201	0.1058485	0.004262

Table 5.5. *Comparison of converged values of the SIFs with those reported by Li et al. [44].*

SIFs	Collocation Trefftz method [44]	SFBIM (present work)
d_1	2.12751351	2.1275134
d_2	−1.0366925	−1.036692
d_3	0.0371711	0.037170
d_4	0.117749	0.11775
d_5	−0.122728	−0.12273
d_6	−0.109909	−0.10991
d_7	−0.002255	−0.00226
d_8	0.006863	0.00686
d_9	−0.005936	−0.00594
d_{10}	−0.011032	−0.01103
c_1	0.1667621	0.166762
c_2	0.0624433	0.062444
c_3	−0.1324738	−0.132474
c_4	−0.010221	−0.01022
c_5	0.105846	0.10585
c_6	0.031153	0.03115
c_7	−0.007149	−0.00714
c_8	−0.001684	−0.00169
c_9	0.009484	0.00950
c_{10}	0.004281	0.00426

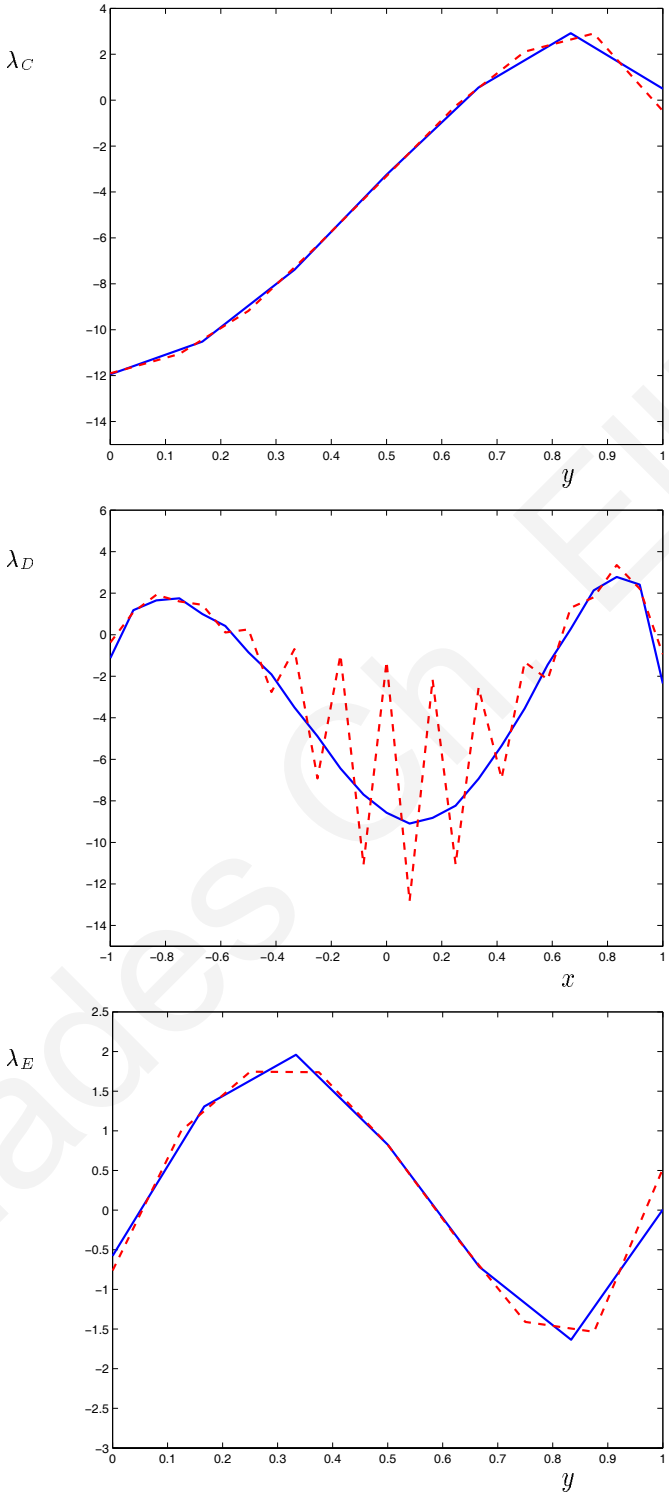

Figure 5.3. *Calculated Lagrange multipliers along* S_C, S_D, S_E, *with* $2N_\alpha = 94$; N_λ=39 *(solid,* N_{λ_C}=N_{λ_E}=7, N_{λ_D}=25*) and* N_λ=43 *(dashed,* N_{λ_C}=N_{λ_E}=9, N_{λ_D}=25*).*

inaccuracies introduced by the high-order singular functions. Tables 5.3 and 5.4 show the effect of varying $N_\lambda = N_{\lambda_C} + N_{\lambda_D} + N_{\lambda_E}$, when $2N_\alpha = 94$. Again, fast convergence is observed initially but as N_λ approaches the value of $2N_\alpha$, the results start diverging slowly, which is attributed to the fact that the stiffness matrix becomes ill-conditioned. These computations suggest that the "optimal" values for the numbers of singular functions and Lagrange multipliers are respectively $2N_\alpha = 94$ and $N_\lambda = 39$. For higher values of $2N_\alpha$ (e.g. $2N_\alpha = 120$) satisfactory values of the SIFs are still obtained, but the quality of the global solution is not very good. When comparing the performance of the method with that in the case of Laplacian problems [22, 23, 29, 30], we note that convergence is slower in the case of the biharmonic equation, which is reasonable since the latter is more complicated than the Laplace equation. If the smoothness of the calculated Lagrange multiplier functions is used as an indication of the quality of the solution, then for the combination of $2N_\alpha = 94$ and $N_\lambda = 39$, the calculated Lagrange multiplier functions along boundary parts S_C, S_D and S_E, are the smoothest possible (see Figure 5.3). We note that for a slightly different value of N_λ the estimated values of the SIFs are essentially unaffected, while the calculated Lagrange multipliers exhibit oscillations.

In Table 5.5 the converged values of coefficients d_i and $c_i, i = 1, ..., 10$, obtained with the SFBIM are compared with the most accurate values obtained by the collocation Trefftz method of Li et al. [44], who reported that the leading SIF, d_1, is converged up to the seventh significant digit. The SFBIM appears to be more accurate as it achieves convergence up to the eighth significant digit. Since Li et al. [44] do not provide information about the convergence of the other SIFs, in Table 5.5 we tabulate their computed values with one additional digit than the converged values of the SFBIM. Nevertheless, there is excellent agreement between the results of the two methods. Finally, Figures 5.4 and 5.5 show the surface plots of the solution u and

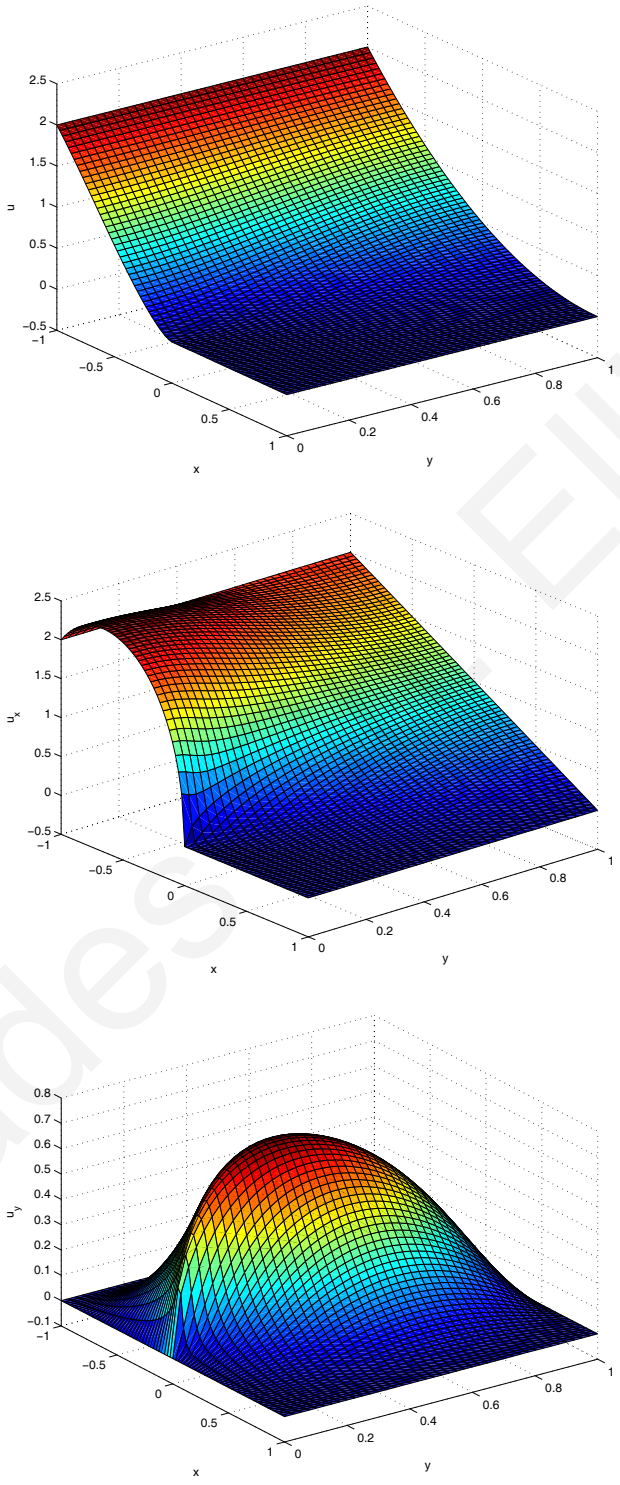

Figure 5.4. *Plots of the converged solution u (top) and its first derivatives u_x (middle) and u_y (bottom).*

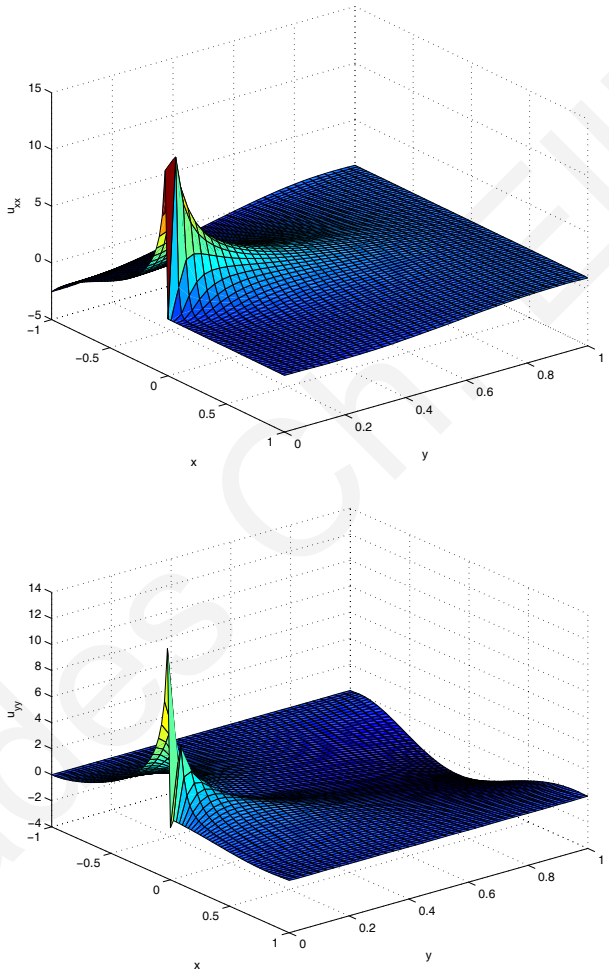

Figure 5.5. *Plots of u_{xx} (top) and u_{yy} (bottom).*

its partial derivatives u_x, u_y, u_{xx}, u_{yy}. The effect of the singularity at O is clearly visible in these profiles.

5.5 Conclusions

The singular function boundary integral method (SFBIM) has been developed for solving two-dimensional fracture problems in terms of the Airy stress function. In this method the leading terms of the asymptotic solution are used to approximate the solution and thus the SIFs are calculated directly (i.e. no post-processing of the numerical solution is required). The governing biharmonic equation is weighted by the singular functions in the Galerkin sense, and the discretized equations are then reduced to boundary integrals by means of a double application of the divergence theorem, which leads to a significant reduction in the computational cost. Another attractive feature of the method is that integration is necessary only along boundary parts that are away from the crack tip. The Dirichlet boundary conditions are weakly enforced by means of Lagrange multipliers which, depending on the type of the boundary conditions, may replace either $\partial u/\partial n$ or $\partial \nabla^2 u/\partial n$ in the integrands of the discretized equations. The Lagrange multipliers are calculated together with the SIFs.

The SFBIM has been applied to a model problem proposed by Schiff et al. [65]. The numerical calculations showed that the method converges very fast with the number of singular functions and the number of Lagrange multipliers, and yields accurate estimates of the leading SIFs. The value of the leading SIF, in particular, is converged up to eight significant digits. Our results agree well with the values obtained by Li et al. [44] using the collocation Trefftz method.

Chapter 6

Analysis of the SFBIM

In this chapter we present the analysis of the singular function boundary integral method (SFBIM) for a two-dimensional Laplace equation problem with only one singular point[1]. Convergence analysis is used to obtain upper bounds on the error created in the approximate solution and in the estimation of the singular coefficients. Throughout this chapter the usual notation $H^{\kappa}(\Omega)$ will be used for spaces containing functions of the domain $\Omega \subset \mathbf{R^2}$ with boundary $\partial\Omega$, having κ generalized derivatives in $L^2(\Omega)$. The norm and semi-norm on $H^{\kappa}(\Omega)$ will be denoted by $||.||_{\kappa,\Omega}$ and $|.|_{\kappa,\Omega}$, respectively.

6.1 The model problem and its formulation

In order to analyse the SFBIM we consider the problem of Figure 6.1:

$$\nabla^2 u = 0, \qquad \text{in } \Omega, \tag{6.1}$$

[1] The material of this chapter appears in [79].

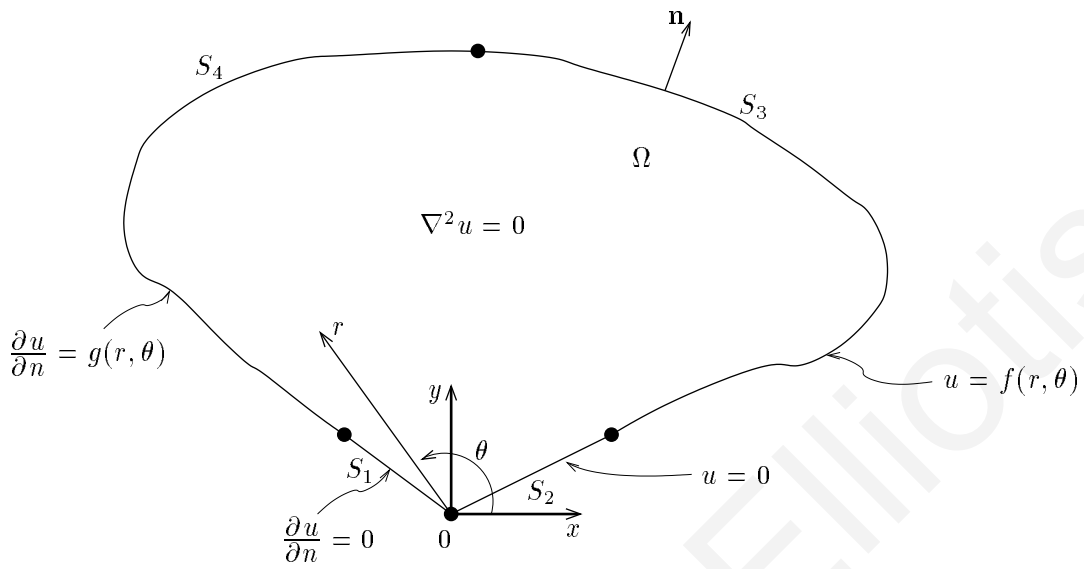

Figure 6.1. *Laplacian problem with one singular point.*

with

$$\left.\begin{array}{lll} \dfrac{\partial u}{\partial n} = 0 & \text{on} & S_1 \\ u = 0 & \text{on} & S_2 \\ u = f(r,\theta) & \text{on} & S_3 \\ \dfrac{\partial u}{\partial n} = g(r,\theta) & \text{on} & S_4 \end{array}\right\}, \tag{6.2}$$

where $\partial\Omega = \cup_{i=1}^{4} S_i$.

Variables (r, θ) denote polar coordinates centered at O, while functions $f(r,\theta)$ and $g(r,\theta)$ are assumed to be smooth and such that there is only one boundary singularity at O. In previous chapters we saw that the local solution near O is given by an expansion of the form

$$u(r,\theta) = \sum_{j=1}^{\infty} \alpha_j \, r^{\mu_j} \, \phi_j(\theta) \,, \tag{6.3}$$

where α_j are the unknown singular coefficients, μ_j are the singularity powers arranged in ascending order, and the functions $\phi_j(\theta)$ represent the θ-dependence of the eigensolution. The coefficients α_j are the so-called (Generalized) Stress Intensity Factors, and μ_j are also known

as the eigenvalues of the problem. Functions $r^{\mu_j}\,\phi_j(\theta)$ are called the singular functions.

Now, suppose v is a function chosen to satisfy

$$\nabla^2 v \;=\; 0, \qquad\qquad \text{in} \;\; \Omega\,, \tag{6.4}$$

with

$$\left.\begin{array}{lll} \dfrac{\partial v}{\partial n} \;=\; 0 & \text{on} & S_1 \\ v \;=\; 0 & \text{on} & S_2 \end{array}\right\}\,. \tag{6.5}$$

(For example, $v{=}r^{\mu_j}\,\phi_j(\theta)$.) Now, multiplying (6.1) by v and integrating over Ω we obtain

$$\int_\Omega v\,\nabla^2 u \;=\; 0\,. \tag{6.6}$$

By employing Green's theorem we get

$$\int_\Omega v\,\nabla^2 u \;=\; -\int_\Omega \nabla v\,\nabla u + \int_{\partial\Omega} v\,\frac{\partial u}{\partial n} \;=\; 0 \tag{6.7}$$

and by considering the boundary conditions (6.2) the above expression takes the following form:

$$\int_\Omega \nabla v\,\nabla u \;-\; \int_{S_2} v\,\frac{\partial u}{\partial n} \;-\; \int_{S_3} v\,\frac{\partial u}{\partial n} \;=\; \int_{S_4} v\,g\,. \tag{6.8}$$

Furthermore, by considering the boundary conditions (6.5) of function v then (6.8) becomes

$$\int_\Omega \nabla v\,\nabla u \;-\; \int_{S_3} v\,\frac{\partial u}{\partial n} \;=\; \int_{S_4} v\,g\,. \tag{6.9}$$

From (6.9), using Green's theorem once more, we get

$$-\int_\Omega u\,\nabla^2 v \;+\; \int_{\partial\Omega} u\,\frac{\partial v}{\partial n} \;-\; \int_{S_3} v\,\frac{\partial u}{\partial n} \;=\; \int_{S_4} v\,g \tag{6.10}$$

and using conditions (6.2) and (6.5) we have

$$\int_{S_3} u\,\frac{\partial v}{\partial n} \;+\; \int_{S_4} u\,\frac{\partial v}{\partial n} \;-\; \int_{S_3} v\,\frac{\partial u}{\partial n} \;=\; \int_{S_4} v\,g \tag{6.11}$$

which is the equation that we have discretized in previous chapters.

Now, let us go back to (6.9). Since $u=f$ on S_3 we have

$$-\int_{S_3} \frac{\partial v}{\partial n}\,(u\,-\,f)\,=\,0\,, \tag{6.12}$$

and therefore by adding this to (6.9) we obtain

$$\int_\Omega \nabla v\,\nabla u\,-\int_{S_3} v\,\frac{\partial u}{\partial n}\,-\int_{S_3}\frac{\partial v}{\partial n}\,(u\,-\,f)\,=\,\int_{S_4} v\,g\,. \tag{6.13}$$

Let

$$\lambda\,=\,\frac{\partial u}{\partial n}\quad\text{and}\quad\mu\,=\,\frac{\partial v}{\partial n}\,. \tag{6.14}$$

Then equation (6.13) can be expressed as the following variational problem:

Problem 1: Find $(u,\lambda)\in V_1\times V_2$ such that

$$B\,(u,v)\,+\,b\,(u,v;\lambda,\mu)\,=\,F\,(v,\mu)\;\forall\;(v,\mu)\,\in\,V_1\times V_2\,, \tag{6.15}$$

where

$$\left.\begin{aligned} B\,(u,v)\,&=\,\textstyle\int_\Omega \nabla v\,\nabla u\\ b\,(u,v;\lambda,\mu)\,&=\,-\textstyle\int_{S_3}\lambda\,v\,-\int_{S_3}\mu\,u\\ F\,(v,\mu)\,&=\,\textstyle\int_{S_4} v\,g\,-\int_{S_3}\mu\,f \end{aligned}\right\}\,. \tag{6.16}$$

The spaces V_1 and V_2 in (6.15) are chosen as

$$V_1\,=\,H^1_*\,(\Omega)\quad\text{and}\quad V_2\,=\,H^{-\frac{1}{2}}\,(S_3)\,, \tag{6.17}$$

where

$$H^1_*\,(\Omega)\,=\,\left\{u\,\in\,H^1\,(\Omega):u|_{S_2}\,=\,0\right\}\,, \tag{6.18}$$

and the space $H^{-\frac{1}{2}}$ is defined as follows: Let

$$H^{\frac{1}{2}}\,(\partial\Omega)\,=\,\left\{u\,\in\,H^1\,(\Omega):u|_{\partial\Omega}\,\in\,L^2\,(\partial\Omega)\right\} \tag{6.19}$$

and let

$$T : H^1(\Omega) \rightarrow H^{\frac{1}{2}}(\partial\Omega)$$

be the trace operator. The norm of $H^{\frac{1}{2}}(\partial\Omega)$ is defined as

$$||\psi||_{\frac{1}{2},\partial\Omega} = \inf_{u \in H^1(\Omega)} \{||u||_{1,\Omega} : Tu = \psi\} . \tag{6.20}$$

Then the space $H^{-\frac{1}{2}}(\partial\Omega)$ is defined as

$$H^{-\frac{1}{2}}(\partial\Omega) = \overline{H^0(\partial\Omega)}^{||.||_{-\frac{1}{2},\partial\Omega}} , \tag{6.21}$$

i.e. the closure of $H^0(\partial\Omega)$ with respect to the norm

$$||\phi||_{-\frac{1}{2},\partial\Omega} = \sup_{\psi \in H^{\frac{1}{2}}(\partial\Omega)} \frac{\int_{\partial\Omega} \phi\, \psi}{||\psi||_{\frac{1}{2},\partial\Omega}} . \tag{6.22}$$

(See [59] for more details on these spaces.)

6.2 Error Analysis

First we present the discrete analog to Problem 1. To this end, let the boundary part S_3 be divided into sections Γ_i, with $i = 1, \cdots, n$ such that $S_3 = \cup_{i=1}^{n} \Gamma_i$. Let $h_i = |\Gamma_i|$ and set $h = \max_{1 \leq i \leq n} h_i$. Now, let

$$v_j = r^{\beta_j} \phi_j(\theta)$$

denote the singular functions, and define the following finite dimensional space:

$$V_1{}^N = span\{v_j\}_{j=1}^{N} . \tag{6.23}$$

We assume that for each segment Γ_i, there exists an invertible mapping $F_i : I \rightarrow \Gamma_i$ which maps the interval I=[-1,1] to Γ_i, and we define the space

$$V_2{}^h = \left\{ \lambda_h : \lambda_h|_{\Gamma_i} \circ F_i^{-1} \in P_k(I),\ i = 1, \cdots, n \right\} , \tag{6.24}$$

where $P_k\,(I)$ denotes the set of polynomials of degree $\leq k$ on S_3. In practice, the representation of the boundary S_3 determines the mappings F_i; i.e., if S_3 is represented by a polynomial then an isoparametric mapping may be used, and if S_3 has some (general) parametric representation, then the *blending map* technique may be used (see Ch. 6 in [71]). Then the discrete version of (6.15) is the following:

Problem 2: Find $(u_N,\lambda_h) \in [{V_1}^N \times {V_2}^h] \subset [H^1_* \times H^{-\frac{1}{2}}\,(S_3)]$ such that

$$B\,(u_N, v) \,+\, b\,(u_N, v; \lambda_h, \mu) \;=\; F\,(v, \mu) \quad \forall\ (v, \mu) \,\in\, {V_1}^N \times {V_2}^h\,, \tag{6.25}$$

with $B\,(u_N, v)$, $b\,(u_N, v; \lambda_h, \mu)$ and $F\,(v, \mu)$ given by (6.16).

We have the following theorem:

Theorem 1: Let (u,λ) and (u_N,λ_h) be the solutions to problems 1 and 2, respectively. Suppose there exist positive constants c_0, c, β and γ, independent of N and h such that the following three conditions hold:

$$B\,(v, v) \geq c_0\,||v||^2_{1,\Omega} \qquad \text{and} \qquad |B\,(u, v)| \leq c\,||u||_{1,\Omega}\,||v||_{1,\Omega} \quad \forall\ v \;\in\; {V_1}^N\,, \tag{6.26}$$

$$\exists\, 0 \neq v_N \;\in {V_1}^N \;\ni\; |\int_{S_3} \mu_h\, v_N| \geq \beta\,||\mu_h||_{-\frac{1}{2},S_3}\,||v_N||_{1,\Omega} \quad \forall\ \mu_h \;\in\; {V_2}^h\,, \tag{6.27}$$

$$|\int_{S_3} \lambda\, v| \leq \gamma\,||\lambda||_{-\frac{1}{2},S_3}\,||v||_{1,\Omega} \quad \forall\ v \in {V_1}^N\,. \tag{6.28}$$

Then,

$$||u \,-\, u_N||_{1,\Omega} \,+ ||\lambda -\, \lambda_h||_{-\frac{1}{2},S_3} \leq C\,\left\{ \inf_{v \in {V_1}^N} ||u -\, v||_{1,\Omega} \,+\, \inf_{\eta \in {V_2}^h} ||\lambda -\, \eta||_{-\frac{1}{2},S_3} \right\}\,, \tag{6.29}$$

with $C \in \mathbf{R}^+$ independent of N and h.

For a proof of the above see [79] or Theorem 6.1 in [41]. Before we verify that (6.26)–(6.28) hold for our problem, consider the following: For any $w \;=\; \sum_{j=1}^{\infty} \alpha_j\, v_j$ we can always write

$$w \;=\; w_N \,+ r_N\,,$$

where

$$w_N = \sum_{j=1}^{N} \alpha_j v_j \in {V_1}^N, \quad \text{and} \quad r_N = \sum_{j=N+1}^{\infty} \alpha_j v_j, \tag{6.30}$$

with α_j the true singular coefficients. We will assume that there exists a constant $\alpha \in (0,1)$ such that

$$|r_N| \leq C\, \alpha^N \tag{A1}$$

and

$$|\frac{\partial r_N}{\partial r}| \leq C\, N\, \alpha^N . \tag{A2}$$

If $r < 1$ in the local solution (6.3), assumptions (A1) and (A2) hold trivially, since then, by the fact that ϕ_j is harmonic and the singular coefficients are bounded we have

$$|r_N| \leq \sum_{j=N+1}^{\infty} |\alpha_j|\, r^{\beta_j} \leq C\, \frac{r^{\beta_N + 1}}{1 - r} \leq C\, \alpha^N ,$$

with $r < \alpha < 1$ and $C \in \mathbf{R}^+$ independent of α and N. Similarly,

$$|\frac{\partial r_N}{\partial r}| \leq \sum_{j=N+1}^{\infty} |\alpha_j|\, r^{\beta_j - 1} = \sum_{j=N+1}^{\infty} |\alpha_j| \left\{ \frac{d}{dr} \int_0^r \rho^{\beta_j - 1}\, d\rho \right\}$$

$$= \frac{d}{dr} \left(\sum_{j=N+1}^{\infty} |\alpha_j| \left\{ \int_0^r \rho^{\beta_j - 1}\, d\rho \right\} \right)$$

$$= \frac{d}{dr} \left(\sum_{j=N+1}^{\infty} |\alpha_j|\, r^{\beta_j} \right) \leq C\, \frac{d}{dr} \left(\frac{r^{\beta_N + 1}}{1 - r} \right) \leq C\, N\, \alpha^N .$$

In the case $r \geq 1$ one may partition the domain Ω into subdomains in which separate approximations may be obtained, including one near 0 that is valid for $r < 1$. The solution over the entire domain can be composed by combining solutions from each subdomain and properly dealing with their interactions across the interfaces separating them (see, e.g., [40]).

We are now ready to verify that (6.26)–(6.28) hold for the problem given by equation (6.25). We may note that $B(v,v)=|v|^2_{1,\Omega}$. So, by Poincaré's inequality we have

$$B\,(v,v) \geq c_0\,||v||^2_{1,\Omega} \quad \forall\ v\ \in H^1_*\,(\Omega)\ . \tag{6.31}$$

Also, by the Cauchy-Schwartz inequality we obtain

$$B\,(u,v)\ \leq\ c\,||u||_{1,\Omega}\,||v||_{1,\Omega} \quad \forall\ u,v\ \in H^1_*\,(\Omega) \tag{6.32}$$

and therefore (6.26) is verified. In order to verify (6.27) we consider the following auxiliary problem:

$$\nabla^2 w\ =\ 0, \qquad \text{in}\ \ \Omega\,, \tag{6.33}$$

with

$$\frac{\partial w}{\partial n}\ =\ \mu_h \quad \text{on}\ \ S_3\,, \tag{6.34}$$

$$w\ =\ 0 \quad \text{on}\ \ S_2\,, \tag{6.35}$$

$$\frac{\partial w}{\partial n}\ =\ 0 \quad \text{on}\ \ S_1 \cup S_4\,, \tag{6.36}$$

where $\mu_h\ \in\ V^h_2$ in (6.34). By using Green's formula and Poincaré's inequality, (6.33) and (6.34) give

$$\int_{S_3} \mu_h w\ =\ \int_{S_3} w\,\frac{\partial w}{\partial n}\ =\ \int_\Omega w\nabla^2 w\ +\ \int_\Omega |\nabla w|^2\,|w|^2_{1,\Omega} \geq c_0\,||w||^2_{1,\Omega} \tag{6.37}$$

with $c_0 \in \mathbf{R}^+$. Now,

$$||\mu_h||_{-\frac{1}{2},S_3}\ =\ ||\frac{\partial w}{\partial n}||_{-\frac{1}{2},S_3} \leq C||w||_{1,\Omega}\,, \tag{6.38}$$

which is a standard inequality [5]. So, by (6.37) and (6.38)

$$\int_{S_3} \mu_h w \geq c_0\,||w||^2_{1,\Omega} \geq \beta\,||w||_{1,\Omega}\,||\mu_h||_{-\frac{1}{2},S_3}\ , \tag{6.39}$$

with $\beta \in \mathbf{R}^+$ independent of w and h. Now, let $w_N \in V_1^N$ be such that $w{=}w_N + r_N$, as given by (6.30). We have

$$\int_{S_3} \mu_h w_N \;=\; \int_{S_3} \mu_h \, w \;-\; \int_{S_3} \mu_h \, r_N \;, \tag{6.40}$$

and also (by standard inequalities and the definition of $||.||_{-\frac{1}{2},\partial\Omega}$, cf. [5])

$$\int_{S_3} \mu_h r_N \leq ||\mu_h||_{-\frac{1}{2},S_3} \, ||r_N||_{\frac{1}{2},S_3} \leq C_1 \, ||\mu_h||_{-\frac{1}{2},S_3} \, ||r_N||_{1,\Omega} \;. \tag{6.41}$$

Now, combining (6.39), (6.40) and (6.41) we obtain

$$\int_{S_3} \mu_h \, w_N \geq \beta \, ||w||_{1,\Omega} \, ||\mu_h||_{-\frac{1}{2},S_3} \;-\; C_1 \, ||\mu_h||_{-\frac{1}{2},S_3} \, ||r_N||_{1,\Omega} \;. \tag{6.42}$$

From the reverse triangle inequality,

$$||w||_{1,\Omega} \;=\; ||w_N \, + r_N||_{1,\Omega} \geq ||w_N||_{1,\Omega} \;-\; ||r_N||_{1,\Omega} \;, \tag{6.43}$$

and (6.42), we get

$$\int_{S_3} \mu_h \, w_N \geq \beta \;(||w||_{1,\Omega} \;- ||r_N||_{1,\Omega}) \; ||\mu_h||_{-\frac{1}{2},S_3} \;-\; C_1 \, ||\mu_h||_{-\frac{1}{2},S_3} \, ||r_N||_{1,\Omega}$$

and therefore

$$\int_{S_3} \mu_h \, w_N \geq \beta \, ||w||_{1,\Omega} \, ||\mu_h||_{-\frac{1}{2},S_3} \;-\; (C_1 \, + \beta) \; ||\mu_h||_{-\frac{1}{2},S_3} \, ||r_N||_{1,\Omega} \;. \tag{6.44}$$

Since by assumption (A1), r_N converges to zero exponentially, we have

$$0 \leq \frac{||r_N||_{1,\Omega}}{||w_N||_{1,\Omega}} \;<\; 1 \;,$$

and for N sufficiently large we may write

$$\frac{||r_N||_{1,\Omega}}{||w_N||_{1,\Omega}} \leq \frac{\beta}{2 \; (C_1 \, + \beta)} \;. \tag{6.45}$$

The combination of (6.44) and (6.45) yields

$$\int_{S_3} \mu_h \, w_N \geq \frac{\beta}{2} \, ||\mu_h||_{-\frac{1}{2},S_3} \, ||w_N||_{1,\Omega} \;, \tag{6.46}$$

which gives (6.27) once we replace w_N by v_N and $\frac{\beta}{2}$ by β.

Finally, condition (6.28) follows from the defition of $H^{-\frac{1}{2}}$-norm. We have

$$\int_{S_3} \lambda\, v \leq ||\lambda||_{-\frac{1}{2},S_3}\, ||v||_{\frac{1}{2},S_3} \quad \forall\ v \in V_1^N\ ,$$

and by the using standard inequality [5]

$$||v||_{\frac{1}{2},S_3} \leq \gamma\, ||v||_{1,\Omega}\ ,\ \gamma \in \mathbf{R}^+$$

we obtain

$$|\int_{S_3} \lambda\, v| \leq ||\lambda||_{-\frac{1}{2},S_3}\, ||v||_{1,\Omega} \quad \forall\ v \in V_1^N\ . \tag{6.47}$$

The above discussion leads to the following theorem.

Theorem 2: Let (u,λ) and (u_N,λ_h) be the solutions to problems 1 and 2, respectively. If $\lambda \in H^{k+1}(S_3)$ then there exists a positive constant C, independent of N and h, such that

$$||u\ -u_N||_{1,\Omega}\ +||\lambda -\ \lambda_h||_{-\frac{1}{2},S_3} \leq C\ \left\{N\,\alpha^N\ +h^{k+1}\right\}\ , \tag{6.48}$$

with $C \in \mathbf{R}^+$ independent of N and h and $k, N \in \mathbf{N}$.

Proof: From Theorem 1 we have

$$||u\ -u_N||_{1,\Omega}\ +||\lambda -\ \lambda_h||_{-\frac{1}{2},S_3} \leq C\ \left\{\inf_{v\in {V_1}^N} ||u-\ v||_{1,\Omega}\ +\ \inf_{\eta\in {V_2}^h} ||\lambda -\ \eta||_{-\frac{1}{2},S_3}\right\}\ . \tag{6.49}$$

Recall that for any $w\ =\ \sum_{j=1}^{\infty}\ \alpha_j\ v_j$ we can always write

$$w\ =\ w_N\ +r_N\ ,$$

where

$$w_N\ =\ \sum_{j=1}^{N}\ \alpha_j\ v_j\ \in\ {V_1}^N\ ,\quad \text{and}\quad r_N\ =\ \sum_{j=N+1}^{\infty}\ \alpha_j\ v_j\ .$$

Then we have

$$\inf_{v\in {V_1}^N} ||u-\ v||_{1,\Omega} \leq ||u-\ w_N||_{1,\Omega}\ =\ ||r_N||_{1,\Omega}\ .$$

Using assumptions (A1) and (A2) and the definitions of $||.||_{0,\Omega}$ and $||.||_{1,\Omega}$ we get

$$\inf_{v \in {V_1}^N} ||u - v||_{1,\Omega} \leq ||r_N||_{1,\Omega} = \left(||r_N||^2_{0,\Omega} + ||\frac{\partial r_N}{\partial r}||^2_{0,\Omega} + ||\frac{1}{r}\frac{\partial r_N}{\partial \theta}||^2_{0,\Omega} \right)^{\frac{1}{2}}$$

$$\leq C_* \left[(C_0\,\alpha^N)^2 + (C_0\,N\,\alpha^N)^2 + (C_0\,N\,\alpha^N)^2 \right]^{\frac{1}{2}} \qquad C_*, C_0 \in \mathbf{R}^+ ,$$

$$\leq C\,N\,\alpha^N , \tag{6.50}$$

where the constant $C > 0$ is independent of N and α. Next let λ_I be the k^{th}-order interpolant of λ. Then, since $\lambda \in H^{k+1}(S_3)$ and λ_h is the best approximation, from the projection theorem we have:

$$||\lambda - \lambda_h||_{-\frac{1}{2},S_3} \leq ||\lambda - \lambda_h||_{0,S_3} \leq ||\lambda - \lambda_I||_{0,S_3} .$$

Also, using the interpolation result

$$||\lambda - \lambda_I||_{0,S_3} \leq h^{k+1}\,||\lambda||_{k+1,S_3} = C\,h^{k+1} , \qquad C \in \mathbf{R}^+ ,$$

we obtain

$$||\lambda - \lambda_h||_{-\frac{1}{2},S_3} \leq C\,h^{k+1} ,$$

which by means of (6.50) gives

$$||u - u_N||_{1,\Omega} + ||\lambda - \lambda_h||_{-\frac{1}{2},S_3} \leq C \left\{ N\,\alpha^N + h^{k+1} \right\} ,$$

with $C \in \mathbf{R}^+$ independent of N, α, h and k. □

Remark: Based on the above theorem, one may obtain the *optimal* matching between N and h, i.e. the relationship between the number of singular functions and the number of Lagrange multipliers used in the method, by choosing $h^{k+1} \approx N\,\alpha^N$. We then have

$$(k+1)\ln h \approx \ln N + N \ln \alpha .$$

For N sufficiently large, $N \gg \ln N$ and therefore

$$(k\ +1)\ln h \approx N\ \ln\ \alpha\ ,$$

from which we have the following approximate expression for N:

$$N \approx (k\ +1)\frac{\ln h}{\ln \alpha}\ . \tag{6.51}$$

In the case of a uniform discretization of boundary S_3, all subintervals Γ_i have length h_i equal to h. Then the number of Lagrange multipliers is $N_\lambda\ =\ \frac{|S_3|}{h}\ +1$. Therefore, (6.51) becomes

$$N \approx (k\ +1)\ \frac{\ln\left(\frac{|S_3|}{N_\lambda\ -1}\right)}{\ln \alpha}\ . \tag{6.52}$$

Let us illustrate how to find the value of α in the case of the Dirichlet problem considered in Chapter 3. Since we are using quadratic basis functions, we have $k\ =\ 2$ while the length of S_3 is equal to 2 (i.e. $|S_3|\ =\ 2$). We fix for a moment the number of elements n, e.g. say $n=\ 8$ which amounts to $N_\lambda\ =\ 17$, and we solve the linear system of discretized equations, which is created by applying the SFBIM for various values of $N > N_\lambda$ (e.g., $N\ =\ 19,\ 21,\ 23, \cdots$). We concentrate only on the calculation of the first singular coefficient α_1 and record our results in Table 6.1 which shows that for the choice N_λ=17 the value of α_1 does not change once N=35. Thus, from (6.52), and with N_λ=17 and N=35, we find that $\alpha \approx\ 0.89$. Now, with α known, we may compute other quantities of interest by choosing N and N_λ via equation (6.52). For example for N_λ=41 (i.e. h=$\frac{1}{10}$) we find that $N \approx\ 60$ which, in fact, is the combination used for the Dirichlet problem discussed in Chapter 3.

The approximation of the singular coefficients is given by the following:

Corollary: Let $u\ =\ \sum_{j=1}^{\infty}\ \alpha_j\ r^{\beta_j}\ \phi_j\,(\theta)$ and $u_N\ =\ \sum_{j=1}^{N}\ \alpha_j^N\ r^{\beta_j}\ \phi_j\,(\theta)$ satisfy problems 1 and 2, respectively, with α_j, α_j^N denoting the true and approximate singular coefficients.

Table 6.1. *Values of* α_1 *with* N_λ=17.

N	α_1
19	1.12797929883135
21	1.12798071689013
23	1.12798444682112
25	1.12798040013968
27	1.12798040107216
29	1.12798040105877
31	1.12798040105983
33	1.12798040105939
35	1.12798040105939

Then, there exists a positive constant $C \in \mathbf{R}^+$, independent of N and α, such that

$$|\alpha_j - \alpha_j^N| \leq C\, \alpha^N \,.$$

Proof: We have already seen that

$$\inf_{v \in V_1^N} ||u - v||_{0,\Omega} \leq ||r_N||_{0,\Omega} \leq C\, \alpha^N \qquad C \in \mathbf{R}^+ \,. \quad (6.53)$$

Now, with

$$u = \sum_{j=1}^{\infty} \alpha_j\, r^{\beta_j}\, \phi_j(\theta) \quad \text{and} \quad u_N = \sum_{j=1}^{N} \alpha_j^N\, r^{\beta_j}\, \phi_j(\theta)\,,$$

we have

$$u - u_N = \sum_{j=1}^{N} (\alpha_j - \alpha_j^N)\, r^{\beta_j}\, \phi_j(\theta) + \sum_{j=N+1}^{\infty} \alpha_j\, r^{\beta_j}\, \phi_j(\theta)\,.$$

Without loss of generality, we assume that singular functions $w_j = r^{\beta_j}\,\phi_j(\theta)$ are orthogonal on Ω. For example, in the case of Dirichlet problem studied in Chapter 3 we have

$$\phi_j(\theta) \;=\; \sin[\frac{2}{3}(2\,j\;-\;1)\,\theta]\,, \qquad -\pi \le\; \theta < \pi\,, \tag{6.54}$$

which is a 2π-periodic function. By multiplying both sides of (6.54) by $\phi_i(\theta)$ and integrating w.r.t. θ form -π to π we see that all terms with $i \neq j$ vanish. Indeed,

$$\int_{-\pi}^{\pi} \sin[\frac{2}{3}\,(2\,j\;-\;1)\,\theta]\;\sin[\frac{2}{3}\,(2\,i\;-\;1)\,\theta]\,d\theta \;=\; \begin{cases} 0\,, & \text{if} \quad i \neq j\,, \\ \\ \pi\,, & \text{if} \quad i \;=\; j \ge\; 1\,. \end{cases}$$

In general, we have

$$\int_{\Omega} w_j\,w_i \begin{cases} \;=\; 0\,, & \text{if} \quad i \neq j\,, \\ \\ \;\neq\; 0\,, & \text{if} \quad i \;=\; j \ge\; 1\,. \end{cases}$$

Therefore,

$$\int_{\Omega}(u\;-\;u_N)\,w_i \;=\; (\alpha_i\;-\alpha_i^N)\int_{\Omega} w_i^2\,, \qquad\qquad i < N\;+\;1\,.$$

Let $\int_{\Omega}\; w_i^2 \;=\; \frac{1}{C_0}$, where $C_0 \in \mathbf{R}^+$. Then,

$$|\alpha_i\;-\alpha_i^N| \;=\; C_0\int_{\Omega}(u\;-u_N)\,w_i \;\le C_0\;\max_{\Omega}|w_i|\;\int_{\Omega}(u\;-u_N)$$

$$\le \bar{C}_0\int_{\Omega}(u\;-\;u_N) \le \bar{C}_0[\int_{\Omega}\,(u\;-\;u_N)^2]^{\frac{1}{2}}\;[\int_{\Omega}\,1^2]^{\frac{1}{2}} \;=$$

$$C_1\,[\int_{\Omega}\,(u\;-\;u_N)^2]^{\frac{1}{2}} \;=\; C_1\,||u\;-\;u_N||_{0,\Omega} \;=\; C_1\,||r_N||_{0,\Omega}\,, \qquad \bar{C}_0, C_1 \in \mathbf{R}^+\,.$$

Thus, by (6.53) we finally have

$$|\alpha_i\;-\alpha_i^N| \le C\;\alpha^N\,, \qquad C \in \mathbf{R}^+\,. \quad \square$$

Note that the above corollary shows the exponential convergence of the SFBIM, which was illustrated in the applications presented in previous chapters on Laplacian and biharmonic problems.

6.3 Conclusions

In this Chapter we analysed the Singular Function Boundary Integral Method for elliptic problems with boundary singularities. We studied, mainly, the convergence of the method and in particular we showed that the method approximates the singular coefficients of the asymptotic expansion at an exponential rate.

We believe that the above analysis of the method can be extended to biharmonic problems with one boundary singularity. This will be one of the goals in our future research.

Chapter 7

Conclusions and future work

In this dissertation a special boundary integral method for the solution of Laplacian and biharmonic problems with boundary singularities has been developed. This method, called the Singular Function Boundary Integral Method (SFBIM), belongs to the family of numerical schemes which incorporate the form of the singularity in the approximation. Two Laplace equation problems over an L-shaped domain, with Dirichlet and mixed boundary conditions (Dirichlet and Neumann), respectively, were solved. In addition, the SFBIM was developed for the case of the stick-slip problem of fluid mechanics and for the case of Schiff's problem of fracture mechanics, both of which are singular biharmonic problems. The observed convergence rate of the SFBIM in singular Laplacian problems was established in Chapter 6.

The application of the SFBIM to the above problems resulted in exponential convergence and results of high accuracy. In fact, comparisons between the results of the present method and those of other methods has indicated that the SFBIM converges faster with respect to the number of singular functions and yields more accurate estimates for the leading singular coefficients and for other parameters (e.g. the values of the velocity components and pressure in the case of the stick-slip problem). In certain cases, numerical results are favorably compared with the analytical solution. The exponential convergence of the method with the number of singular functions, is established theoretically in the last part of the dissertation for the case

of Laplacian problems.

With the SFBIM the governing equation (Laplace or biharmonic) is weighted by the singular functions in the Galerkin sence. A very important characteristic of the method is that the area integrals are reduced to boundary integrals, by means of the divergence theorem, and therefore the computational cost of the method is significantly reduced. Furthermore, with the SFBIM the Dirichlet boundary conditions which are away from the singularity, are weakly enforced by means of Lagrange multipliers, which are expressed in terms of quadratic basis functions. Then, the resulting linear system of the discretized equations is solved directly for the leading singular coefficients and the Lagrange multipliers. It should be emphasized that all the integrations are carried out far from the singularity. The fact that the leading singular coefficients of the local solution expansion are calculated directly together with the Lagrange multipliers, without any post-processing procedure, is another main advantage of the method.

On the other hand, however, the number of Lagrange multipliers should be large enough in order to assure accuracy in the integrations along the boundary (which is subdivided into quadratic elements) but it must be much lower than the number of singular functions, in order to avoid ill-conditioning of the stiffness matrix. Furthermore, the number of singular functions cannot be very high, since the computer accuracy cannot handle the contributions of the higher-order singular functions, which become very small for $r < 1$ or very large for $r > 1$. Finally, the fact that the SFBIM is based on the approximation of the solution by the leading terms of the local solution expansion, implies that the method is restricted to problems in which the domain is a subset of the domain of convergence of the asymptotic expansion.

Several questions still remain open for future research. We list here a few of them:

(i) Analysis of the method in the case of biharmonic problems (rate of convergence,

etc.).

(ii) Study of the condition number of stiffness matrix and of other solution techniques in order to further improve the performance of the method.

(iii) Application of the SFBIM to planar linear elasticity problems where the singular coefficients are, indeed, the *stress intensity factors* (SIFs).

(iv) Combination of the method with other numerical schemes in order to extend the SFBIM to a much wider class of problems than those that can efficiently and effectively be handled by the method (e.g. local application of the SFBIM together with FEM elsewhere in the domain of the problem).

A concluding remark of this work would be that as applied mathematics is playing an ever important role in numerous areas of science, I hope that this dissertation has provoked an interest in using the SFBIM, apart from other numerical schemes, for the solution of singular elliptic and biharmonic problems, which model mathematical problems in physical and biological sciences, in order to obtain results with high accuracy and with low computational cost.

Bibliography

[1] Y.C. Ahn and M.E. Ryan, "A finite difference analysis of the extrudate problem," *Int. J. Numer. Methods Fluids* **13**, 1289-1310 (1991).

[2] M. Arad, Z. Yosibash, G. Ben-Dor and A. Yakhot, "Comparing the flux intensity factors by a boundary element method for elliptic equations with singularities," *J. Commun. Numer. Meth. Eng.* **14**, 657-670 (1998).

[3] F.P.T. Baaijens, "Numerical experiments with a discontinuous Galerkin method including monotonicity enforcement on the stick-slip problem," *J. Non-Newtonian Fluid Mech.* **51**, 141-159 (1994).

[4] F.P.T. Baaijens, "Application of low-order discontinuous Galerkin methods to the analysis of viscoelastic flows," *J. Non-Newtonian Fluid Mech.* **52**, 37-57 (1994).

[5] I. Babuška, "The finite element method with Lagrangian multipliers," *J. Numer. Math.* **20**, 179-192 (1973).

[6] I. Babuška and B. Guo, "The $h-p$ version of the finite element method. Part I : The basic approximation results," *J. Comp. Mech.* **1**, 21-41 (1986).

[7] I. Babuška and M. Suri, "The p and $h-p$ versions of the finite element method, basic principles and properties," *SIAM Review* **36**, No. 4, 578-632 (1994).

[8] I. Babuška and A. Miller, "The post-processing approach in the finite element method – Part 1: Calculation of displacements, stresses and other higher derivatives of the displacements", *Int. J. Numer. Meth. Eng.* **20**, 1085-1109 (1984).

[9] I. Babuška and A. Miller, "The post-processing approach in the finite element method – Part 2: The calculation of stress intensity factors", *Int. J. Numer. Meth. Eng.* **20**, 1111-1129 (1984).

[10] I. Babuška and R. Werner, *Adaptive finite element processes in structural mechanics*, Elliptic problem solvers, II (Monterey, Calif., 1983), 345-377, Academic Press, Orlando, FL (1984).

[11] E.B. Becker, G.F. Carey and J.T. Oden, *Finite Elements*, Prentice Hall, Englewood Cliffs, NJ (1981).

[12] S.C. Brenner, "Overcoming corner singularities using multigrid methods," *SIAM J. Numer. Anal.* **35**, 1883-1892 (1998).

[13] S.C. Brenner, "Multigrid methods for the computation of singular solutions and stress intensity factors I: Corner singularities," *J. Math. Comp.* **68**, 559-583 (1999).

[14] S.C. Brenner and L.R. Scott, *The Mathematical Theory of Finite Element Methods*, Springer-Verlag, New York (1994).

[15] F. Brezzi and M. Fortin, *Mixed and Hybrid Finite Element Methods*, Springer-Verlag, New York (1991).

[16] A.T. Chen and J.R. Rice, "On grid refinement at point singularities for $h-p$ methods," *Int. J. Numer. Meth. Eng.* **33**, 39-57 (1992).

[17] P. G. Ciarlet, *The Finite Element Method for Elliptic Problems*, Classics in Appl. Math. **40**, *SIAM* (2002).

[18] M. Costabel, M. Dauge and S. Nicaise, *Boundary Value Problems and Integral Equations in Nonsmooth Domains*, Marcel Dekker, Inc., New York (1995).

[19] W.R. Dean and P.E. Montagnon, "On the steady motion of viscous liquid in a corner," *Proc. Camb. Phil. Soc.* **45**, 389-394 (1949).

[20] L. Demkowicz, P. Devloo and J.T. Oden, "On an h-type mesh-refinement strategy based on minimization of interpolation errors," *Comput. Methods Appl. Mech. Eng.* **53**, No. 1, 67-89 (1985).

[21] A.A. Dosiyev, "The high accurate block-rigid method for solving Laplace's boundary value problem with singularities," *SIAM J. Numer. Anal.* **42**, 153-178 (2004).

[22] M. Elliotis, G. Georgiou and C. Xenophontos, " The solution of a Laplacian problem over an L-shaped domain with a singular function boundary integral method," *J. Commun. Numer. Meth. Eng.* **18**, 213-222 (2002).

[23] M. Elliotis, G. Georgiou and C. Xenophontos, " Solving Laplacian problems with boundary singularities: A comparison of a singular function boundary integral method with the p/hp version of the finite element method," *J. Appl. Math. Comput.*, in press (2005).

[24] M. Elliotis, G. Georgiou and C. Xenophontos, " Solution of the planar Newtonian stick-slip problem with a singular function boundary integral method," *Int. J. Numer. Methods Fluids*, in press (2005).

[25] M. Elliotis, G. Georgiou and C. Xenophontos, " The singular function boundary integral method for a two-dimensional fracture problem," *J. Engin. Anal. Bound. Elem.*, submitted (2004).

[26] G.J. Fix, 'Singular finite element methods', *Finite Elements. Theory and Application. Chapter 3: " Singular finite element methods,"*, D.L. Dwoyer, M.Y. Hussaini and R.G. Voigt (Eds.), Springer-Verlang, New York (1988).

[27] G.C. Georgiou, L.G. Olson, W.W. Schultz and S. Sagan, "A singular finite element for Stokes flow: the stick-slip problem," *Int. J. Numer. Methods Fluids* **9**, 1353-1367 (1989).

[28] G.C. Georgiou, L.G. Olson and W.W. Schultz, "The integrated singular basis function method for the stick-slip and the die-swell problems," *Int. J. Numer. Methods Fluids* **13**, 1251-1265 (1991).

[29] G.C. Georgiou, L.G. Olson and Y. Smyrlis, "A singular function boundary integral method for the Laplace equation," *J. Commun. Numer. Meth. Eng.* **12**, 127-134 (1996).

[30] G.C. Georgiou, A. Boudouvis and A. Poullikkas, "Comparison of two methods for the computation of singular solutions in elliptic problems," *J. Comput. Appl. Math.* **79**, 277-290 (1997).

[31] P. Grisvard, *Elliptic Problems in Nonsmooth Domains*, Pitman Publishers, Oxford (1995).

[32] I. Herrera and M. Diaz, "Indirect methods of collocation: Trefftz-Herrera collocation," *J. Numer. Meth. Partial Diff. Eqns* **15**, 709-738 (1999).

[33] H. Igarashi and T. Honma, "A boundary element method for potential fields with corner singularities," *J. Appl. Math. Model.* **20**, 847-852 (1996).

[34] D.B. Ingham and M.A. Kelmanson, *Boundary Integral Equation Analyses of Singular Potential and Biharmonic Problems*, Springer-Verlag, Berling pp. 21-51 (1984).

[35] G.R. Irwin, "Analysis of stresses and strains near the end of a crack traversing a plate," *Trans. ASME J. Appl. Mech.* **24**, 361-364 (1957).

[36] W.G. Jin, Y.K. Cheung and O.C. Zienkiewicz, "Trefftz method for Kirchoff plate bending problems," *Int. J. Numer. Meth. Eng.* **36**, 765-781 (1993).

[37] A. Karageorghis, "Modified methods of fundamental solutions for harmonic and biharmonic problems with boundary singularities," *J. Num. Meth. Partial Diff. Eqns* **8**, 1-19 (1992).

[38] M.A. Kelmanson, "An integral equation method for the solution of singular and slow flow problems," *J. Comp. Physics* **51**, 139-158 (1983).

[39] D. Lefeber, *Solving problems with singularities using boundary elements*, Comp. Mech. Publications, Southampton (1984).

[40] Z.C. Li, R. Mathon and P. Sermer, "Boundary methods for solving elliptic problems with singularities and interfaces," *SIAM J. Numer. Anal.* **24**, 487-498 (1987).

[41] Z.C. Li, "Penalty combinations of Ritz-Galerkin and finite-difference methods for singularity problems," *J. Comput. Appl. Math.* **81**, 1-17 (1997).

[42] Z.C. Li, *Combined Methods for Elliptic Equations with Singularities, Interfaces and Infinities*, Kluwer Academic Publishers, Boston (1998).

[43] Z.C. Li and T.T. Lu, "Singularities and treatments of boundary value problems," *J. Math. Comput. Model.* **31**, 97-145 (2000).

[44] Z.C. Li, T.T. Lu and H.Y. Hu, "The collocation Trefftz method for biharmonic equations with crack singularities," *J. Engin. Anal. Bound. Elem.* **28**, 79-96 (2004).

[45] Z.C. Li, Y.L. Chan, G. Georgiou and C. Xenophontos, "Special boundary approximation methods for Laplace's equation with singularities," *J. Comp. Maths. Appl.*, in press (2005).

[46] H.J. Lugt and E.W. Schwiderski, "Flows around dihedral angles, I. Eigenmotion analysis," *Proc. Roy. Soc. London* **A285**, 382-399 (1965).

[47] J. Marsden and A. Tromba, *Vector Analysis*, Transl. by A. Giannopoulos, University of Crete Editions, Heraklion (1992).

[48] F. Michavila, L. Gavete and F. Diez, "Two different approaches for the treatment of boundary singularities," *J. Num. Meth. Partial Diff. Eqns* **43**, 255-282 (1988).

[49] A. Mpakopoulos, *Finite Elements*, National Technical University, Athens (1983).

[50] N.K. Mukhopadhyay, S.K. Maiti and A. Kakodkar, "A review of SIF evaluation and modelling of singularities in BEM," *J. Comp. Mech.* **25**, 358-375 (2000).

[51] V. Ngamaramvaranggul and M.F. Webster, "Computation of free surface flows with a Taylor-Galerkin/pressure-correction algorithm," *Int. J. Numer. Methods Fluids* **33**, 993-1026 (2000).

[52] V. Ngamaramvaranggul and M.F. Webster, "Viscoelastic simulations of stick-slip and die-swell flows," *Int. J. Numer. Methods Fluids* **36**, 539-595 (2001).

[53] M. Normandin, D.G. Radu, A. Mahmoud and J.R. Clermont, "Finite-element and stream-tube formulations for flow computations - two-dimensional applications," *J. Math. and Computers in Simulation* **60**, 129-134 (2002).

[54] L.G. Olson, G.C. Georgiou and W.W. Schultz, "An efficient finite element method for treating singularities in Laplace's equation," *J. Comp. Physics* **96**, 391-410 (1991).

[55] R.G. Owens and T.N. Phillips, "A spectral domain decomposition method for the planar non-Newtonian stick-slip problem," *J. Comp. Appl. Math.* **41**, 43-79 (1991).

[56] R.G. Owens and T.N. Phillips, "Mass and momentum-conserving spectral methods for Stokes flow," *J. Comp. Appl. Math.* **53**, 185-206 (1994).

[57] T. Papanastasiou, G. Georgiou and A. Alexandrou, *Viscous fluid flow*, CRC Press: Boca Ranton, FL (1999).

[58] N. Papamichael and G.T. Symm, "Numerical techniques for two-dimensional Laplacian problems," *Comput. Methods Appl. Mech. Eng.* **6**, 175-194 (1975).

[59] J. Pitkaranta, "Boundary subspaces for the finite element method with Lagrange multipliers," *J. Numer. Math.* **33**, 273-289 (1973).

[60] A. Portela, M.H. Aliabadi and D.P. Rooke, "Efficient bounday element analysis of sharp notched plates," *Int. J. Numer. Meth. Eng.* **32**, 445-470 (1991).

[61] A. Poullikas, A. Karageorghis and G.C. Georgiou, "Methods of fundamental solutions for harmonic and biharmonic boundary value problems," *J. Comp. Mech.* **21**, 416-423 (1998).

[62] S. Richardson, "A stick-slip problem related to the motion of a free jet at low Reynolds numbers," *Proc. Camb. Phil. Soc.* **67**, 477-489 (1970).

[63] P. Rahulkumar, S. Saigal and S. Yunus, "Singular p-version finite elements for stress intensity factor computations," *Int J. Numer. Meth. Eng.* **40**, 1091-1114 (1997).

[64] T.R. Salamon, D.E. Bornside, R.C. Armstrong and R.A. Brown, "The role of surface tension in the dominant balance in the die-swell singularity," *J. Phys. Fluids*, **7**, 2328-2344 (1995).

[65] B.D. Schiff, D. Fishelov and J.R. Whiteman, *Determination of a stress intensity factor using local mesh refinement*, In: J.R. Whiteman (editor) "The mathematics in finite elements and applications III," London: Academic Press, 55-64 (1979).

[66] E. Schnack, *Singularities of cracks with generalized finite elements*, Lecture Notes in Math, 1121:258-277, London (1985).

[67] H. Schulz, C. Schwab and W. L. Wendland, "The computation of potentials near and on the boundary by an extraction technique for boundary element methods," *Comput. Methods Appl. Mech. Eng.* **157**, 225-238 (1998).

[68] J.M. Shi, M. Breurer and F. Durst, "A combined analytical-numerical method for treating corner singularities in viscous flow predictions," *Int. J. Numer. Methods Fluids* **45**, 659-688 (2004).

[69] L.D. Sturges, *Ph.D. Thesis*, Univerity of Minnesota, Minneapolis (1977).

[70] G.T. Symm, "Treatment of singularities in the solution of Laplace's equation by an integral equation method," *National Physical Laboratory Report NAC31* (1973).

[71] B. Szabó and I. Babuška, *Finite Element Analysis*, John Wiley & Sons, Inc., New York (1991).

[72] B.A. Szabó and Z. Yosibash, "Numerical analysis of singularities in two dimensions. Part 1: Computation of the eigenpairs," *Int. J. Numer. Meth. Eng.* **38**, 2055-2082 (1995).

[73] B.A. Szabó and Z. Yosibash, "Numerical analysis of singularities in two dimensions. Part 2: Computation of generalized flux/stress intensity factors," *Int. J. Numer. Meth. Eng.* **39**, 409-434 (1996).

[74] R.I. Tanner and X. Huang, "Stress singularities in non-Newtonian stick-slip and edge flows," *J. Non-Newtonian Fluid Mech.*, **50**, 135-160 (1993).

[75] D.M. Tracey, "Finite elements for determination of crack tip elastic stress intensity factors," *J. Eng. Fract. Mech.* **3**, 255-265 (1971).

[76] S.A. Trogdon and D.D. Joseph, "The stick-slip problem for a round jet. I. Large surface tension," *Rheol. Acta* **19**, 404-420 (1980).

[77] N.M. Wigley, "An efficient method for subtracting off singularities at corners for Laplace's equation," *J. Comp. Physics* **78**, 369-377 (1988).

[78] L.S. Xanthis, M.J.M. Bernal and C. Atkinson, " The treatment of singularities in the calculation of stress intensity factors using the boundary integral equation method," *Comput. Methods Appl. Mech. Eng.* **26**, 285-304 (1981).

[79] C. Xenophontos, M. Elliotis and G. Georgiou, " A singular function boundary integral method for elliptic problems with singularities," *SIAM J. Sci. Comp.*, submitted (2005).

[80] Z. Yosibash, "Computing singular solutions of elliptic boundary value problems in polyhedral domains using the p-FEM," *J. Appl. Numer. Math.* **33**, 71-99 (2000).